MEMORANDUM REPORT BRL-MR-3659

BRL

1938 – Serving the Army for Fifty Years – 1988

SIMULATION TECHNIQUES FOR THE PREDICTION OF BLAST FROM UNDERGROUND MUNITIONS STORAGE FACILITIES

GEORGE A. COULTER
GERALD BULMASH
CHARLES N. KINGERY

APRIL 1988

U.S. ARMY LABORATORY COMMAND

BALLISTIC RESEARCH LABORATORY
ABERDEEN PROVING GROUND, MARYLAND

DESTRUCTION NOTICE

Destroy this report when it is no longer needed. DO NOT return it to the originator.

Additional copies of this report may be obtained from the National Technical Information Service, U.S. Department of Commerce, Springfield, VA 22161.

The findings of this report are not to be construed as an official Department of the Army position, unless so designated by other authorized documents.

The use of trade names or manufacturers' names in this report does not constitute indorsement of any commercial product.

UNCLASSIFIED

SECURITY CLASSIFICATION OF THIS PAGE

AD-A192 262

REPORT DOCUMENTATION PAGE

Form Approved OMB No. 0704-0188

1a. REPORT SECURITY CLASSIFICATION
UNCLASSIFIED

1b. RESTRICTIVE MARKINGS

2a. SECURITY CLASSIFICATION AUTHORITY

2b. DECLASSIFICATION / DOWNGRADING SCHEDULE

3. DISTRIBUTION / AVAILABILITY OF REPORT
Approved for public release; distribution is unlimited.

4. PERFORMING ORGANIZATION REPORT NUMBER(S)
BRL-MR-3659

5. MONITORING ORGANIZATION REPORT NUMBER(S)

6a. NAME OF PERFORMING ORGANIZATION
U.S. Army Ballistic Research Laboratory (BRL)

6b. OFFICE SYMBOL (If applicable)
SLCBR-TB-B

7a. NAME OF MONITORING ORGANIZATION

6c. ADDRESS (City, State, and ZIP Code)
Aberdeen Proving Ground, MD 21005-5066

7b. ADDRESS (City, State, and ZIP Code)

8a. NAME OF FUNDING / SPONSORING ORGANIZATION
DOD Explosive Safety Board

8b. OFFICE SYMBOL (If applicable)

9. PROCUREMENT INSTRUMENT IDENTIFICATION NUMBER

8c. ADDRESS (City, State, and ZIP Code)
2461 Eisenhower Avenue
Alexandria, VA 22331-0600

10. SOURCE OF FUNDING NUMBERS

PROGRAM ELEMENT NO.	PROJECT NO.	TASK NO.	WORK UNIT ACCESSION NO.
	4A665805M857		

11. TITLE (Include Security Classification)
Simulation Techniques for the Prediction of Blast from Underground Munitions Storage Facilities

12. PERSONAL AUTHOR(S)
Coulter, George A., Bulmash, Gerald, and Kingery, Charles N.

13a. TYPE OF REPORT	13b. TIME COVERED	14. DATE OF REPORT (Year, Month, Day)	15. PAGE COUNT
Memorandum	FROM Sep 86 TO Sep 87	88 February 16	95

16. SUPPLEMENTARY NOTATION

17. COSATI CODES

FIELD	GROUP	SUB-GROUP
20	04	
14	02	

18. SUBJECT TERMS (Continue on reverse if necessary and identify by block number)
Airblast, Baffles, Blast Waves, Blast Suppression, Converging Area, Exit Blast, Munitions Storage, Overpressure, Shock Tube, Tunnel Attenuation, Underground Storage,

19. ABSTRACT (Continue on reverse if necessary and identify by block number)

Results are presented from a series of shock tube and 1:50 scale model high explosive (PETN) tunnel tests, designed to simulate underground chamber/tunnel explosions. Models consisted of straight and smooth chamber/tunnel configurations with converging area changes. Experimental data are compared with predictions from a modified INBLAST computer code to which was added the blast wave propagation along the tunnel. Modifications were made either by the addition to INBLAST of shock tube equations for converging area change at the diaphragm, or by addition of the BRL-Q1D one-dimensional hydrocode. Effects of baffle induced tunnel area changes were included in the hydrocode when needed. Otherwise, the algebraic shock tube equations were used. The field test, in addition to internal blast pressure, measured the exit field pressures as a function of the chamber charge loading density. The free-field blast pressure was measured as a function of radial distance and angle of propagation with respect to the tunnel's long axis. Results were

(OVER)

20. DISTRIBUTION / AVAILABILITY OF ABSTRACT
☐ UNCLASSIFIED/UNLIMITED ☒ SAME AS RPT. ☐ DTIC USERS

21. ABSTRACT SECURITY CLASSIFICATION
UNCLASSIFIED

22a. NAME OF RESPONSIBLE INDIVIDUAL
George A. Coulter

22b. TELEPHONE (Include Area Code)
301-278-6719/4913

22c. OFFICE SYMBOL
SLCBR-TB-B

DD Form 1473, JUN 86 Previous editions are obsolete. SECURITY CLASSIFICATION OF THIS PAGE

UNCLASSIFIED

REPORT DOCUMENTATION PAGE

19. ABSTRACT (Cont)

found to be consistent with those found in the literature. Data from the test results will be incorporated into quantity-distance standards for underground storage of munitions. This will result in a more comprehensive data base for airblast effects from ordnance.

ACKNOWLEDGMENTS

The authors wish to thank Messrs. William B. Sunderland and Lowell K. Bryant for their most useful participation on the field project as data acquisition engineer and charge handler, respectively.

TABLE OF CONTENTS

FIGURES

Page

FIGURES (Cont)

TABLES

1. INTRODUCTION

1.1 Background. The Department of Defense Explosives Safety Board (DDESB) has as a part of its mission the characterization of airblast hazards for determining quantity-distance (Q-D) standards (airblast effects) for ordnance. The research effort reported here deals with the approximate Q-D standards to be applied when there are explosions of munitions stored underground. A survey of a large number of model experiments[1] reported in the literature indicates a rather large error band in the data. This is reflected in Q-D standards that may be overly conservative.

1.2 Objectives. The general objective of the research sponsored by DDESB here is to develop a comprehensive database and analytical models for airblast effects from ordnance. In particular, immediate objectives are: a) to conduct, analyze, and report shock tube tests simulating explosions of munitions in underground chamber/tunnel storage facilities and compare the results with empirical models for external airblast effects; b) modify the Internal Blast Damage Mechanisms Computer Program (INBLAST) computer code[2] to simulate blast wave propagation down tunnels; c) conduct scale model tunnel tests to improve the empirical model for external airblast effects; and d) to propose improved Q-D standards (airblast effects) for underground storage of munitions.

2. TEST PROCEDURES

Two types of tests were designed to meet the desired objectives. A smooth-walled steel pipe chamber/tunnel model of 1:50 scale was constructed and operated as a converging shock tube with a helium driver to simulate a TNT explosive. The second test was with a similar chamber/tunnel configuration but was operated with primarily PRIMACORD (PETN) explosive.[3] The tests are described in detail in the sections below.

2.1 Shock Tube Model. The 1:50 scale shock tube model is shown sketched in Figure 1. A straight configuration with a single area change was chosen for simplicity. Construction was of thick smooth-walled steel pipes and, since it was to be operated indoors, was terminated with a dump tank. Pertinent dimensions and ratios are listed on Figure 1. Quartz pressure transducers[4] were mounted along the tunnel section to monitor the airblast wave traveling in the tunnel. Transducers were placed at locations of 20 to 45 tunnel diameters. Helium gas was used in the driver for two reasons: a) to enhance the airblast wave in the tunnel for a given driver pressure; and b) to obtain a higher sound velocity ratio in the driver chamber to more nearly simulate the chamber mixture from the real case of an explosion of munitions. The comparison is to TNT in this case.

NOTES ~

1. ALL SECTIONS ARE SMOOTH WALL PIPE
2. NOT TO SCALE
3. DUMP TANK USED INDOORS

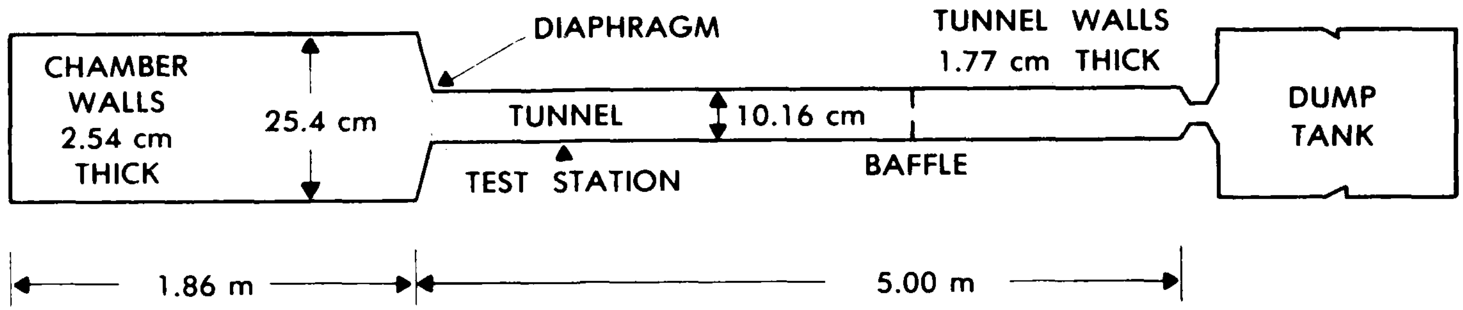

CHAMBER / TUNNEL

$\frac{\text{TUNNEL AREA}}{\text{CHAMBER AREA}} = 0.16$

CHAMBER VOLUME = 0.0942 m^3

TUNNEL VOLUME = 0.0405 m^3
(FOR 5 m)

TOTAL VOLUME = 0.1347 m^3

BAFFLE STATIONS

27 TUNNEL DIA.
36

TEST STATIONS

20 TUNNEL DIA.
25
30
33
45

FIGURE 1. 1:50 Scale Shock Tube Model

Diaphragms were installed at the converging area from the driver chamber to the tunnel. Mylar, aluminum, and copper diaphragms were used to contain the driver chamber pressure until self-rupture occurred. One set of pressure-time records was obtained without tunnel baffles and a second set with installed baffles, as indicated on Figure 1.

The objective of the baffle study was to determine the feasibility of using baffles in tunnels to attenuate the blast.

2.2 Field Model. The model used for the shock tube tests was modified slightly and moved to one of the U.S. Army Ballistic Research Laboratory's (BRL's) outdoor ranges. The dump tank had been removed so the blast would now exit from the open tunnel. Pressure transducers were mounted in ground baffles on blast radials located at 0°, 45°, 90°, and 135° from the tunnel exit - 0° being defined as the long axis of the tunnel. Other transducers were placed in the chamber and the tunnel.

Ground distances for transducer stations were chosen so as to record equal predicted pressures on all blast lines at corresponding stations. The field layout is shown in Figure 2. Photographs of the test site and charge centering device are given in the Results section. The PRIMACORD was cut in lengths, bundled, and centered in a tube within the driver chamber to give the desired loading density. This corresponds to a distributed storage of munitions in the chamber of an underground storage facility. Detonation was from the closed-chamber end by means of a Type 2023 detonator. A single charge of C-4 was placed and detonated near the center of the chamber. In Tests 1, 2, 3, and 4 the charges were 0.03320 kg, 0.06337 kg, 0.13585 kg, and 0.31697 kg of PETN, respectively. On Test 5, the charge was 0.3670 kg of C-4 explosive.

Results of both sets of experiments are given in the Results section below.

2.3 Instrumentation. Standard recording instrumentation was used in both sets of experiments. The shock tube tests needed only a few channels, so they were recorded with a digitizing oscilloscope. The field tests required more channels of data, so those shots were recorded with two analog tape recorders. Data reduction procedures were very similar. Figure 3 shows a schematic of the two systems used in the tests.

3. RESULTS

The results are listed separately for the two sets of firings according to location.

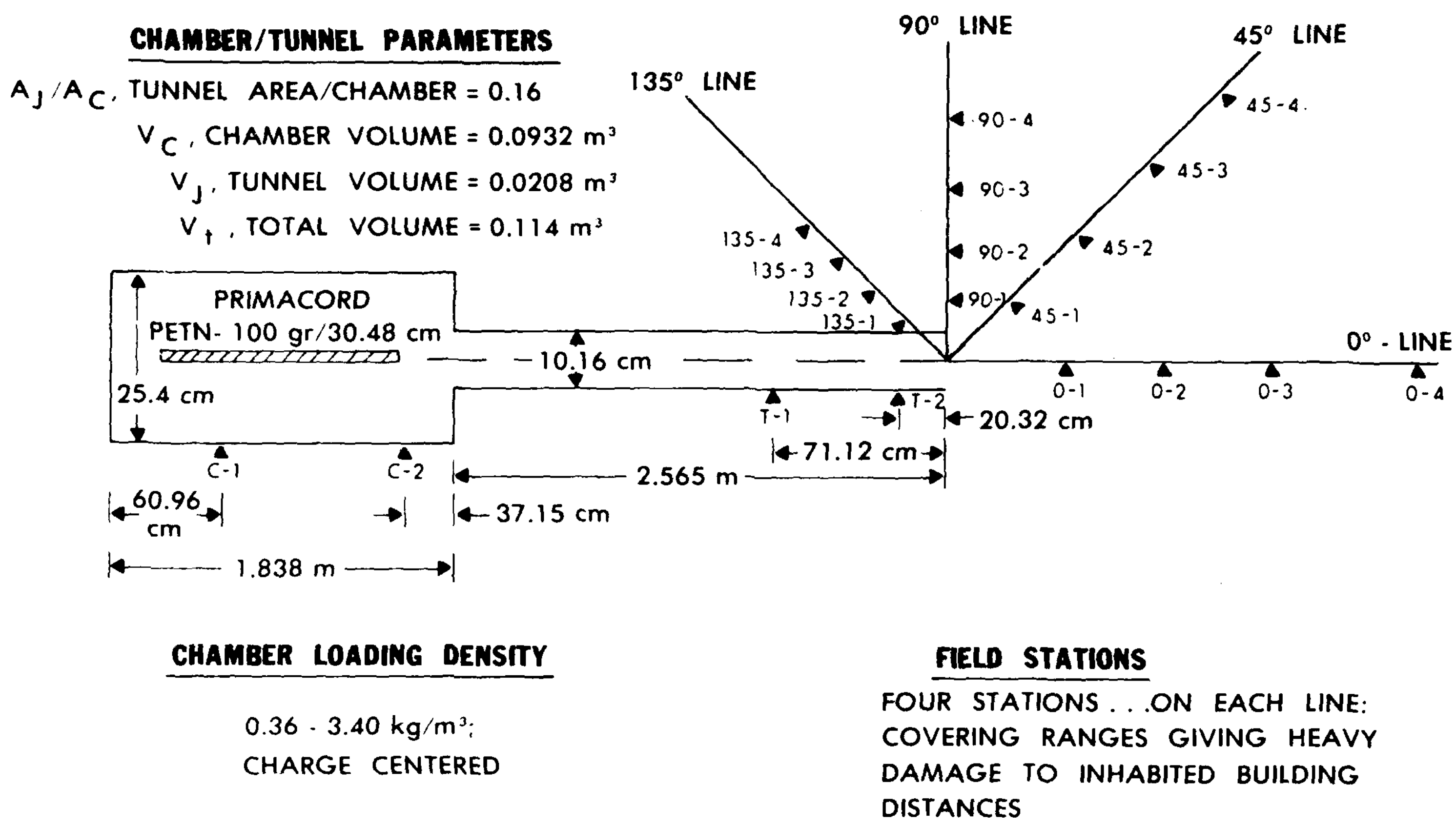

FIGURE 2. Tunnel Configuration for Field Shots

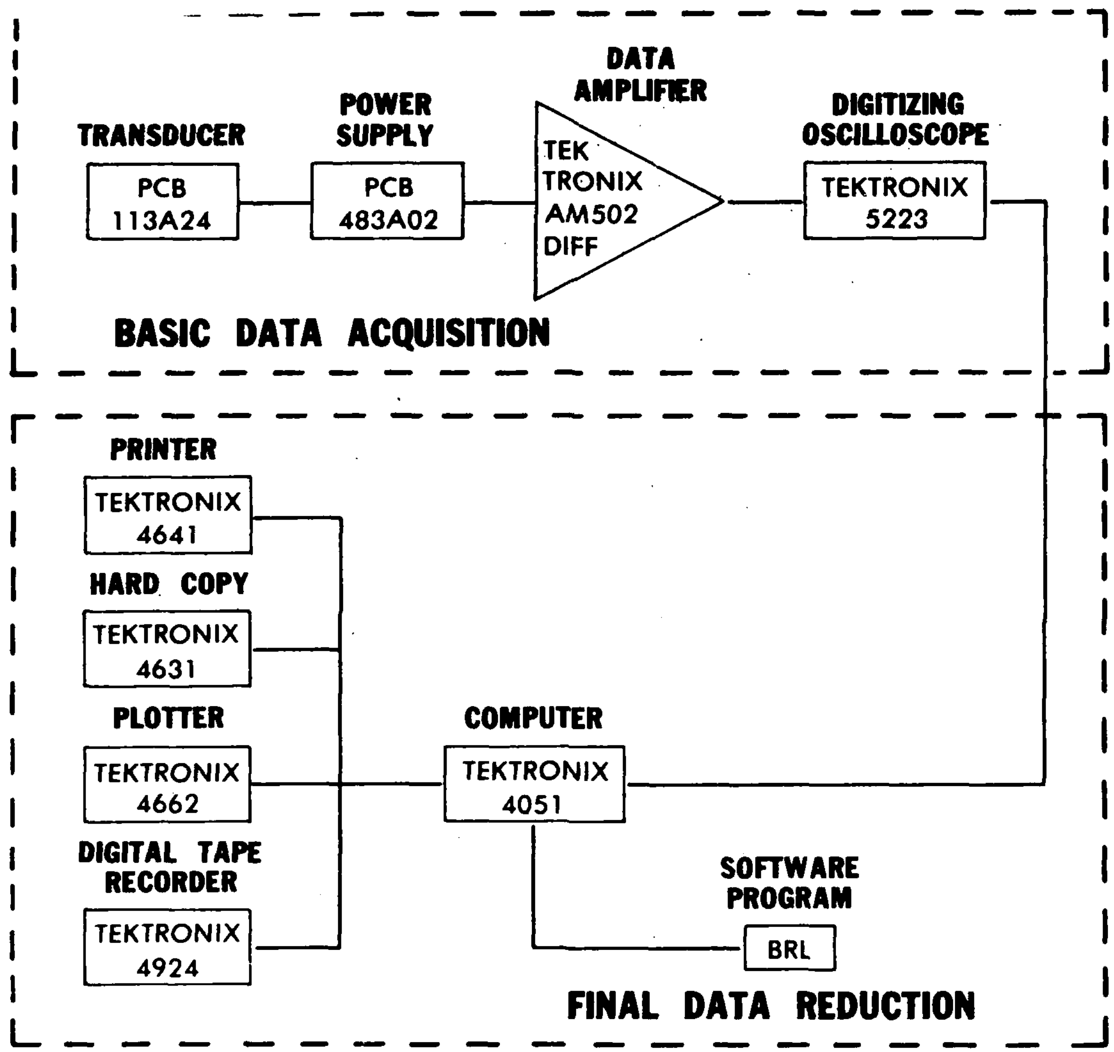

A. Shock Tube Tests

FIGURE 3. Schematic of Data Acquisition - Reduction System

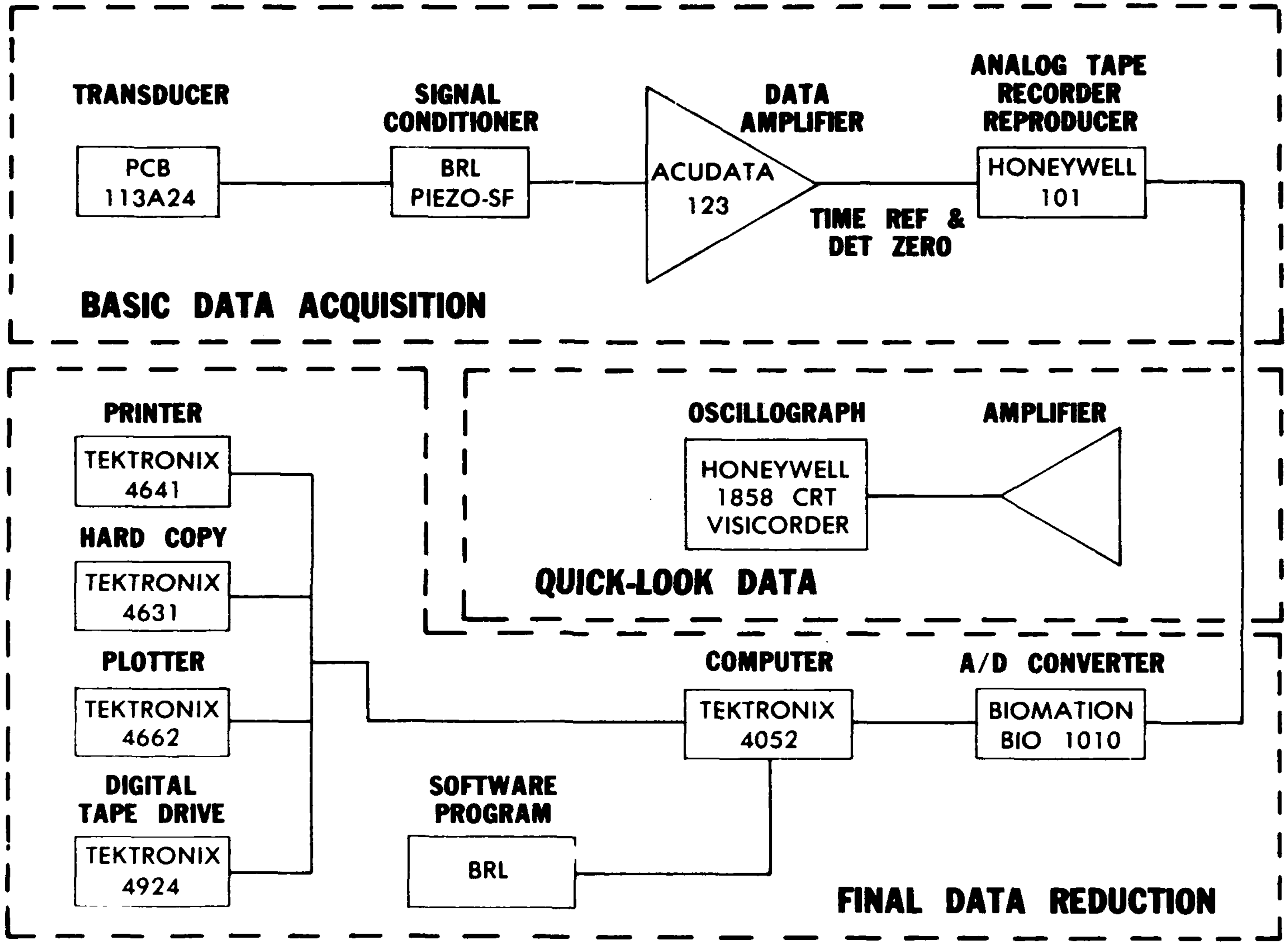

B. Field Tests

FIGURE 3. Schematic of Data Acquisition - Reduction System (Cont)

3.1 Shock Tube Tests. Diaphragms, and therefore the driver chamber pressures, were selected to correspond to gas pressures generated from the munitions stored at low to medium charge density. The chamber loading density (Q/V_c) for the field test ranged from 0.36 to 3.4 kg/m^3. From the INBLAST code, this would give a quasi-static chamber pressure for TNT of 1300 to 4600 kPa. Helium gas was used in the shock tube driver because it could very nearly match initial sound-ratio conditions of a TNT explosion. The chamber pressure ranged from 814 kPa to 5454 kPa. The objectives of these tests are to determine the feasibility of using the shock tube to determine the exit pressure that might be expected in a field test, as well as to check the accuracy of using INBLAST and shock tube equations to predict the measured exit pressure. The results of Tests 4 through 7 are listed in Table 1.

The test series was repeated with sets of baffles placed at locations of 27 and 36 tunnel diameters. Table 1 summarizes the results from the two sets of shots fired in the shock tube model. Tunnel overpressures are listed as a function of the given driver chamber pressure, with and without baffles.

The smooth wall attenuation (no baffles) is 0.5 to 3.5%, and also includes transducer calibration error. With two baffles, each blocked 26.2%, the attenuation between 25 and 45 tunnel diameters was 7.5-10.3%. These values include the unobstructed smooth wall attenuation also. With two baffles, each blocked 50%, the attenuation was between 39.7 and 43.1%, including the smooth wall unobstructed values. A more complete baffle/attenuation program will be needed to determine baffle location dependence to maximize baffle efficiency.

Figures 4-7 show portions of the pressure-time records from the shots where there were no baffles in the tunnel section of the model. The second peak is caused by the blast wave reflecting from the entrance throat to the dump tank. Figures 8-11 show records obtained when baffles were used in the test tunnel. Figures 12 and 13 compare the waveforms obtained at 45 tunnel diameters from the unobstructed tests with those taken when the baffles were on either side of the test stations. The larger blockage of 50% each for the two baffles indicates a substantial reduction in the blast wave. This much blockage may not be practical for a full-size tunnel to an underground storage facility. This would be particularly the case where the tunnel may not be overly large in the first place.

The attenuation values are in agreement with those established in Reference 5. For a 50% blockage, there should be a 22% attenuation going through each plate. In Table 1, Shot 8, the value through the first plate measures 331 kPa versus a predicted 335 kPa, and through the second plate, the measured value is 245 kPa versus 261 kPa. On Shot 9, the value after the second plate is 566 kPa versus a predicted value of 570 kPa.

TABLE 1. Shock Tube Test Results

Shot No.	Station	Baffles	Chamber Pressure, kPa	Side-On Wall Pressure, kPa	Percent Change	P_1, kPa	T_1, °C
5	20	None	813.6	435.3		103.0	22.0
	25			438.9			
	33			429.0			
	45			423.1	- 3.5	(St25-45)	
4	20	None	1447.9	639.1		103.0	22.6
	25			659.8			
	33			643.1			
	45			639.1	- 3.1	(St25-45)	
6	20	None	2695.8	997.5		102.9	22.8
	25			1006.2			
	33			987.2			
	45			972.6	- 3.3	(St25-45)	
7	20	None	5453.8	1463.3		102.8	23.3
	25			1559.5			
	33			1559.7			
	45			1551.8	- 0.4	(St25-45)	
8	20	2-50%	792.9	409.5		102.7	23.0
	25	Blocked.		430.3			
	33	@ 27 dia.		331.2			
	45	@ 36 dia.		244.8	-43.1	(St25-45)	
9	20	Same as 8	2682.1	931.0		102.3	23.2
	25			939.1*			
	30			741.4			
	33			785.7			
	45			566.1	-39.7	(St25-45)	
10	20	2-26%	834.3	421.3		103.3	21.5
	25	Blocked.		424.8*			
	30	@ 27 dia.		429.8			
	33	@ 36 dia.		412.8			
	45			380.8	-10.3	(St25-45)	
12	20	Same as	2626.9	902.2		102.7	23.4
	25	10		910.1*			
	30			999.2			
	33			942.1			
	45			841.7	- 7.5	(St25-45)	

*Extrapolated

P_1 - Local ambient pressure.

T_1 - Local ambient temperature.

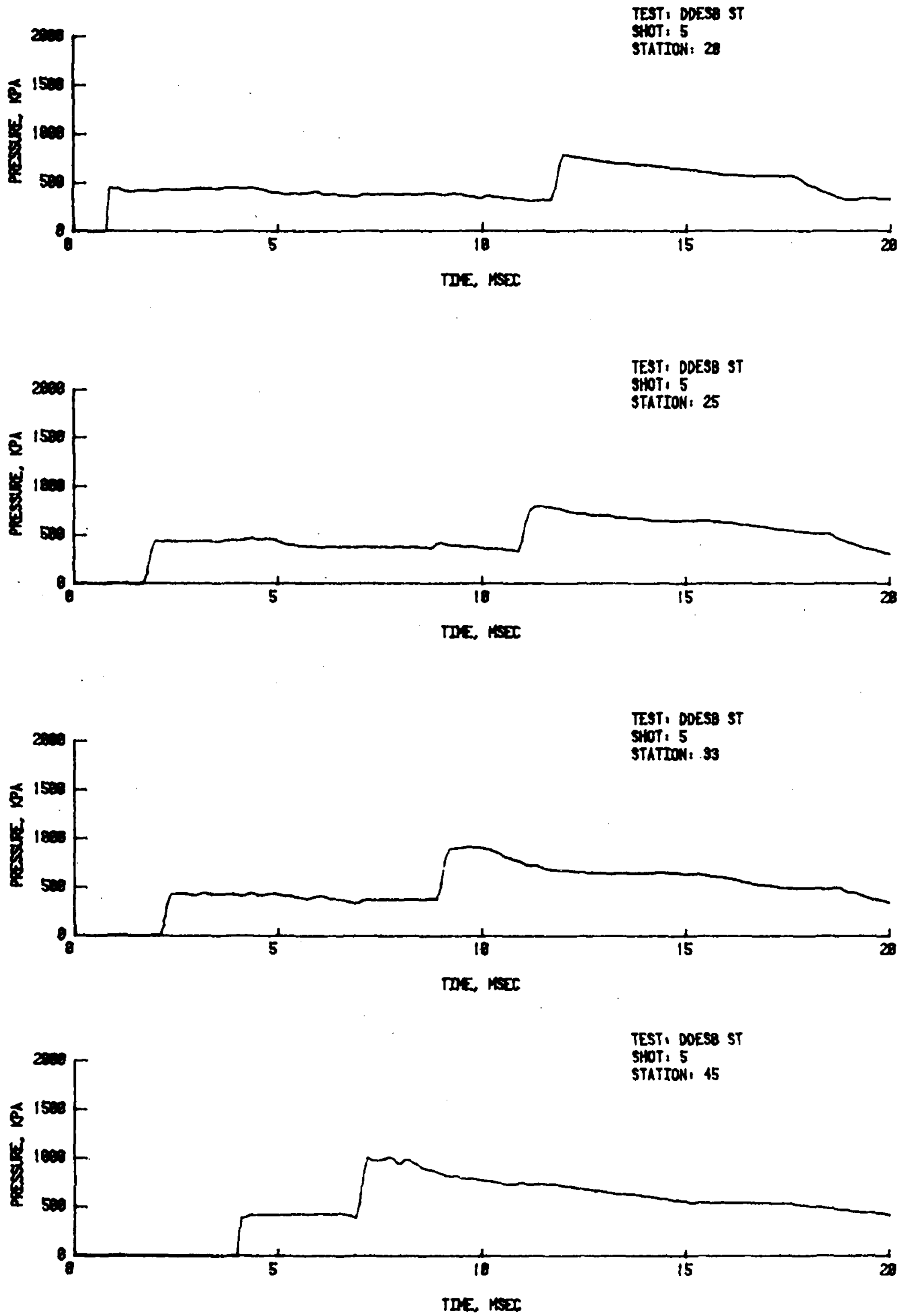

FIGURE 4. Driver Pressure 813.6 kPa-No Baffle

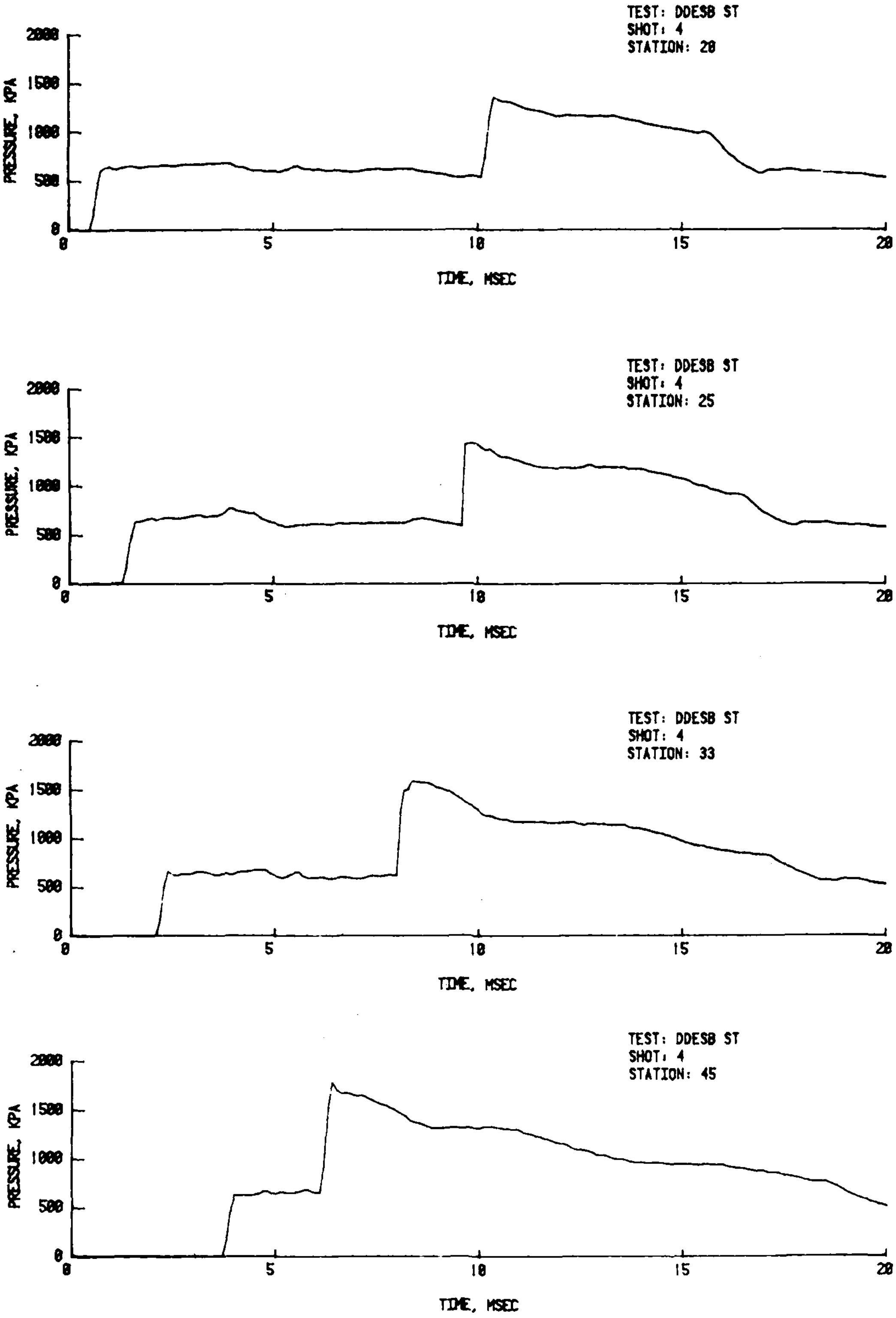

FIGURE 5. Driver Pressure 1447.9 kPa-No Baffle

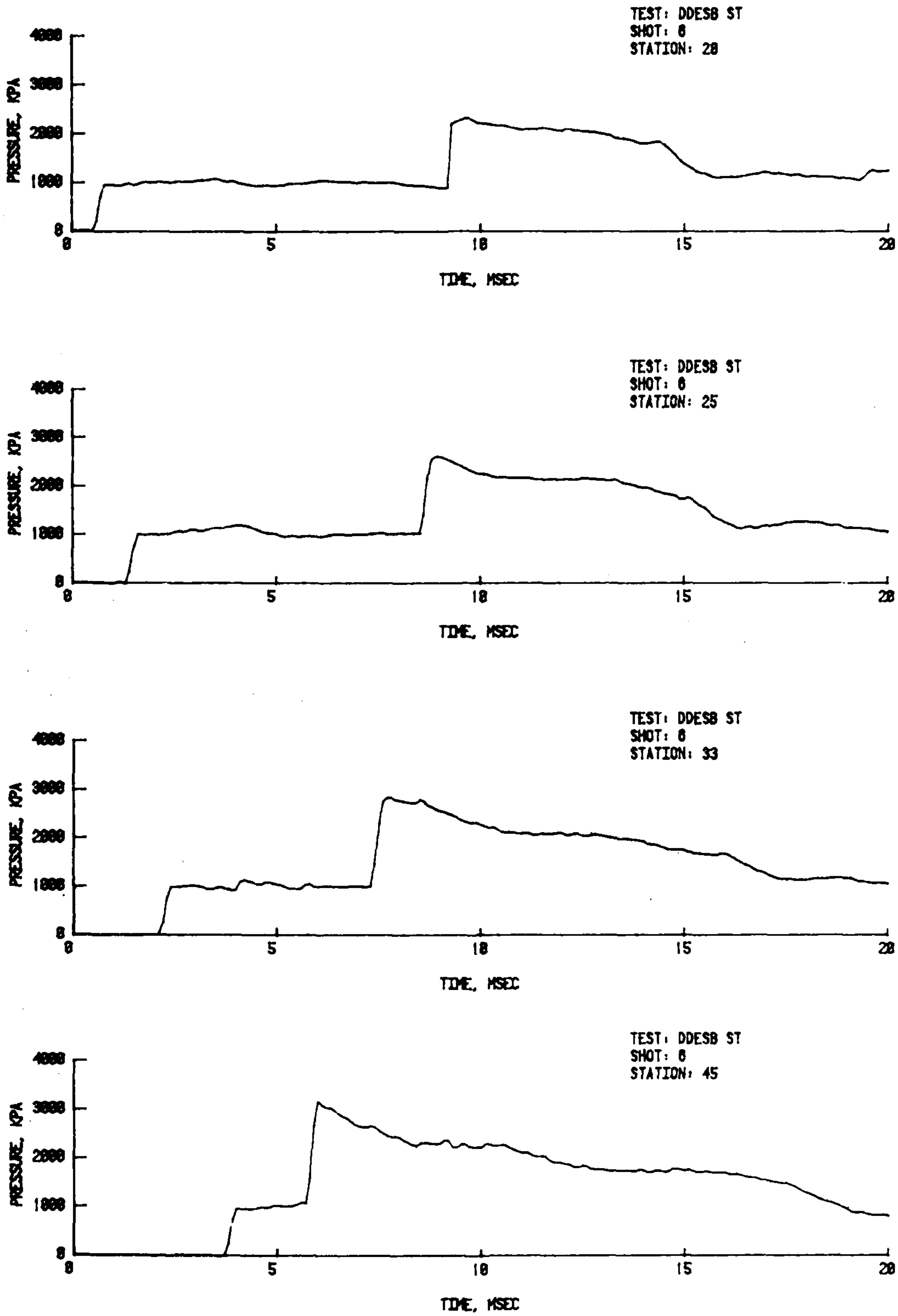

FIGURE 6. Driver Pressure 2695.8 kPa-No Baffle

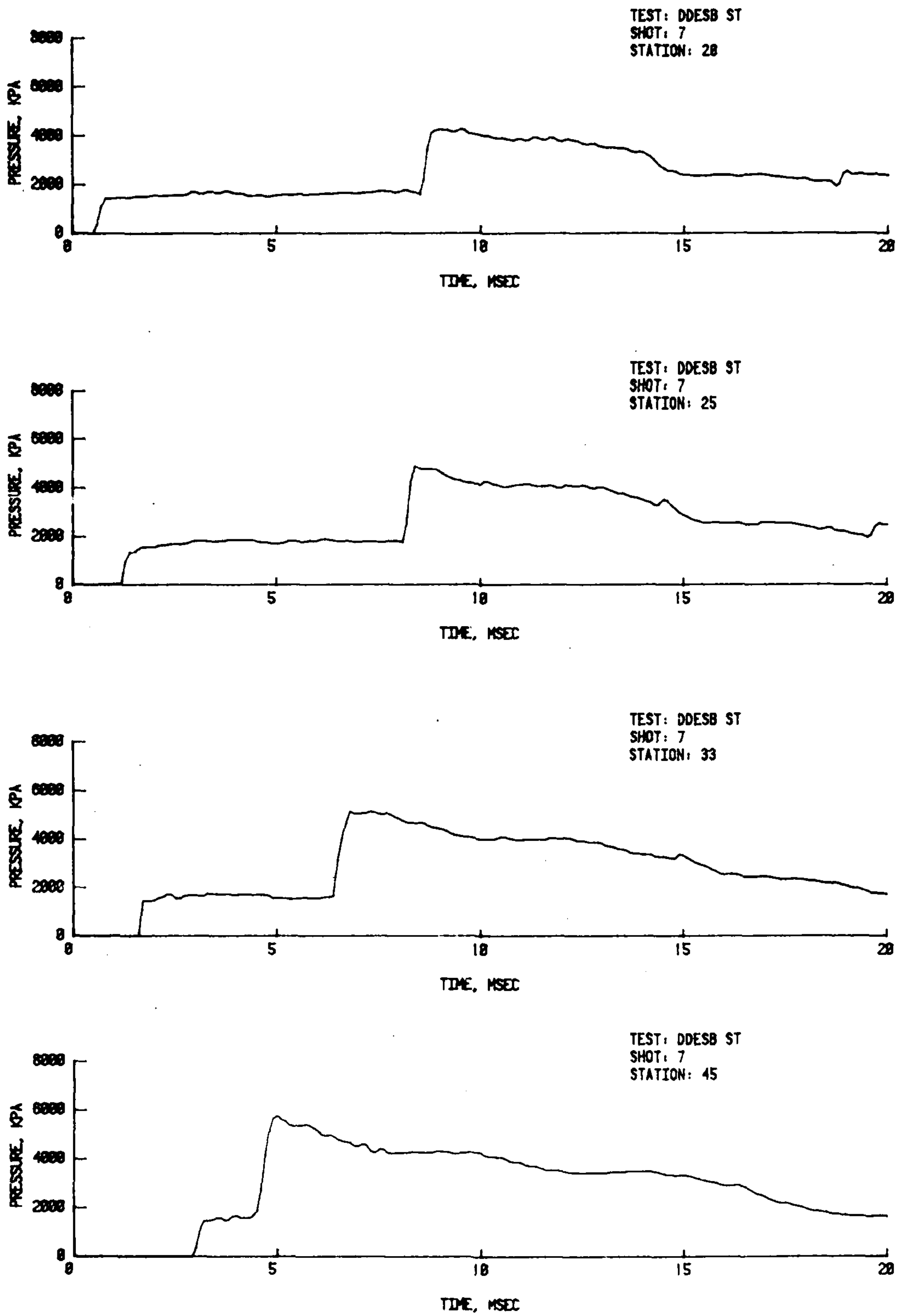

FIGURE 7. Driver Pressure 5453.8 kPa-No Baffle

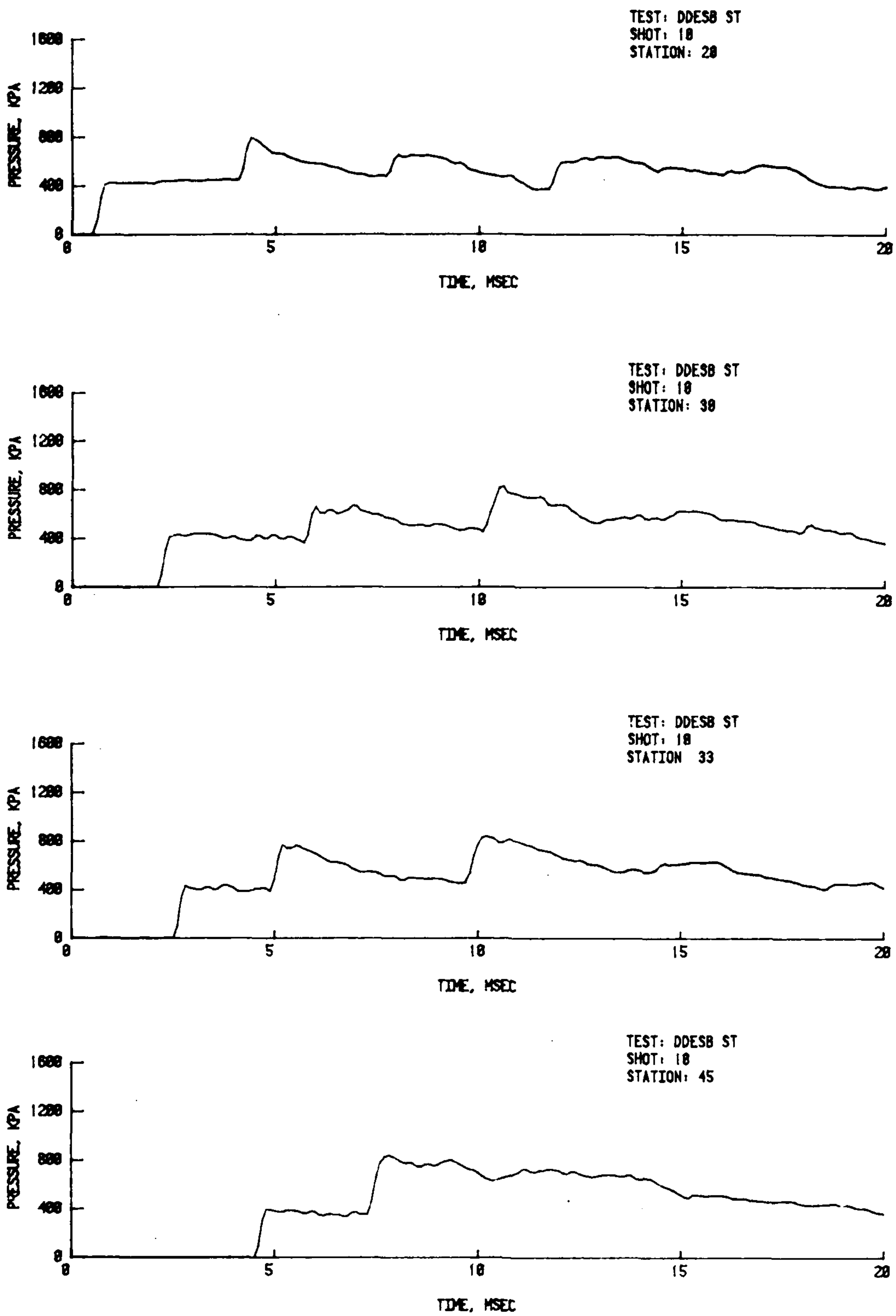

FIGURE 8. Driver Pressure 834.3 kPa-2 Baffles, Each Blocked 26%

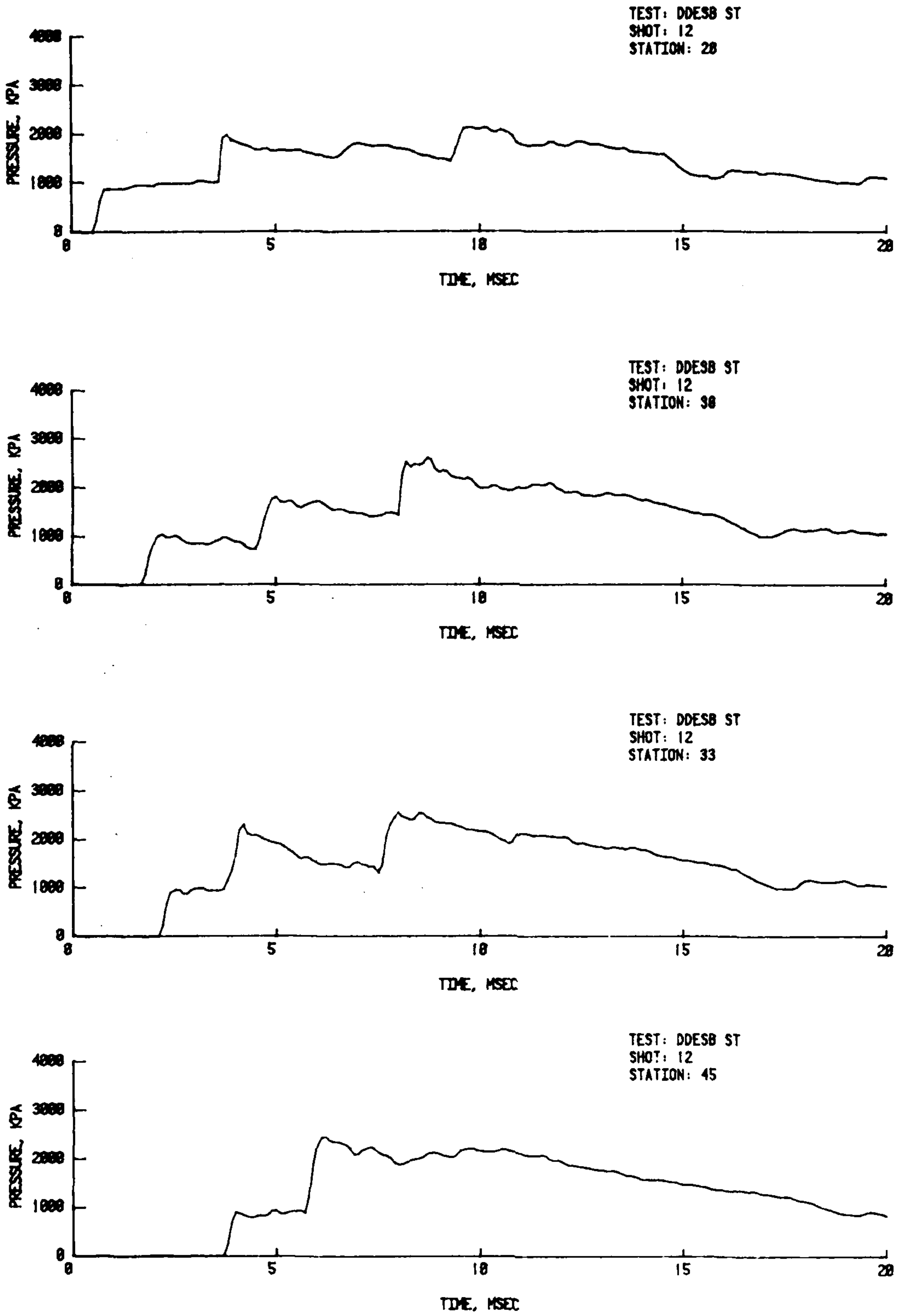

FIGURE 9. Driver Pressure 2626.9 kPa-2 Baffles, Each Blocked 26%

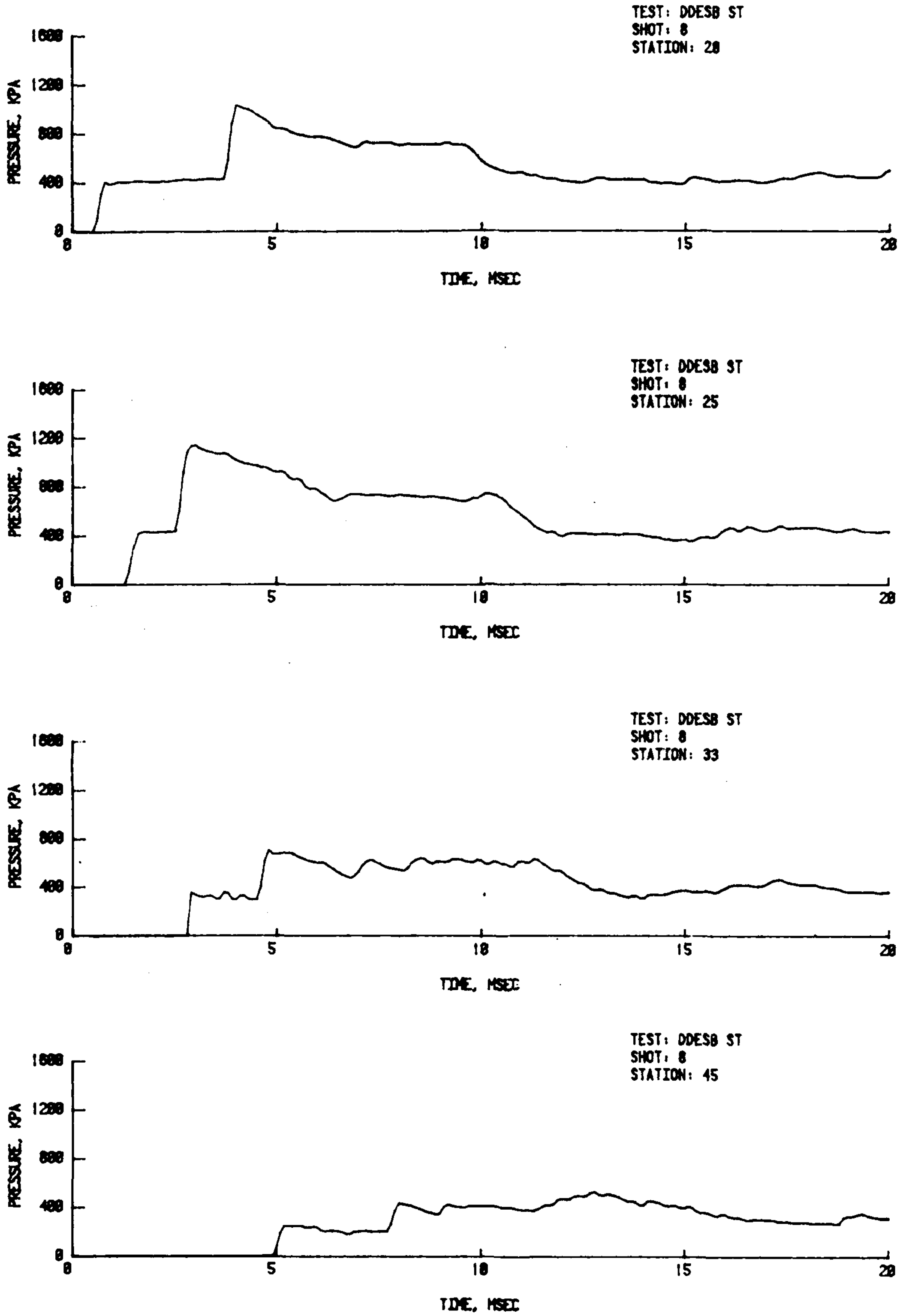

FIGURE 10. Driver Pressure 792.9 kPa-2 Baffles, Each Blocked 50%

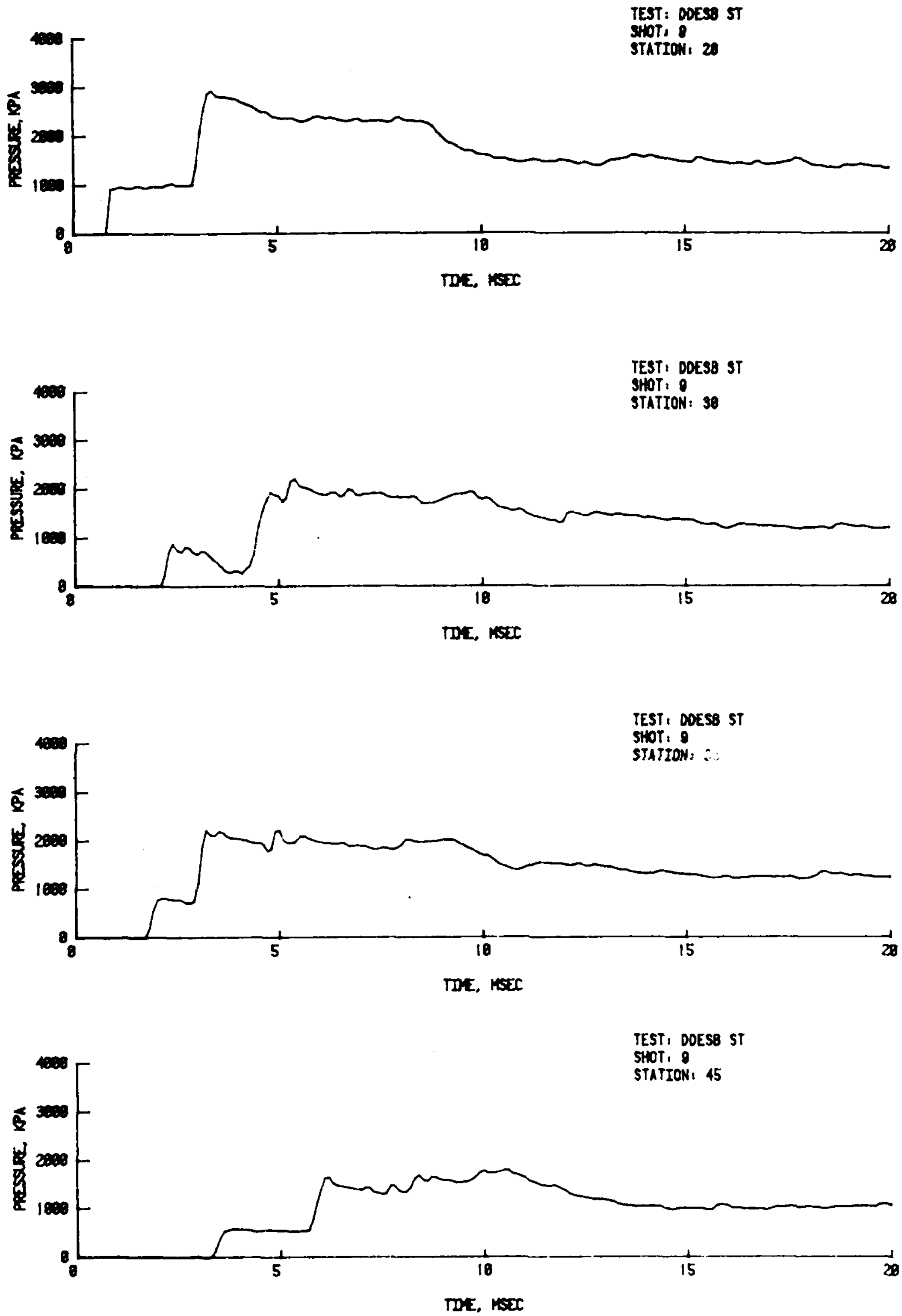

FIGURE 11. Driver Pressure 2682.1 kPa-2 Baffles, Each Blocked 50%

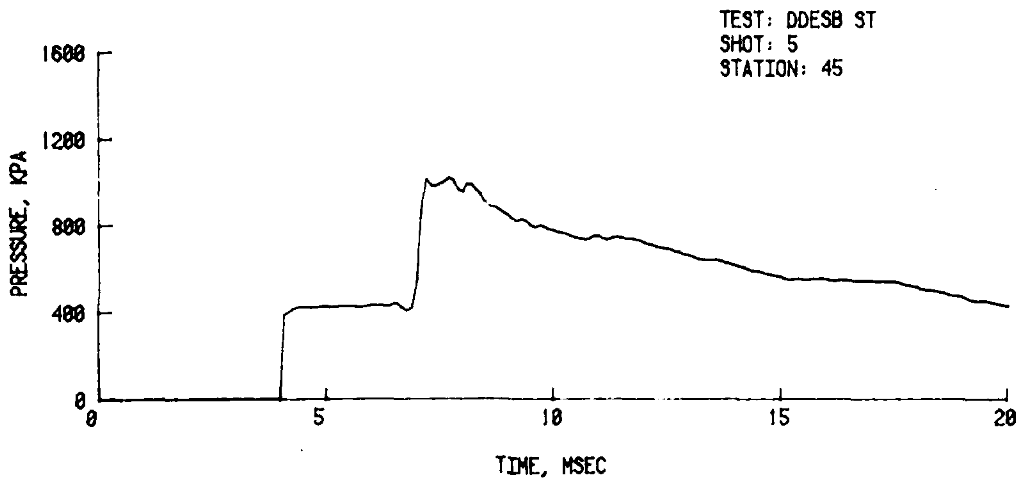

A. NO BAFFLES

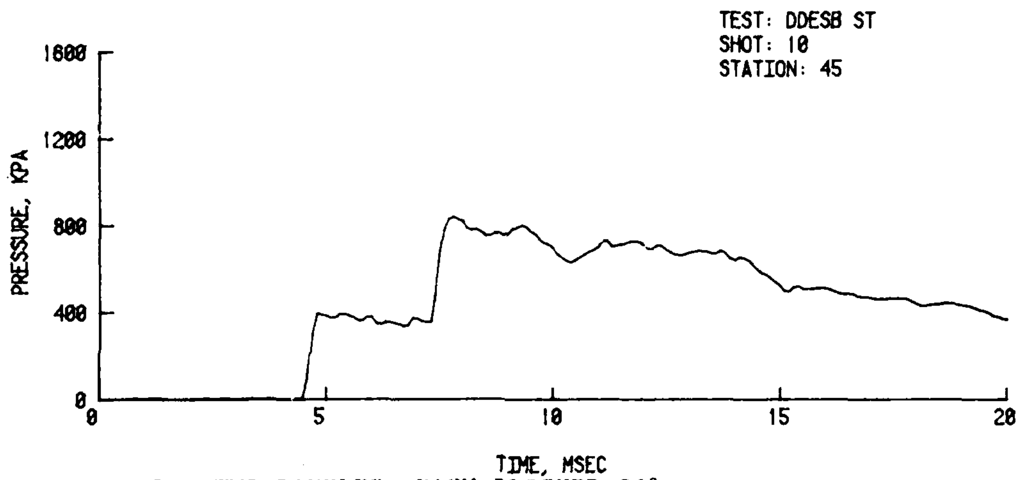

B. TWO BAFFLES, EACH BLOCKED 26%

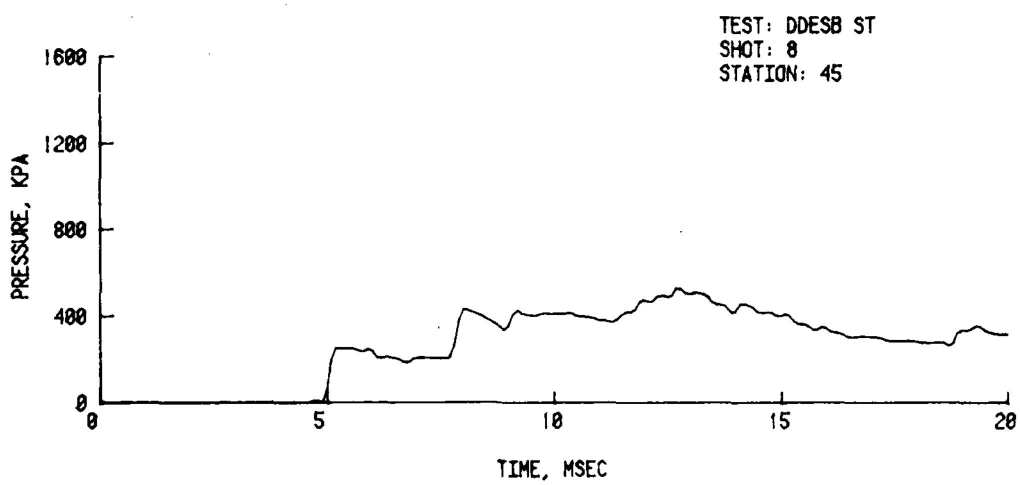

C. TWO BAFFLES, EACH BLOCKED 50%

FIGURE 12. Attenuation Over 45 Test Section Diameters, Average Driver Pressure 814 kPa

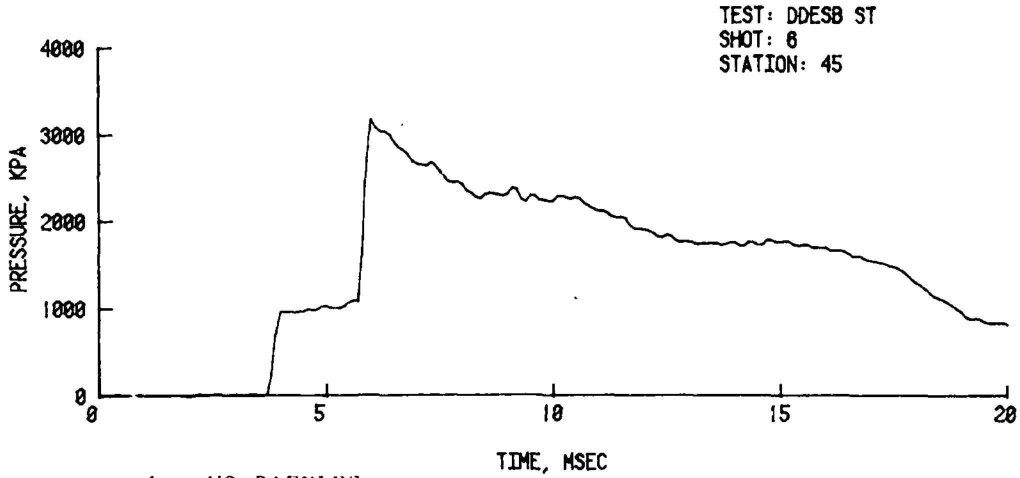

A. NO BAFFLES

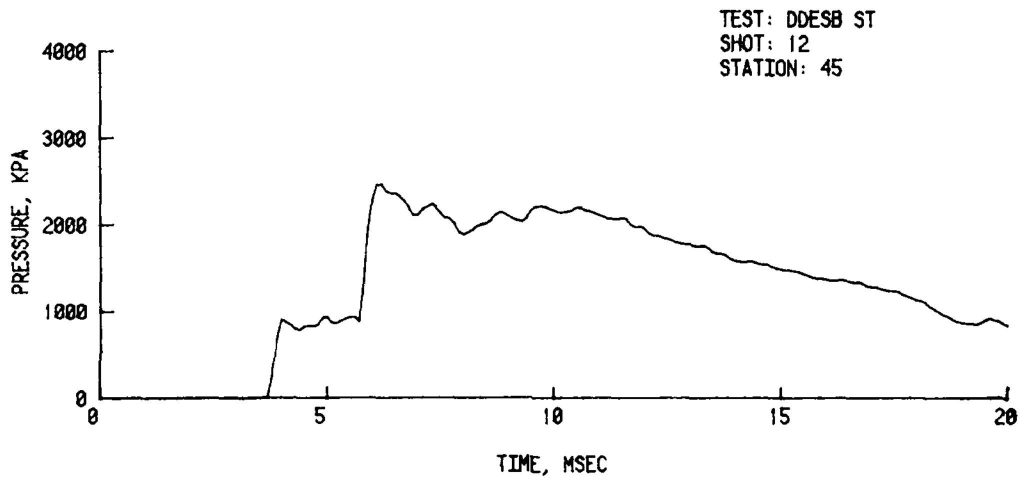

B. TWO BAFFLES, EACH BLOCKED 26%

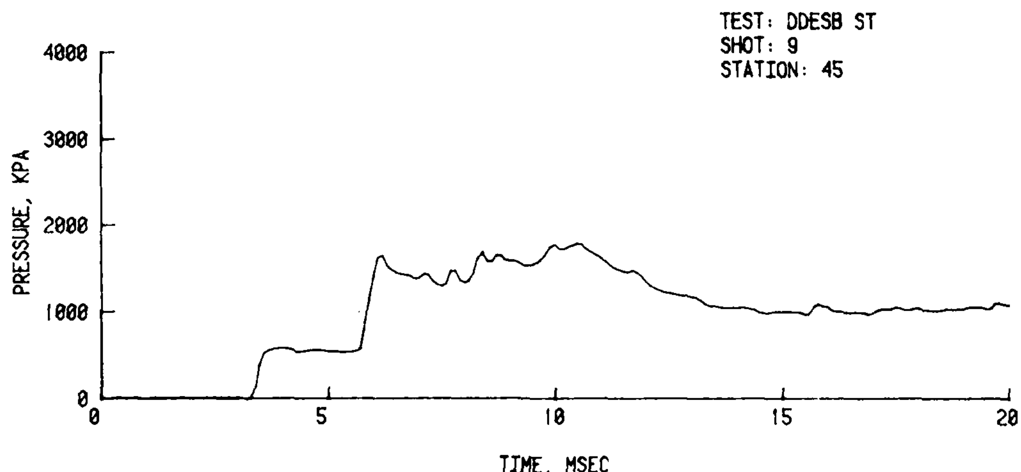

C. TWO BAFFLES, EACH BLOCKED 50%

FIGURE 13. Attenuation Over 45 Test Section Diameters, Average Driver Pressure 2668 kPa

3.2 Field Tests. Figures 14 and 15 are photographs of the field model. A small crane was used to remove the end plate for loading the explosives into the driver chamber. Figure 15 shows three of the blast lines with the transducers placed in ground baffles along these lines. The 135° line is hidden from view behind the exit cover.

Figure 16 shows the centering device for the bundled strands of PRIMACORD. The charge was loaded into the long cardboard tube, then into the driver chamber. Firing lines to the detonator and lines for a time-zero closure were brought out through a hole in the bolted end plate.

Figures 17 and 18 show post-shot photographs of the damage to the sand test bed surface. There was some cratering near the exit and enough soot from the explosion to mark a path along the 0° line. The 90° line was relatively free from the soot.

Figure 19 displays pressure-time records from the driver chamber, records from the tunnel, and records from each station of the blast lines. Notice at Station C-2, in the chamber, the records show that large blast reflections occur from the detonating charge. Then the pressure builds up to some average quasi-steady pressure and decays by exhausting into the tunnel and out the exit. Some transducers were broken due to the very harsh environment of the detonation. A comparison of records from Stations T-1 and T-2 in the tunnel each follows the blast wave profile seen in the chamber, although at a reduced initial peak pressure.

The blast wave propagation can be seen by comparing the records from each of the stations on each of the blast lines. Large double peaked waveforms are seen along the 0° line, but are not present in the other records from the other three blast lines. Whether or not the peaks catch up determines the maximum pressure at a given station. Multiple values of pressure are listed in Table 2 to show the extra peaks.

Table 2 lists pertinent data for each shot at the different explosive loading densities. PRIMACORD (PETN) was used for all shots except Shot 5, which used C-4. In this shot, all the explosive was placed in about the center of the storage chamber, approximately a cylinder 5 cm in diameter x 20 cm long.

The test model configuration was not varied during the shots. However, to maintain the predicted pressure levels of 68.95 kPa at Station 1, 24.13 kPa at Station 2, 11.72 kPa at Station 3, and 5.00 kPa at Station 4, the transducers were moved for each shot. For location of chamber and tunnel transducers, see Figure 2.

The results are discussed and compared with predictions in the Analysis section below.

FIGURE 14. <u>View From Chamber of Field Model</u>

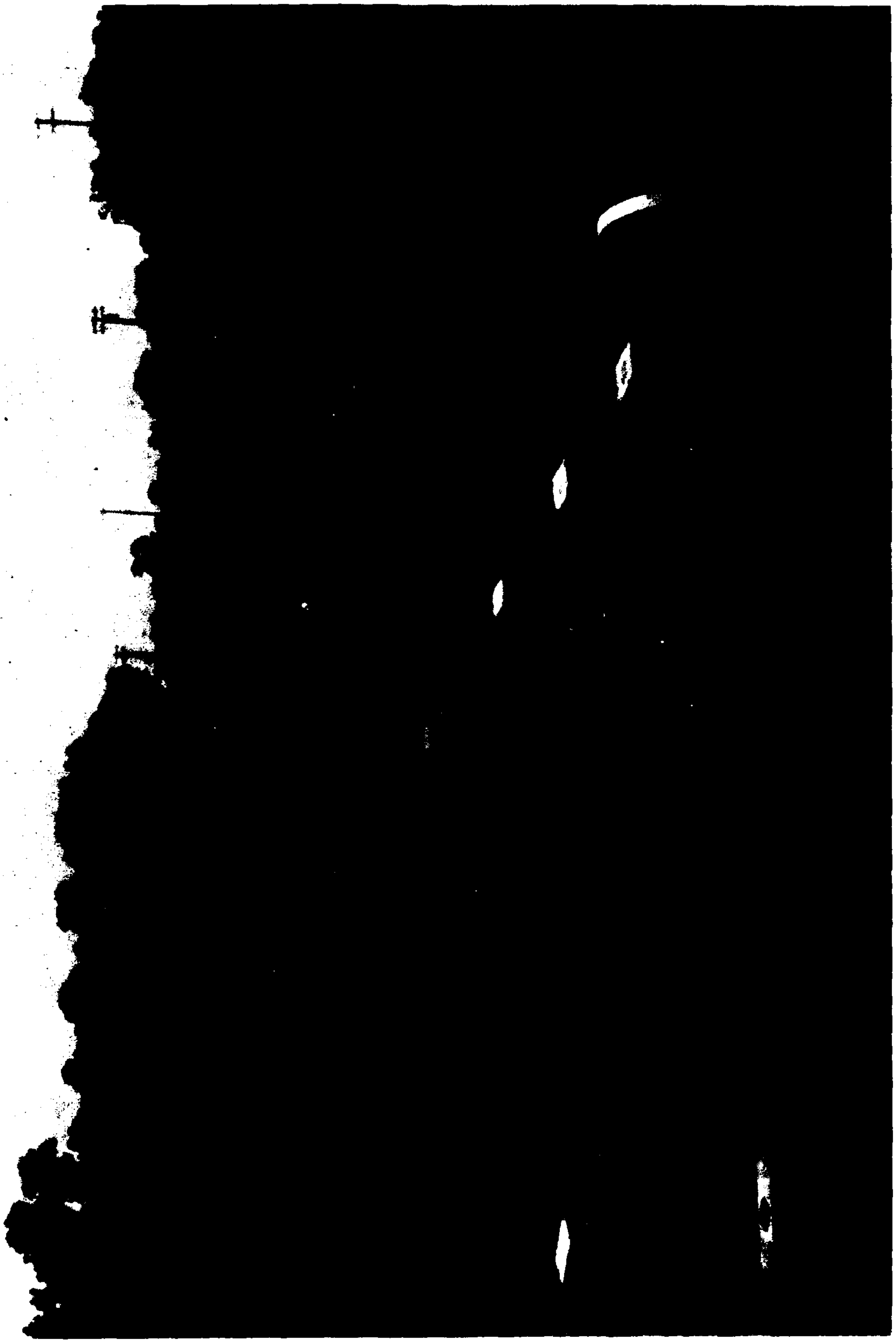

FIGURE 15. View From Exit Tunnel of Field Model

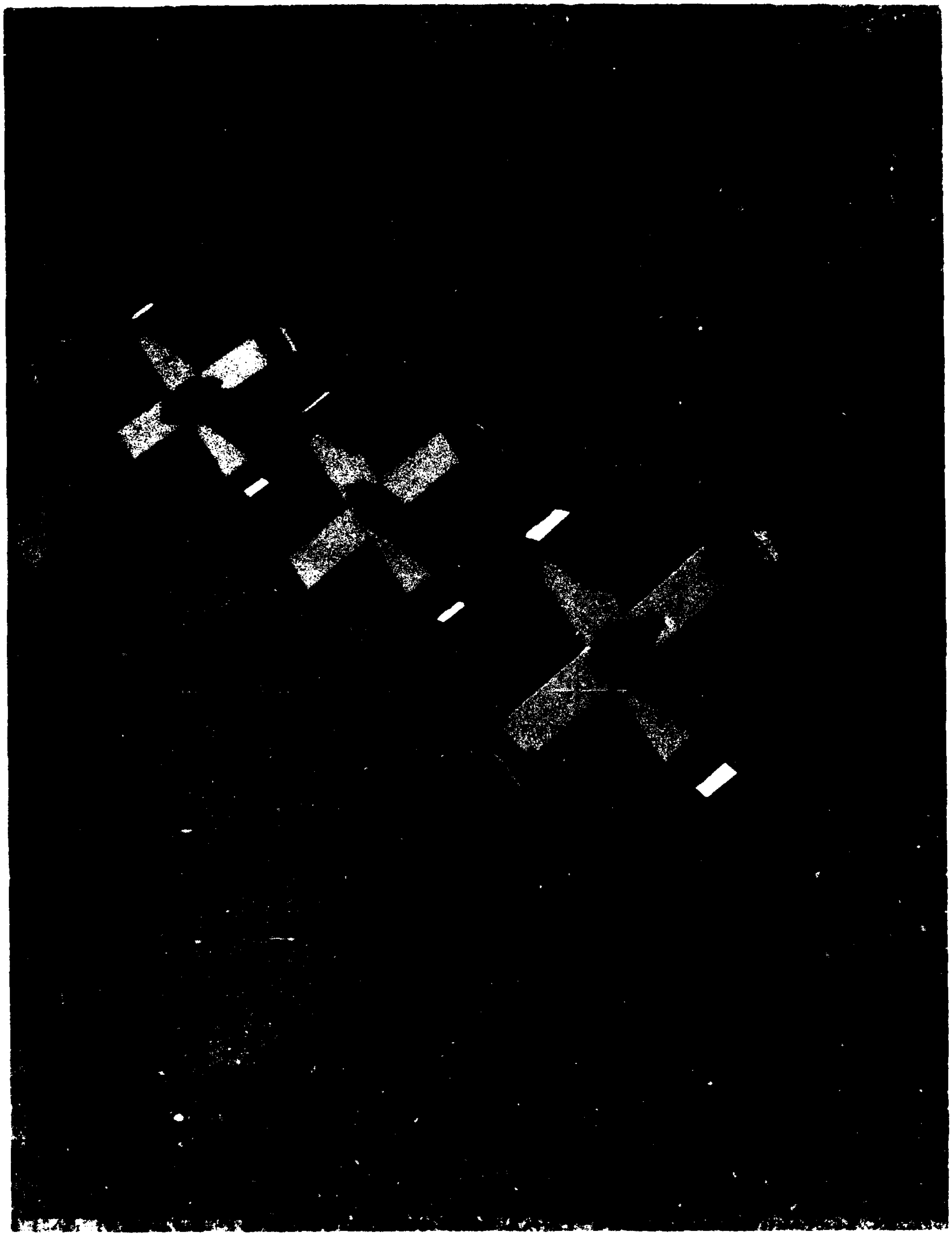

FIGURE 16. Centering Mount for PRIMACORD

FIGURE 17. Post-Shot, View Along 0^{o} Line, Shot 4

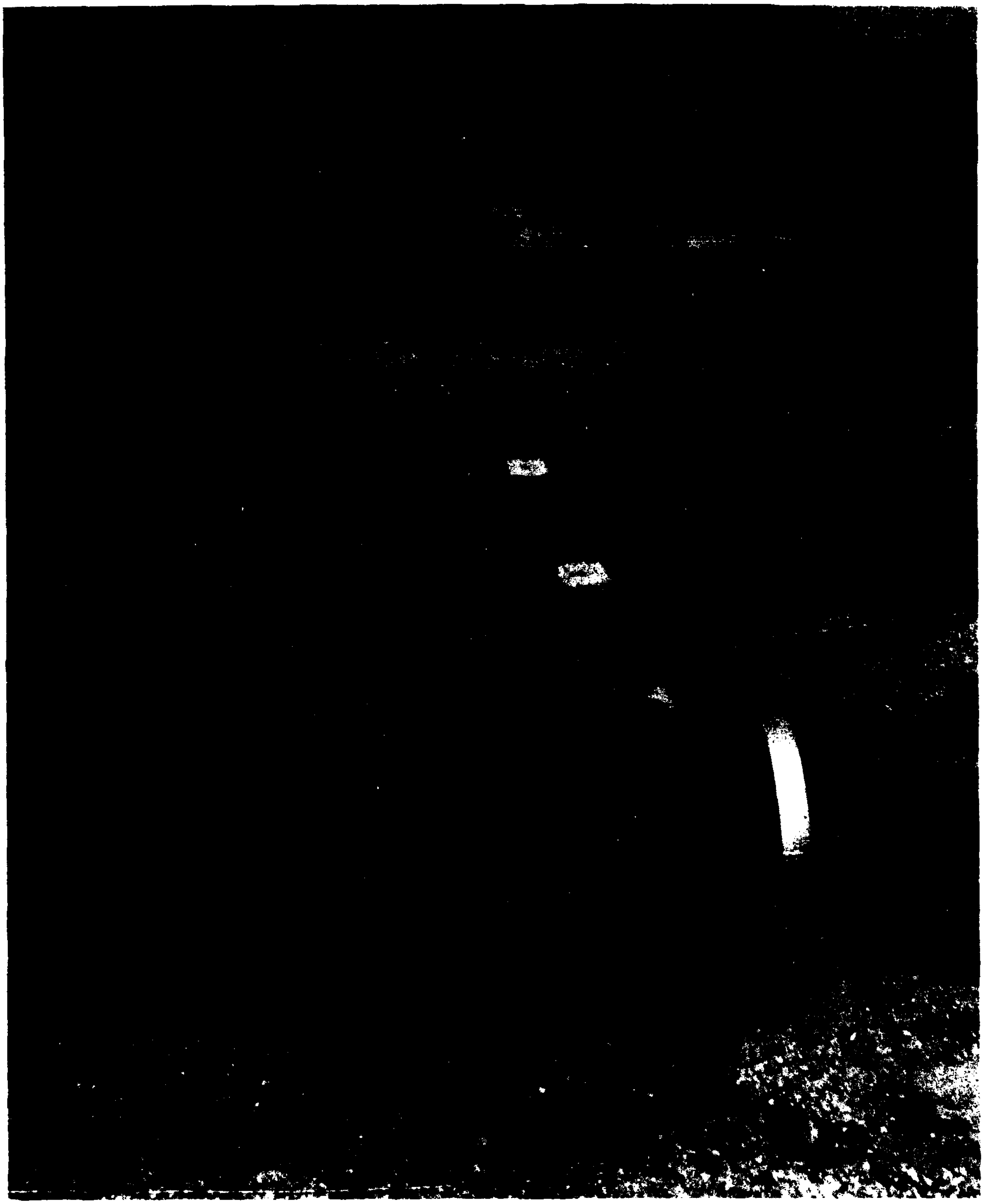

FIGURE 18. Post-Shot, View Along 90° Line, Shot 4

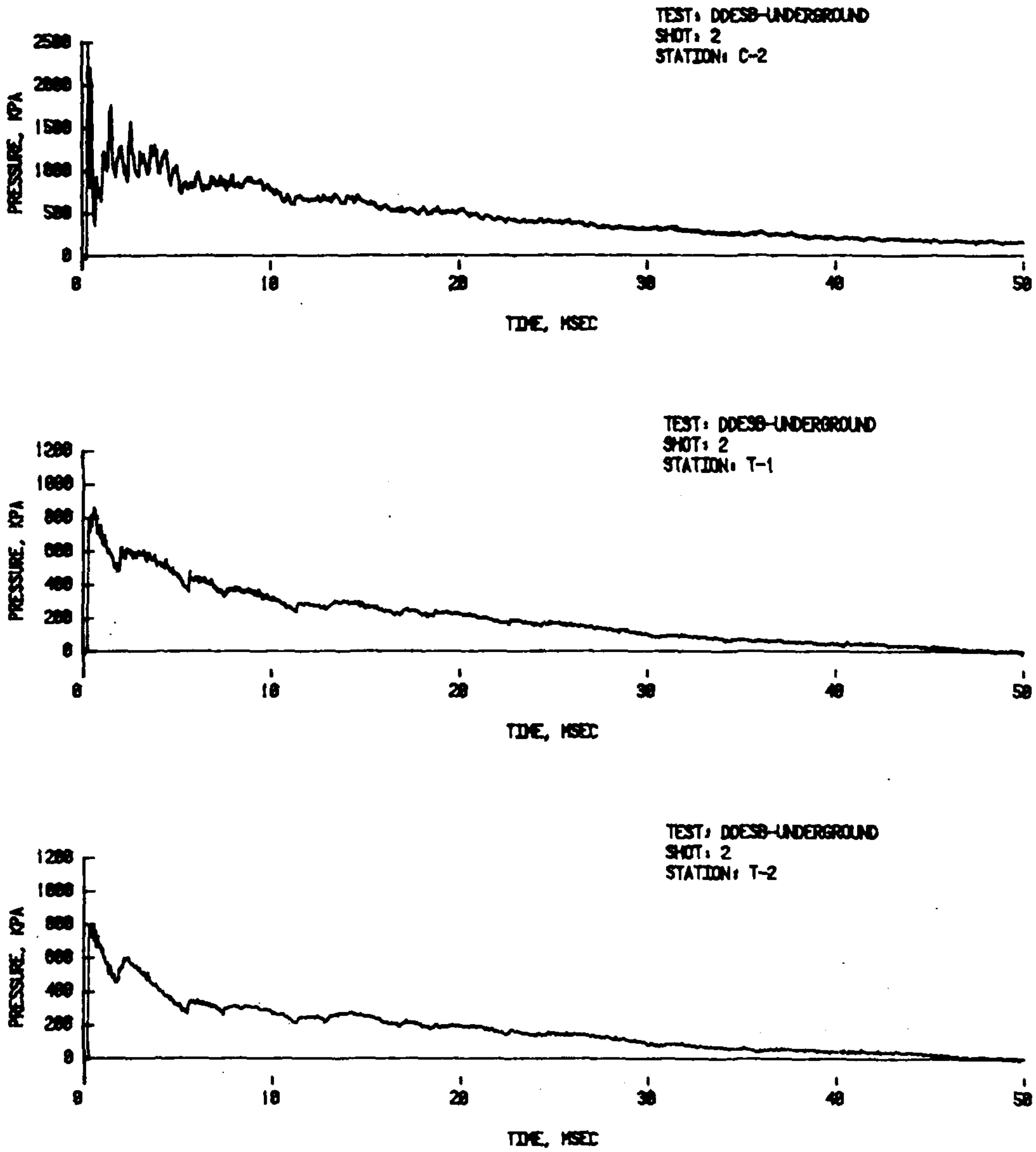

FIGURE 19. Pressure-Time Records From Field Test

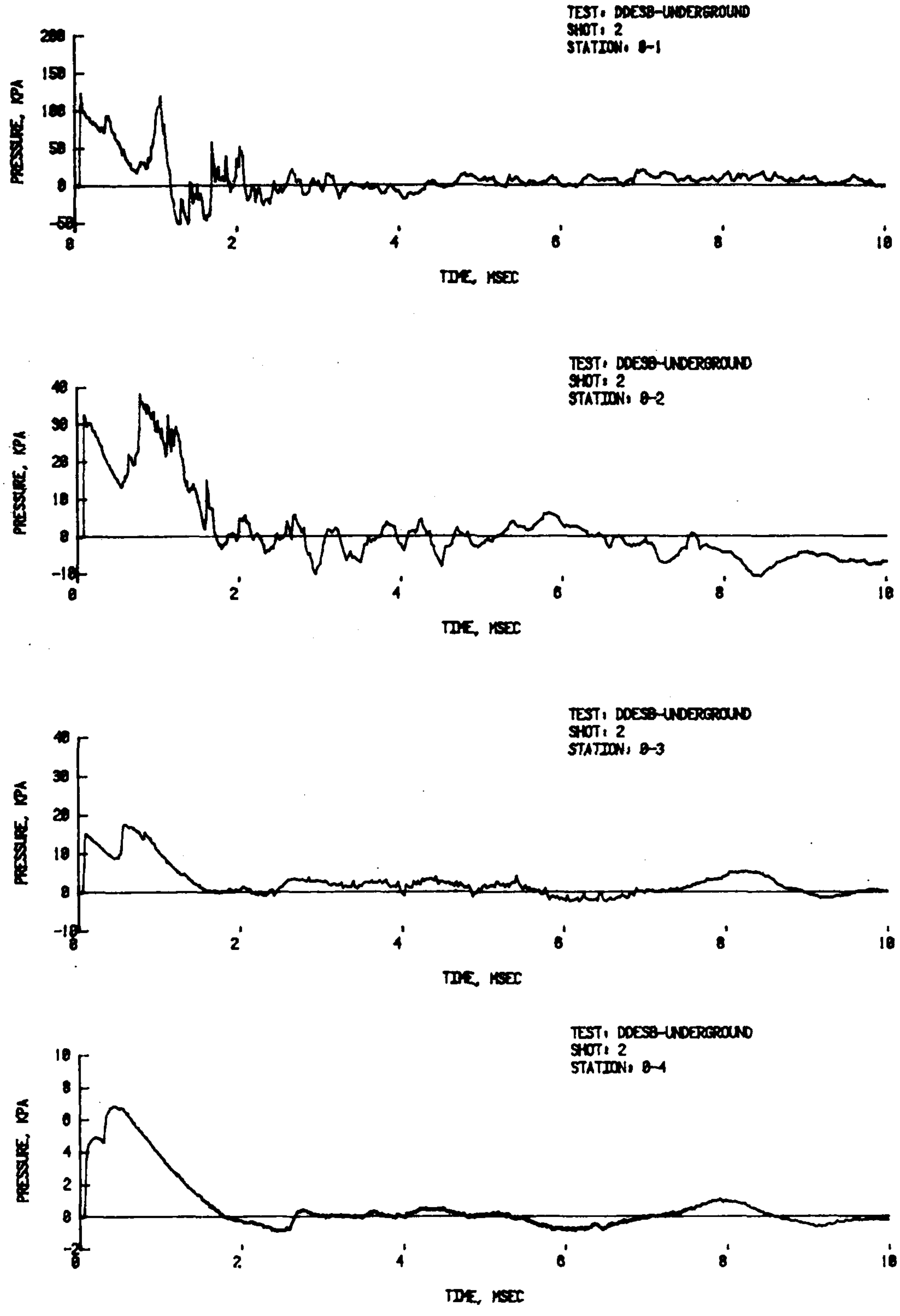

FIGURE 19. Pressure-Time Records From Field Test (Cont)

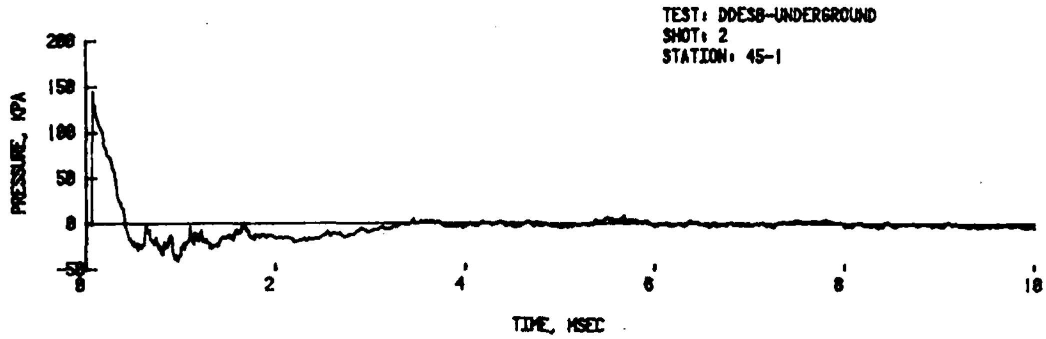

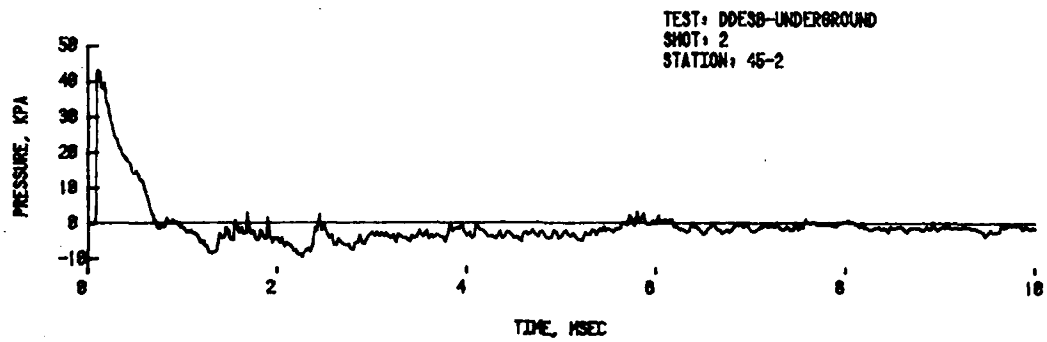

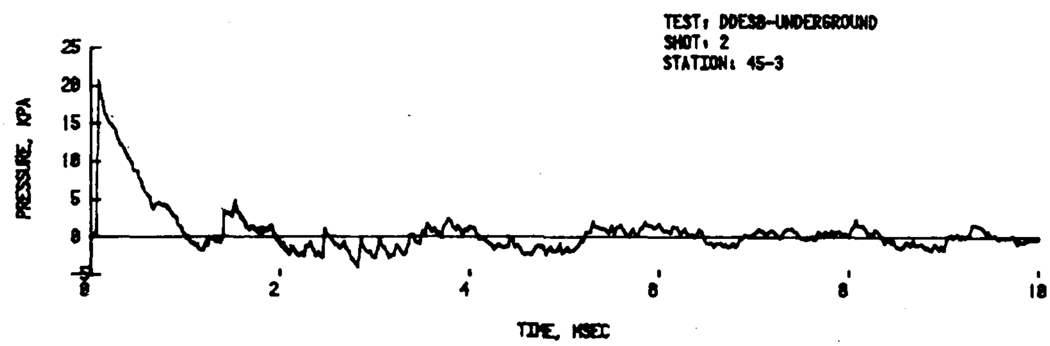

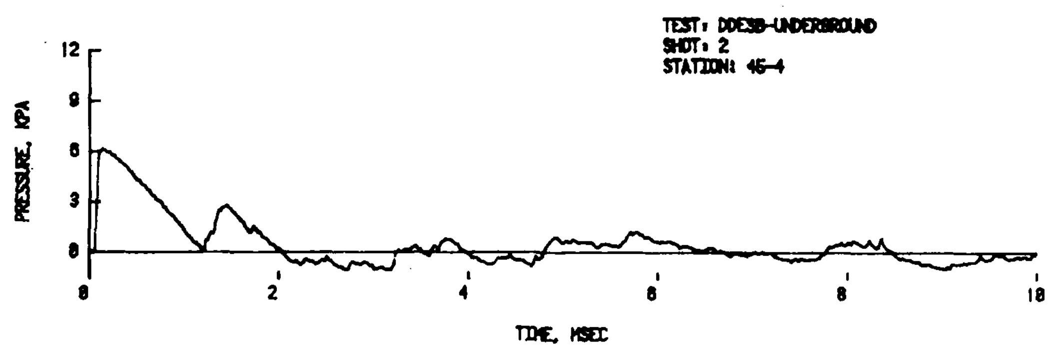

FIGURE 19. Pressure-Time Records From Field Test (Cont)

STATION: 90-1

NO RECORD

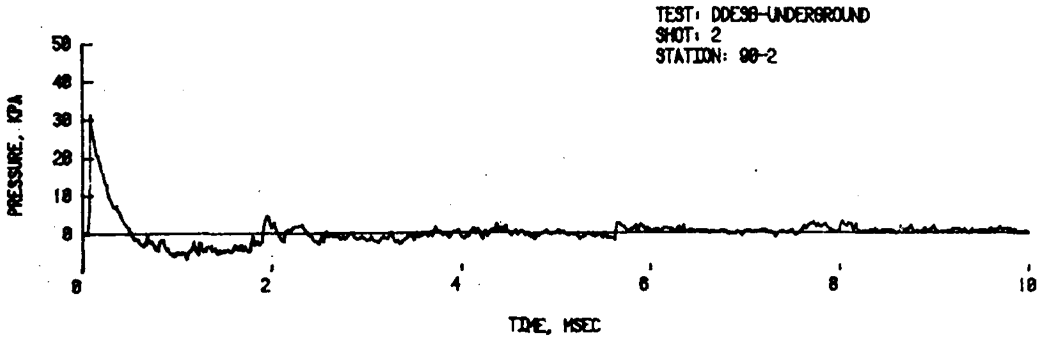

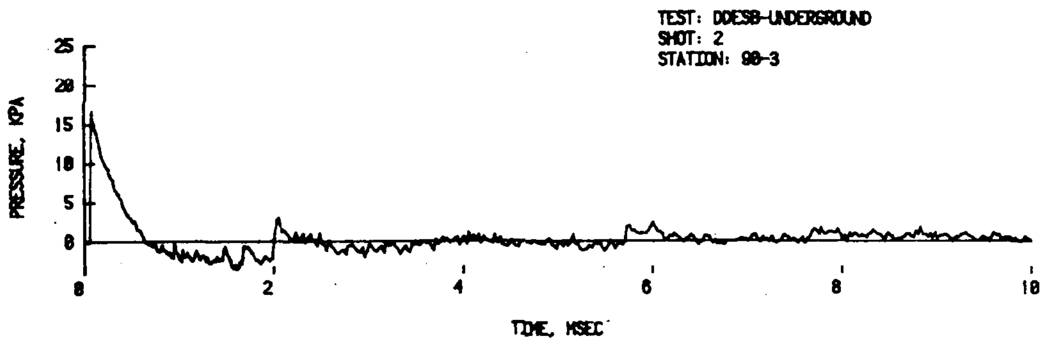

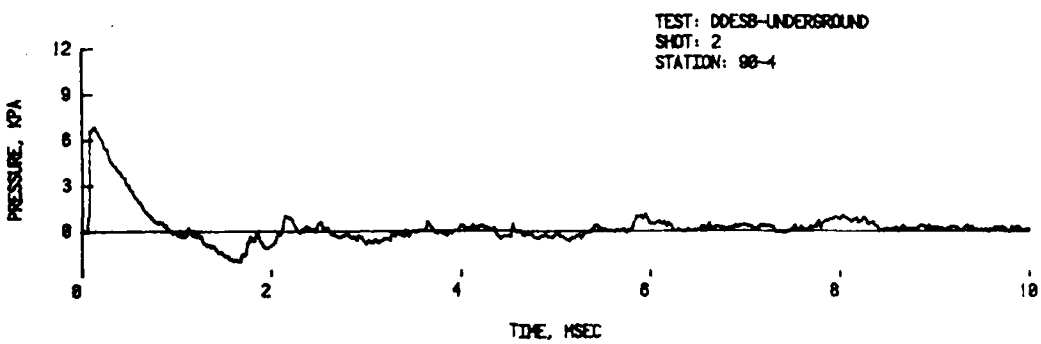

FIGURE 19. Pressure-Time Records From Field Test (Cont)

STATIONS: 135-1, AND 135-2

NO RECORDS

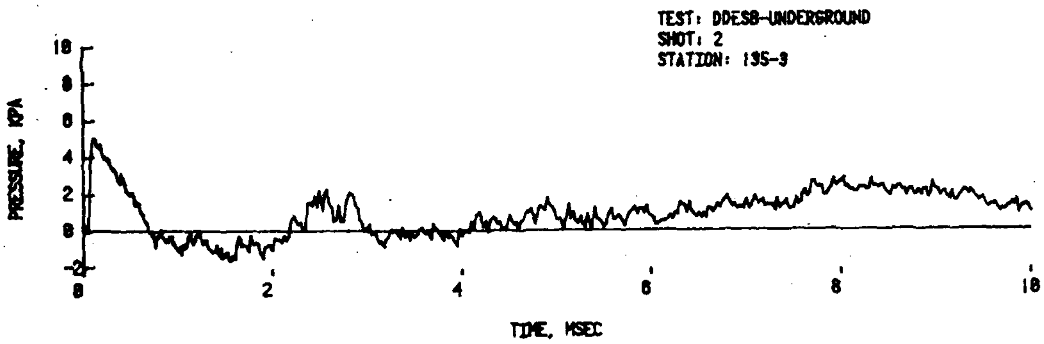

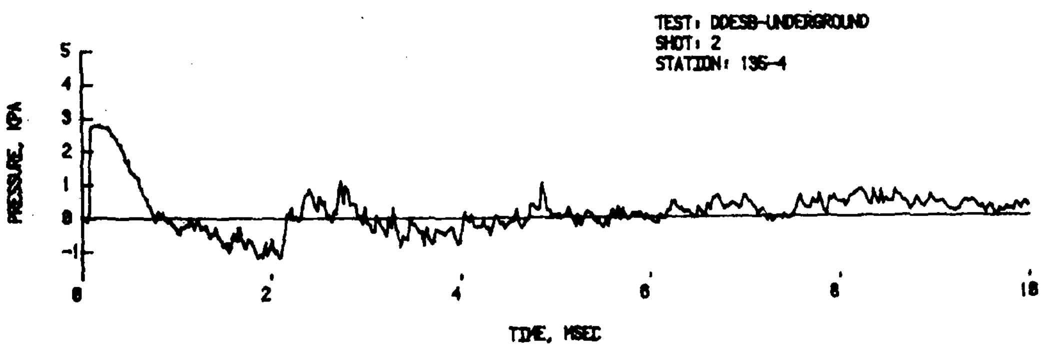

FIGURE 19. Pressure-Time Records From Field Test (Cont)

TABLE 2. Field Test Results

Shot No.	Station	ΔP,kPa	R,m	R/D_T**	$\Delta P/P_W$	Remarks
1	C-1	--	--	--	--	
	C-2	807/1551 (827*)	--	--	--	Q=0.03320 kg, PETN***
	T-1	538/676	--	--	--	Q/V_c=0.3562 kg/m^3
	T-2	(P_W)475/ 627	--	--	--	Q/V_t=0.2912 kg/m^3
	0-1	90/175	0.465	4.58	0.190	
	0-2	35.2/50.3	1.011	9.95	0.074	P_1=102.2 kPa
	0-3	31.0	1.725	16.98	0.065	
	0-4	9.9	3.240	31.89	0.021	T_1=20.0°C
	45-1	--	0.321	3.16	--	
	45-2	44.1/49.0	0.699	6.88	0.093	
	45-3	21.7/24.5	1.193	11.74	0.046	
	45-4	11.4	2.241	22.06	0.024	
	90-1	--	0.181	1.78	--	
	90-2	33.2	0.393	3.87	0.070	
	90-3	15.9	0.671	6.60	0.033	
	90-4	7.2	1.260	12.40	0.015	
	135-1	--	0.112	1.10	--	
	135-2	--	0.244	2.40	--	
	135-3	--	0.417	4.10	--	
	135-4	3.38	0.783	7.71	0.0071	

*INBLAST Calculation, 827 kPa
**Tunnel Diameter, D_T = 0.1016 m
***Explosive in this shot was centered at the rear half of the driver chamber.

TABLE 2. Field Test Results (Cont)

Shot No.	Station	P,kPa	R,m	R/D_T	P/P_W	Remarks
2	C-1	1379	--	--	--	
	C-2	2500/1127 (1380*)	--	--	--	Q=0.6337 kg, PETN
	T-1	821	--	--	--	
	T-2	(P_W)765	--	--	--	Q/V_c=0.681 kg/m^3
	0-1	123	0.702	6.91	0.16	
	0-2	33.1/35.9	1.529	15.05	0.043	Q/V_t=0.556 kg/m^3
	0-3	15.4/17.6	2.614	25.73	0.020	
	0-4	4.90/6.86	4.893	48.16	0.0064	P_1=101.8 kPa
	45-1	145	0.486	4.78	0.19	T_1=32.2°C
	45-2	43.1	1.057	10.40	0.056	
	45-3	20.9	1.808	17.80	0.027	
	45-4	6.14	3.384	33.31	0.0080	
	90-1	--	0.273	2.69	--	
	90-2	31.4	0.594	5.85	0.041	
	90-3	16.8	1.022	10.06	0.022	
	90-4	6.89	1.903	18.73	0.0090	
	135-1	--	0.170	1.67	--	
	135-2	--	0.370	3.64	--	
	135-3	5.03	0.730	7.19	0.0066	
	135-4	2.76	1.183	11.64	0.0036	

*INBLAST value of quasi-static chamber pressure, 1380 kPa.

TABLE 2. Field Test Results (Cont)

Shot No.	Station	ΔP, kPa	R, m	R/D_T	$\Delta P/P_W$	Remarks
3	C-1	--	--	--	--	
	C-2	(2896*)	--	--	--	Q=0.13585 kg PETN
	T-1	1358	--	--	--	
	T-2	(P_W)1103	--	--	--	Q/V_c=1.459 kg/m^3
	0-1	98	1.118	11.00	0.089	Q/V_t=1.192 kg/m^3
	0-2	20.3/31.0	2.430	23.92	0.018	
	0-3	11.7/12.1	4.167	41.01	0.011	P_1=102.2 kPa
	0-4	3.79	7.792	76.69	0.0034	
	45-1	--	0.774	7.62	--	T_1=20.6°C
	45-2	28.8	1.680	16.54	0.026	
	45-3	11.7	2.882	28.37	0.011	
	45-4	4.27	5.389	53.04	0.0039	
	90-1	--	0.441	4.34	--	
	90-2	18.5	0.945	9.30	0.017	
	90-3	10.1	1.621	15.95	0.0092	
	90-4	4.96	3.030	29.82	0.0045	
	135-1	--	0.270	2.66	--	
	135-2	--	0.587	5.78	--	
	135-3	4.69	1.007	9.91	0.0043	
	135-4	2.21	1.884	18.54	0.0020	

*INBLAST calculated value of chamber pressure, 2896 kPa.

TABLE 2. Field Test Results (Cont)

Shot No.	Station	ΔP,kPa	R,m	R/D_T	$\Delta P/P_W$	Remarks
4	C-1	--	--	--	--	
	C-2	(5654*)	--	--	--	Q=0.31697 kg PETN
	T-1	1551/1758	--	--	--	
	T-2	(P_W)1551/ 1606	--	--	--	Q/V_c=3.405 kg/m^3
	0-1	47.6/88.9	1.861	18.30	0.031	Q/V_t=2.780 kg/m^3
	0-2	15.2/25.2	4.044	39.80	0.0098	
	0-3	13.9	6.960	68.50	0.0090	P_1=101.7 kPa
	0-4	4.96	13.014	128.09	0.0032	
	45-1	--	1.286	12.66	--	T_1=26.7°C
	45-2	23.7	2.797	27.53	0.015	
	45-3	10.6	4.814	47.38	0.0068	
	45-4	3.65	9.000	88.58	0.0024	
	90-1	--	0.723	7.12	--	
	90-2	21.0	1.573	15.48	0.014	
	90-3	11.9	2.707	26.64	0.0077	
	90-4	4.76	4.890	48.13	0.0031	
	135-1	--	0.450	4.43	--	
	135-2	7.31	0.978	9.63	0.0047	
	135-3	5.03	1.683	16.56	0.0032	
	135-4	2.28	3.146	30.97	0.0015	

*INBLAST calculation of chamber pressure, 5654 kPa.

TABLE 2. Field Test Results (Cont)

Shot No.	Station	ΔP,kPa	R,m	R/D_T	$\Delta P/P_W$	Remarks
5	C-1	--	--	--	--	
	C-2	(6540*)	--	--	--	Q=0.3670 kg, C-4
	T-1	4137	--	--	--	
	T-2	(P_W)4137	--	--	--	Q/V_c=3.942 kg/m^3
	0-1	150	1.861	18.30	0.036	Q/V_t=3.219 kg/m^3
	0-2	18.9/24.7	4.044	39.80	0.0046	
	0-3	8.89/11.7	6.960	68.50	0.0022	P_1=102.1 kPa
	0-4	--	13.014	128.09	--	
	45-1	136.2	1.286	12.66	0.033	T_1=23.3°C
	45-2	27.6	2.797	27.53	0.0067	
	45-3	11.7	4.814	47.38	0.0028	
	45-4	4.41	9.000	88.58	0.0011	
	90-1	--	0.723	7.12	--	
	90-2	37.9	1.573	15.48	0.0092	
	90-3	17.9	2.707	26.64	0.0043	
	90-4	7.17	4.890	48.13	0.0017	
	135-1	--	0.450	4.43	--	
	135-2	18.6	0.978	9.63	0.0045	
	135-3	11.8	1.683	16.56	0.0029	
	135-4	3.59/4.34	3.146	30.97	0.0087	

*INBLAST calculation of chamber pressure, 6540 kPa.

4. ANALYSIS

Modifications are shown for INBLAST where predictions are compared to shock tube experiments and model chamber/tunnel PETN and C-4 explosive field data.

4.1 Modification of INBLAST. INBLAST was developed at the Naval Ordnance Laboratory (NOL) to describe the shock and blast loading characteristics of detonation of a high explosive internal to a structure. Documentation of the code can be found in Reference 2.

In the application to underground explosions of stored munitions, INBLAST was used to predict the confined-explosion gas pressure in the storage chamber. One modification included an addition of shock tube equations with area change.[6] A second modification used the BRL-Q1D hydrocode.[7] If the exit tunnel of the underground storage facility is short (<35 tunnel diameters), is relatively smooth, and the tunnel length of about the same magnitude as the storage chamber length, then the relatively simple algebraic expressions from the shock tube theory can be used. This modification works in the following way.

The INBLAST program computes the maximum internal gas pressure in the storage chamber for detonation of the given stored munitions. The computed chamber pressure is assumed to be the same as a shock tube driver gas of the magnitude computed. The shock tube equations are then solved by iteration procedures. It is assumed that the internal gas pressure would force the chamber doors open analagous to the shock tube diaphragm breaking. The equations needed are listed below from Reference 6:

$$\frac{gP_{41}}{P_{21}} = \left[1 - \frac{(\gamma_4 - 1)\, U_{21}}{2\, A_{41}} (g)^{-\frac{\gamma_4 - 1}{2\gamma_4}}\right]^{-\frac{2\gamma_4}{\gamma_4 - 1}} \qquad (1)$$

$$g = \left[\frac{2 + (\gamma_4 - 1)\, M_5^2}{2 + (\gamma_4 - 1)\, M_e^2}\right]^{\frac{\gamma_4}{\gamma_4 - 1}} \left[\frac{2 + (\gamma_4 - 1)\, M_e}{2 + (\gamma_4 - 1)\, M_5}\right]^{\frac{2\gamma_4}{\gamma_4 - 1}} \qquad (2)$$

$$M_5 \frac{S_4}{S_1} = M_e \left[\frac{2 + (\gamma_4 - 1)\, M_5^2}{2 + (\gamma_4 - 1)\, M_e^2}\right]^{\frac{\gamma_4 + 1}{2(\gamma_4 - 1)}} \qquad (3)$$

$$M_3 = \frac{U_{21}}{A_{41}\,(g)^{\frac{\gamma_4 - 1}{2\gamma_4}} - \frac{\gamma_4 - 1}{2}\,U_{21}} \qquad (4)$$

$$U_{21} = \frac{P_{21} - 1}{\gamma_1\left[\left(\frac{\gamma_1 - 1}{2\gamma_1}\right)\left(\frac{\gamma_1 + 1}{\gamma_1 - 1}\,P_{21} + 1\right)\right]^{\frac{1}{2}}} \qquad (5)$$

Given parameters from the INBLAST calculations are the chamber pressure ratio P_{41}, chamber sound speed ratio A_{41}, ratio of specific heats for chamber, γ_4, and ambient air, γ_1. Given also is S_4/S_1, the chamber cross-section area to tunnel cross-section area ratio. For the case of most interest for strong shocks, the mach number $M_e=1$, at the chamber/tunnel area change and the factor g depends only on S_4/S_1 and γ_4.

Equation 3 is solved for M_5 by an iterative procedure on both sides of the equation. Equation 2 is then solved for g after substituting the value of M_5 found in Equation 3 along with γ_4. Substitute U_{21}, the shock pressure ratio P_{21}, and the shock overpressure P_w, where:

$$P_W = P_1(P_{21} - 1) \qquad (6)$$

This is the pressure at the tunnel exit when the blast wave attenuation along the tunnel can be ignored.

If a decaying blast wave should occur because of short chamber/long tunnel configuration or attenuation, by baffles for example, then a hydrocode may be coupled to the INBLAST program to take into account the additional effects. This may be done, for example, with the BRL-Q1D[7] code.

Predictions from the modified INBLAST/shock tube method and a method obtained from fitting published field data[8] will be compared with data from the present work. Table 3 and Figure 20 show the comparisons of three prediction methods for predicting P_W, along with the measured values obtained in the shock tube experiment.

TABLE 3. Comparison of Smooth Wall Shock Tube Results With Predictions

Shot No.	Simulated Charge-TNT Q,kg	Charge Density Q/V_c,kg/m^3	Q/V_t,kg/m^3	Chamber* Pressure P_c,kPa	Area Ratio A_J/A_c	Exit Tunnel Pressure P_W,kPa: Ref. 1	Ref. 8	INBLAST/Shock Tube	Exp. St 25
5	0.0185	0.196	0.137	814	0.16	348	256	538	439
4	0.0424	0.450	0.315	1448	0.16	611	424	779	660
6	0.160	1.70	1.188	2696	0.16	1010	948	1028	1006
7	0.424	4.50	3.148	5454	0.16	1694	1683	1566	1560

*NOTES: 1) Results in bars have been changed to kPa: 1 bar equals 100 kPa.

2) Ambient pressure, P_1 = 102.73 kPa.

A_c - Chamber cross-section area, m^2.

A_j - Tunnel cross-section area, m^2.

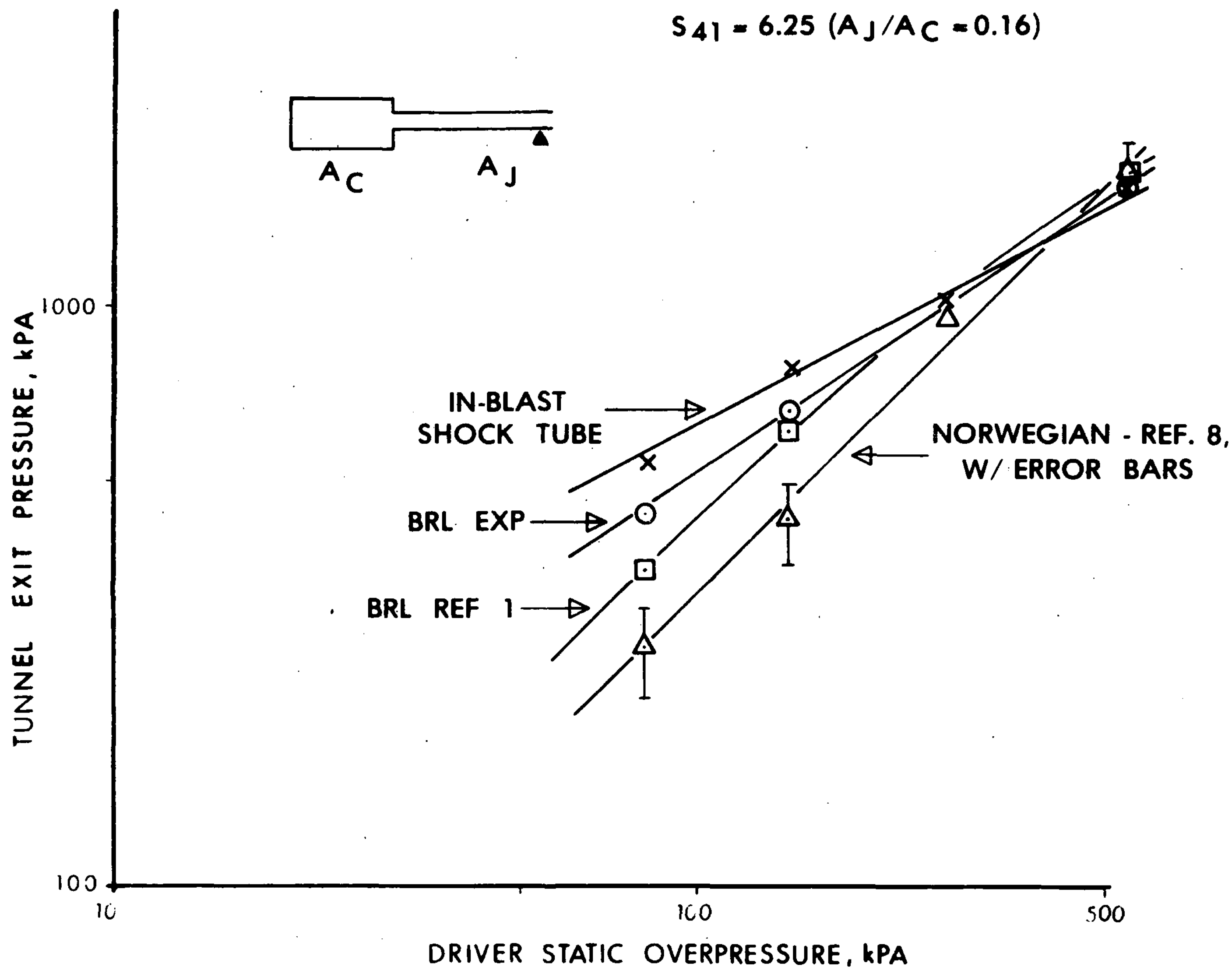

FIGURE 20. Comparison of Prediction Methods for Tunnel Exit Pressure

It is seen that at three lower loading densities, the INBLAST/shock tube method overpredicts the tunnel exit pressure, P_W. At the three larger loading densities, the shock tube experimental value compares well with the BRL equation.[1] The Norwegian values[8] are lower than the shock tube experimental results.

The next section shows how these methods may be used to predict the blast at the exit tunnel when the driver pressure is obtained from high explosive.

4.2 Predictions of Blast at Tunnel Exit. Large amounts of data from underground storage model experiments have been used by Norwegian researchers[8] to develop Equation 7 to predict the pressure at the end of the exit tunnel.

$$P_W = 12.1 \left(\frac{Q}{V_t}\right)^{0.607} \left(\frac{A_J}{A_C}\right)^{0.19} . \qquad (7)$$

Here P_W is the blast pressure in bars predicted to arrive at the end of an access tunnel to an underground storage magazine in which an explosion has occurred. The loading density, Q/V_t, is the stored charge, Q, in kilograms for the total volume V_t, m^3; storage chamber plus access tunnel volumes. The tunnel junction cross-section area to chamber cross-section ratio is given as A_J/A_c.

Kingery[1] has developed an equation of the form of Equation 7 to account for different explosives which are not accounted for in Equation 7. The term for charge density has been replaced by the pressure, P_{V_t}, generated by the explosion throughout the total volume, V_t. Equation 8 shows this expression:

$$P_W = 1.1 \left(P_{V_t}\right)^{0.83} \left(\frac{A_J}{A_C}\right)^{0.19} , \qquad (8)$$

where P_W and P_{V_t} are both in bars. Tables or graphs generated by the INBLAST code are used to find P_{V_t} for a given kind of charge and storage configuration modeled. Figure 21 shows three such curves plotted from Reference 9. PETN is plotted to be used in predicting the PRIMACORD pressure and RDX for the C-4 explosive, which is made to 91% RDX.[11] The remaining material in the C-4 is plastic binder. It is assumed that the binder does not contribute to the chamber pressure.

The TNT values are plotted to show the difference in chamber pressure versus loading density between TNT and PETN. This also is the rationale for using the pressure (P_{V_t}) associated with the total volume in Equation 8 rather than the loading density (Q/V_t) within the total volume in Equation 7.

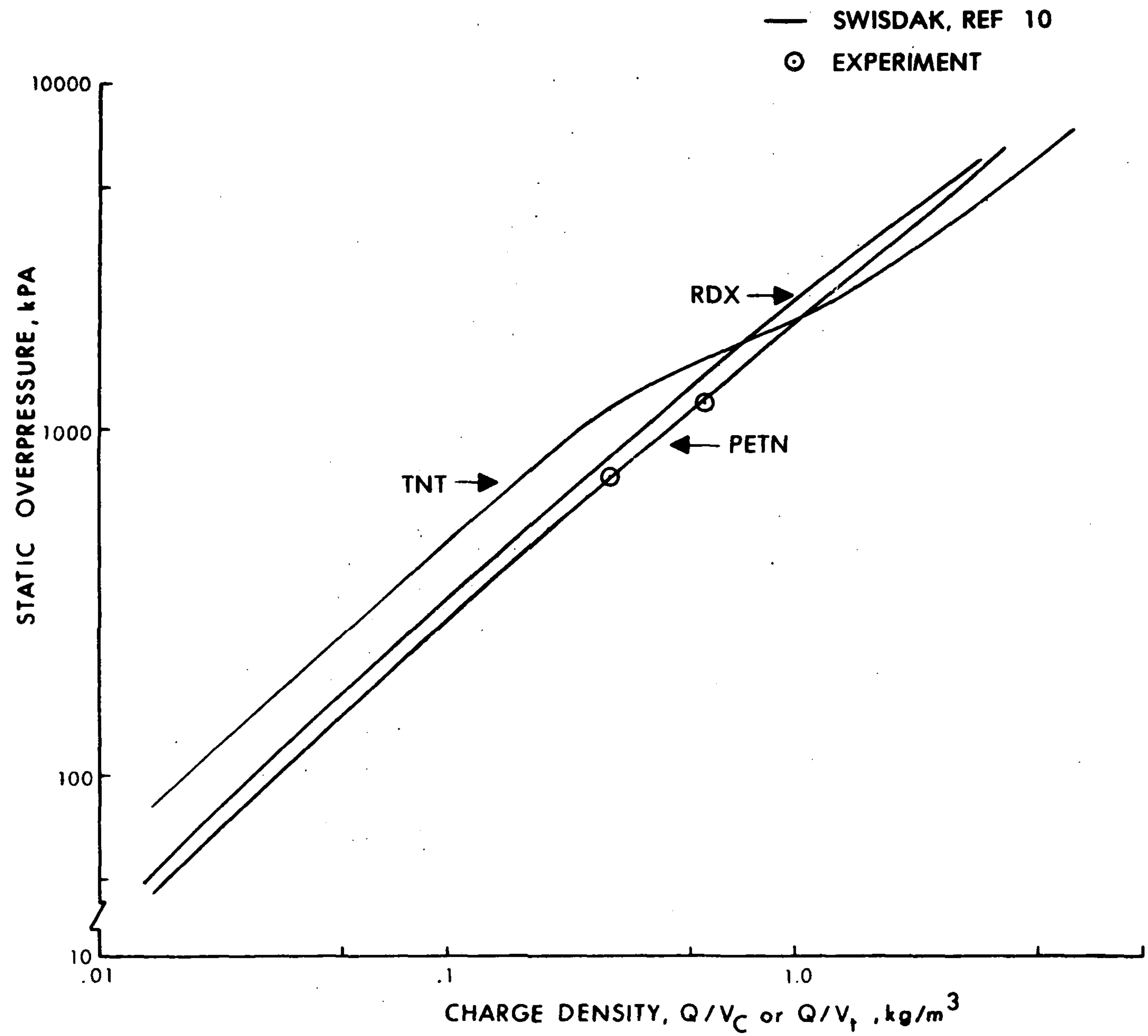

FIGURE 21. Static Overpressure as a Function of Loading Density from Explosives in Confined Spaces

The experimental environment inside the chamber was quite harsh for the transducers; several were broken during the test series. Few data were obtained there except for Shots 1 and 2. The two values listed in Table 2 are shown as the two experimental points plotted in Figure 21.

Figure 21 provides the total volume storage chamber pressure (P_{V_t}) for Equation 8 to calculate P_W. Results from the two methods for predicting P_W (Equations 7 and 8) are listed in Table 4 along with the measured values from Table 2. The values from Table 4 are plotted in Figure 22 to show this comparison. The scatter in the measured data and the predicted data is reasonable with the exception of the C-4 test (Shot 5). If the record in Appendix A from the tunnel transducer at Station T-2 is examined, it can be seen that the latter portion of the record is in question but the initial portion of the record has a faster decay from the peak value than the record from Station T-2 on Shot 4. It is surmised that a large reflection of the blast wave from the centered C-4 explosive may have propagated to the tunnel exit as measured at Station T-2. Whereas in the earlier tests, the PRIMACORD explosive was stretched along the center line of the storage chamber giving a slower decaying wave at the exit. The first station (0-1) along the outside blast line also recorded a higher than expected peak overpressure, but it also had a very rapid decay in pressure versus time from the peak value.

The next section will discuss the free-field records and compare them with predictions.

4.3 <u>Predictions of Blast Outside Tunnel</u>. After the exit pressure, P_W, is calculated for the end of the tunnel, the free-field blast pressure may be calculated from Equation 9. This is a variation of the equation given in Reference 10.

$$\Delta P/P_W = 1.24\ (R/D_t)^{-1.35}/(1 + (\theta/56)^2), \qquad (9)$$

where $\Delta P/P_W$ is the free-field blast pressure to exit pressure ratio found at a radial distance to tunnel diameter ratio R/D_t and angle θ in degrees from the tunnel exit. The field experiments were designed to find distances at which certain key free-field blast overpressure would be predicted. Equation 9 may be rearranged to give the distances for the required pressure levels. Equations 10 and 11 show two such useful forms.

$$R_o = 1.173\ D_t\ (\Delta P/P_W)^{-0.74} \quad (10)$$

and $R = R_o\ A_F$, where A_F (11)

is the angle correction factor $(1 + (\theta/56)^2)^{-0.74}$ applied to the zero radial from the tunnel exit.

For example, the present field tests were designed to give predictions of distances to obtain overpressures of 68.94 kPa (10psi), 24.13 kPa (3.5psi), 11.72 kPa (1.7psi), and 5.00 kPa (0.725psi). Radial lines at 0°, 45°, 90°, and 135° were used to predict each of the distances of interest. The predictions are compared to the free-field data from the experiments as listed in Table 5. Graphically, the comparison may be seen in the normalized plots of Figures 23-26. It should be noted that for the loading densities and explosives used for these experiments, References 1 and 10 predict almost the same values of pressure for the free field. No distinction has been made in the predictions here (see Equation 10).

The data are generally higher than predicted for the 0°, 45°, and 90° lines. The exception is the 135° line where all the data fall below the predictions. Two reasons may be given for the higher values on the first three radials. If the experimental P_W is lower than predicted, then the pressure ratio is too large. Or, if the value of ΔP is too large because a double pressure peak has caught up at a particular station, then the pressure ratio will again be too large. This appears to be a functi[illegible] of the interior charge distributions and/or the detonation within the storage chamber for the model used. A variation in free-field pressure of a factor of two may, therefore, be expected.

The low data values for the 135° line occur probably because of the particular configuration of sand bags used for topography at the tunnel exit. Other, less restricted tunnel exits might give higher values of pressure along the 135° line, more nearly the values predicted.

Predictions for the pressure-time and impulse-time records at each of the four stations along the 0° line from our simulation model are shown in Appendix B. A comparison of these impulse curves, over the chamber charge loading density range of 0.36 - 3.9 kg/m^3 does not show enough change in total impulse to justify establishing free-field prediction equations for this range to account for larger loading densities.

TABLE 4. Comparison of Field Test Results With Predictions

Shot No.*	Q, kg	Q/V_c, kg/m^3	Q/V_t, kg/m^3	P_{V_t}, kPa	A_J/A_c	P_W, kPa Eq. 7	P_W, kPa Eq. 8	P_W, kPa Exp.
1	0.0332	0.356	0.291	710	0.16	404	395	475
2	0.0634	0.680	0.556	1200	0.16	598	611	765
3	0.1359	1.458	1.192	2300	0.16	950	1048	1103
4	0.3170	3.401	2.780	4700	0.16	1589	1897	1551
5	0.3670	3.938	3.219	5700	0.16	1737	2226	4100

*Tests 1, 2, 3, and 4 are with PRIMACORD.
Test 5 is with C-4.

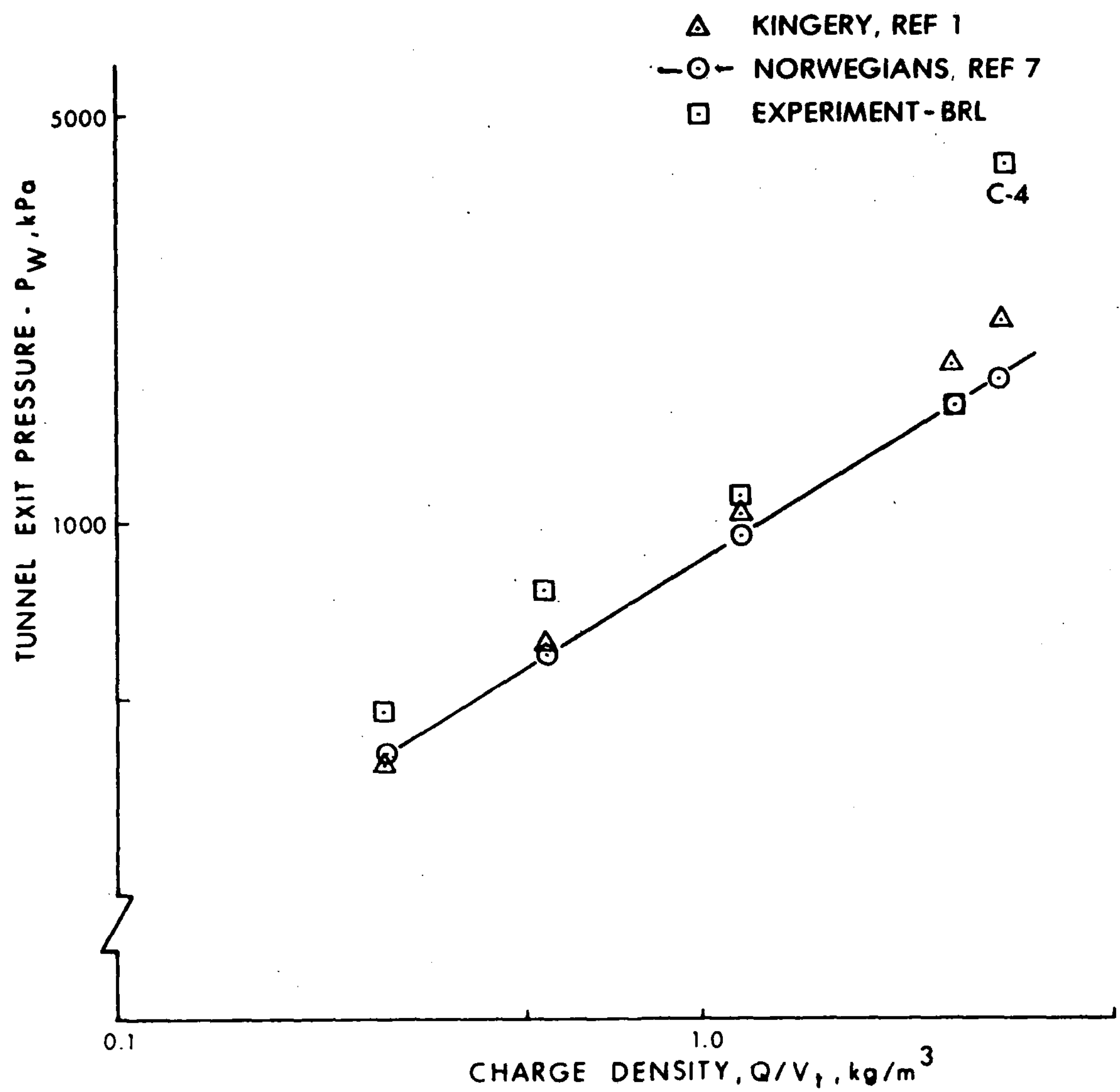

FIGURE 22. Tunnel Exit Pressure as a Function of Charge Density

TABLE 5. Comparison of Free-Field Overpressures

Station	Shot 1	Shot 2	Shot 3	Shot 4	Shot 5
			Pressure, kPa		
0-1		123	98	47.6/88.9*	150
0-2	35.2/50.3	33.1/35.9	20.3/31.0	15.2/25.2	18.9/24.7
0-3	31.0	15.4/17.6	11.7/12.1	13.9	8.9/11.7
0-4	9.9	4.9/6.9	3.79	4.96	--
45-1	--	145	--	--	136
45-2	44.1/49.0	43.1	28.8	23.7	27.6
45-3	21.7/24.5	20.9	11.7	10.6	11.7
45-4	11.4	6.1	4.27	3.65	4.41
90-1	--	--	--	--	--
90-2	33.2	31.4	18.5	21.0	37.9
90-3	15.9	16.8	10.1	11.9	17.9
90-4	7.2	6.9	4.96	4.76	7.2
135-1	--	--	--	--	--
135-2	--	--	--	7.31	18.6
135-3	--	5.03	4.69	5.03	11.8
135-4	3.38	2.76	2.21	2.28	3.59/4.34

*Second value is given for second peak, if present.

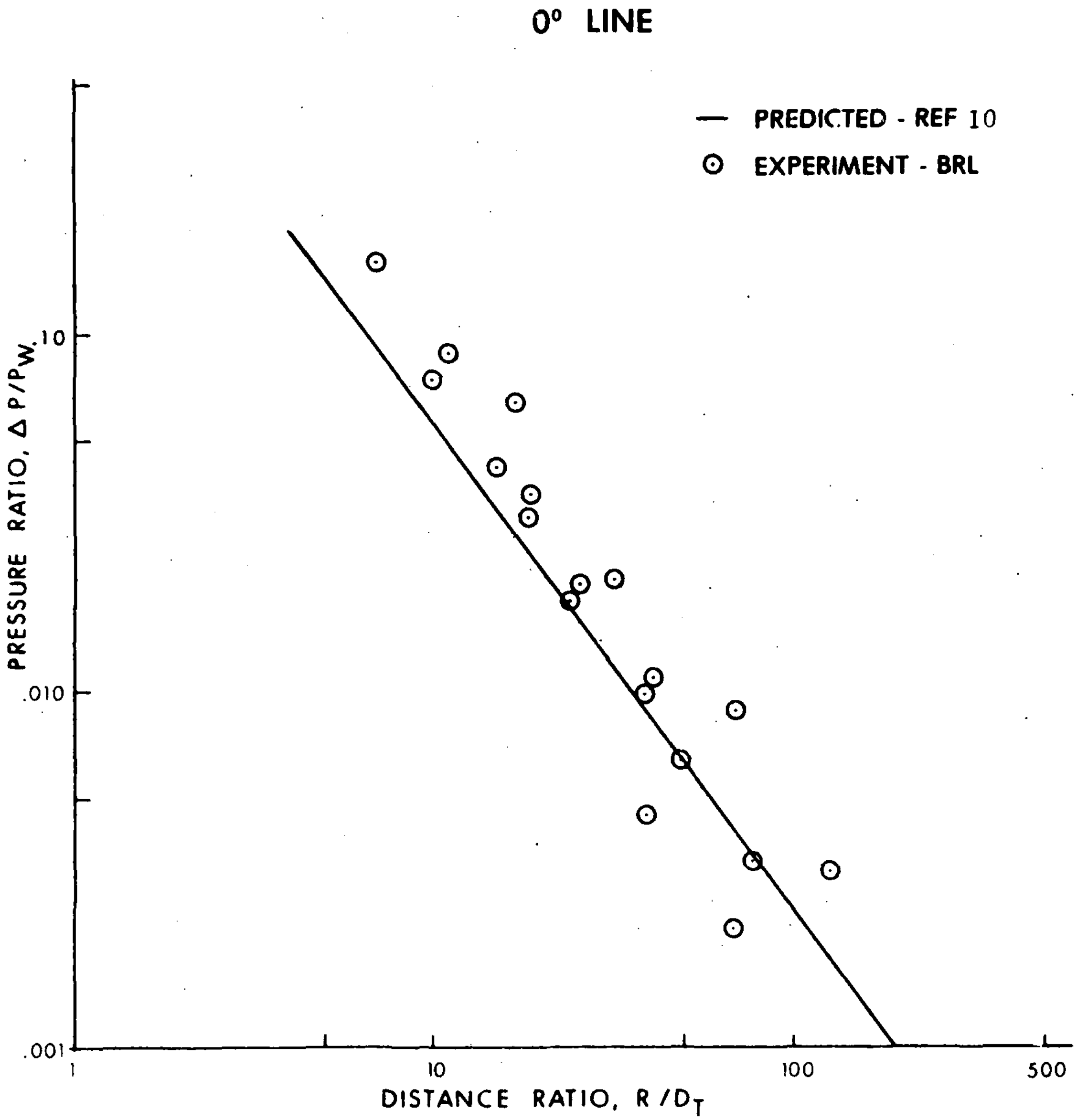

FIGURE 23. Pressure on 0° Line Outside Tunnel

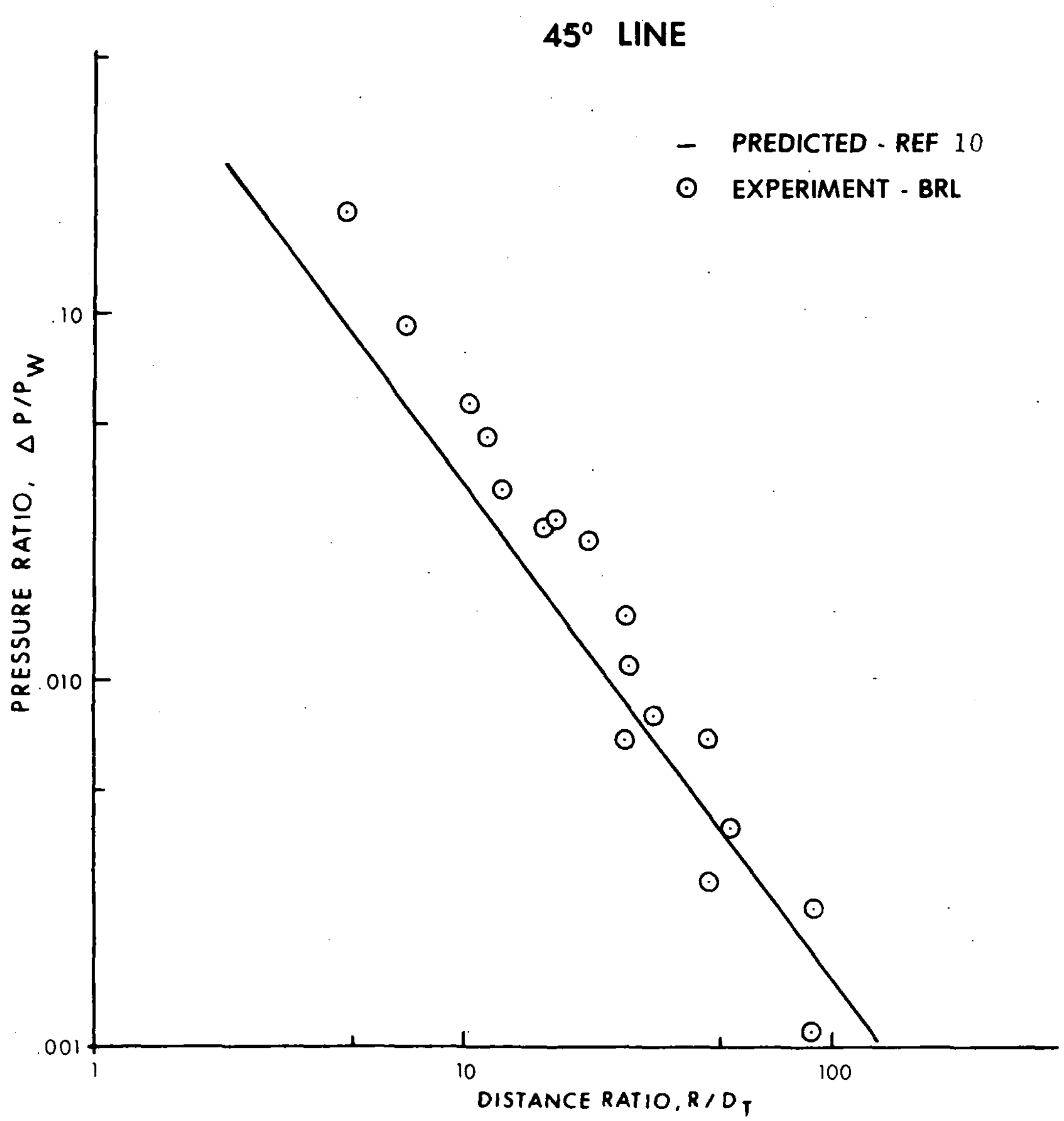

FIGURE 24. Pressure on 45° Line Outside Tunnel

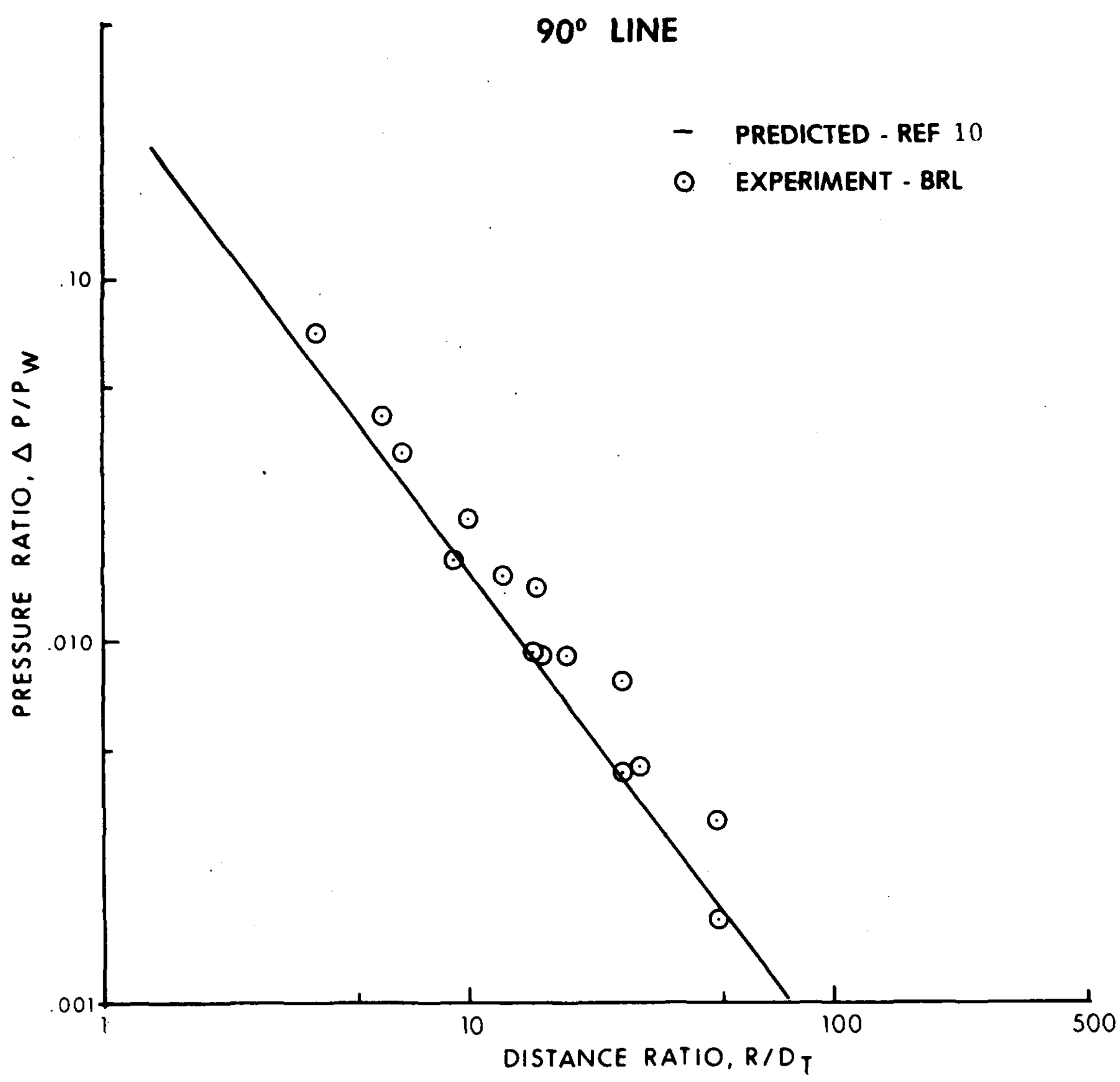

FIGURE 25. Pressure on 90° Line Outside Tunnel

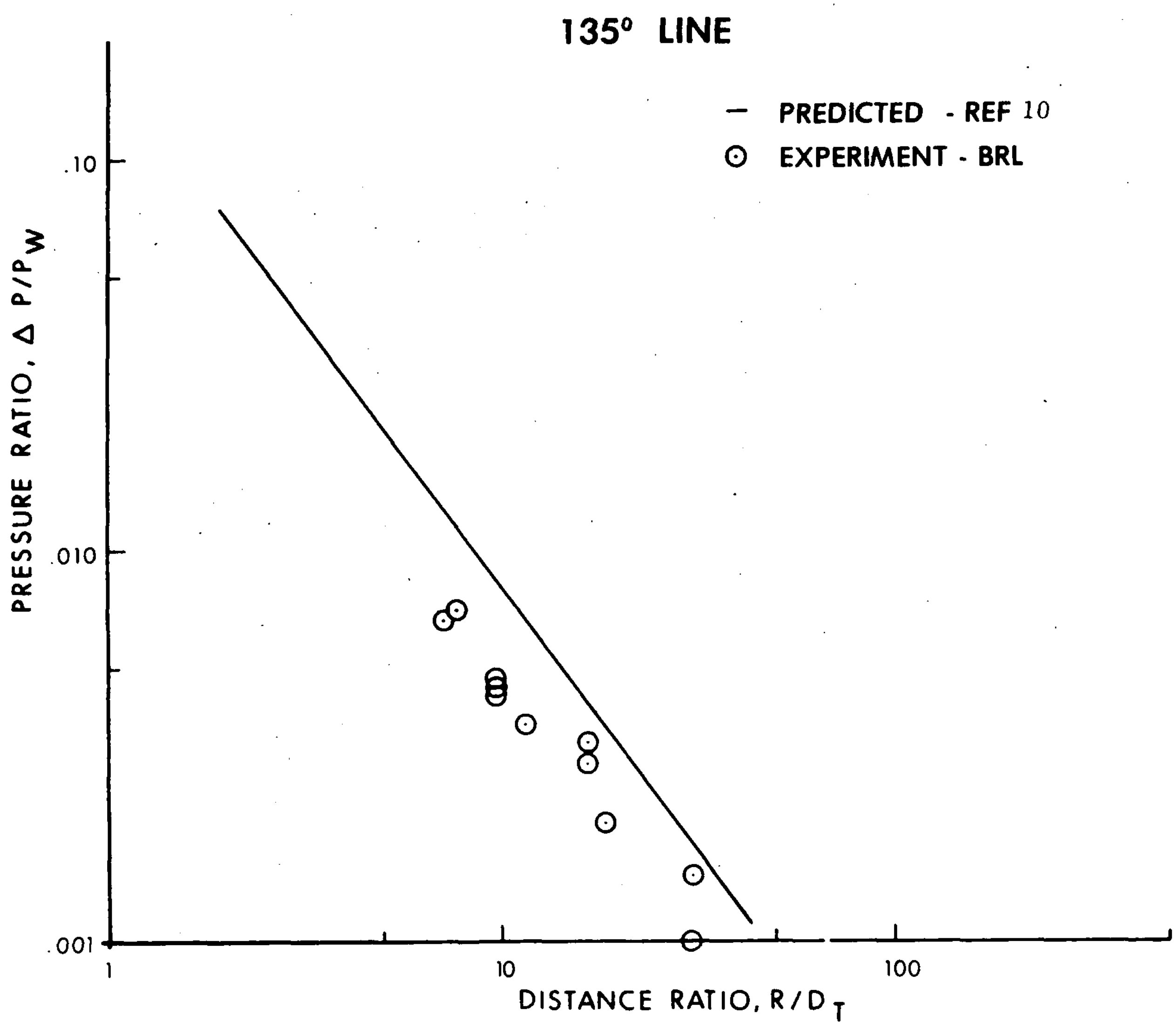

FIGURE 26. Pressure on 135° Line Outside Tunnel

5. SUMMARY AND CONCLUSIONS

Results have been presented from a series of shock tube and field tests which were used to model the blast effects expected from explosions within underground munitions storage facilities. Pressure-time records were obtained and presented for the explosively produced driver pressures within the model storage chamber or driver, within the access tunnel, and over the area outside the tunnel exit. Measurements were obtained on test radials of 0^{o}, 45^{o}, 90^{o}, and 135^{o} - as measured from the long axis of the tunnel - which was taken as 0^{o}.

The shock tube results compared favorably to predictions from a modified INBLAST computer code which included standard shock tube equations with area change. Predictions of the explosive chamber pressures from INBLAST were used to predict access tunnel exit pressures from the methods given by Kingery[1] and Skjeltorp et al.[8]

Generally, the prediction methods used were satisfactory. It should be noted that charge location and charge shape within a given storage chamber hamper accurate predictions of the blast pressure at the exit tunnel. This, in turn, of course, will cause inaccurate predictions for the free-field region outside the tunnel. An uncertainty factor of about two was present in the free-field blast measurements.

A preliminary effort was also made to determine the effect of baffles on attenuation of the blast waves within the access tunnel for the shock tube experiments. It was necessary to add two 50% blocked baffles within the tunnel to attenuate the blast wave approximately 40% over a 20-tunnel diameter's travel. It was felt that probably in many access tunnels it might not be practical to use this amount of baffling due to size limitation. However, if the facility access tunnel is large enough, depending on traffic requirements, then baffling would be useful in attenuating the blast wave within the tunnel. No baffling or rough walls were tried in the tunnel during the field tests due to a time constraint. See References 12-16 for discussion of wall roughness effects on blast waves. This kind of attenuation should be included for rough wall tunnels.

Also, no attempt was made to define the danger zone created by the high speed jet flow following behind the free-field blast wave. It is recommended that further experiments be designed to study this phenomenon.

In conclusion, the INBLAST or similar code may be used to predict the storage chamber pressure from the munitions' explosion. Equations from either Kingery[1] or Skjeltorp et al[8] may be used to predict the tunnel exit blast pressure. The free-field blast pressure outside the exit tunnel may be predicted along desired radials at various distances from equations given by Skjeltorp et al.[10]

It is suggested that for a study of blast attenuation devices or topography, a shock tube model be used first to narrow the choices to those considered to be most useful. The selected attenuation or topography choices might then be built into models of certain specific storage facilities for field testing. Results from the model field tests might then be applied to the full-size storage facilities selected for appraisal.

REFERENCES

1. Kingery, Charles N., "Survey of Airblast Data Related to Underground Munitions Storage Sites," BRL technical report to be published.

2. Proctor, James F., "Internal Blast Damage Mechanisms Computer Program," Naval Ordnance Laboratory Technical Report NCLTR 72-231, 31 August 1972 (AD 759002).

3. "PRIMACORD Detonating Cord Handbook," Ensign Bickford Co., Simsbury, Connecticut 06070, Ninth Printing 1963.

4. "Quartz Sensors," PCB Piezotronics, Inc., Catalog 884, 1984.

5. Kingery, Charles and Coulter, George, "Shock Wave Attenuation by Single Perforated Plates," BRL Memorandum Report BRL-MR-2664, August 1976.

6. Glass, I.I. and Hall, J. Gordon, "Handbook of Supersonic Aerodynamics, Section 18, Shock Tubes," NAVORD Report 1488 (Vol 6), December 1959.

7. Opalka, Klaus O. and Mark, Andrew, "The BRL-Q1D Code: A Tool for the Numerical Simulation of Flows in Shock Tubes With Variable Cross-Sectional Area," BRL Technical Report BRL-TR-2763, October 1986 (A 174254).

8. Skjeltorp, A.T., Hegdahl, T., and Jenssen, A., "Underground Ammunition Storage, Blast Propagation in the Tunnel System, Report IIIA," Norwegian Defence Construction Service Office of Test and Development, Fortifikatorisk Notat Nr. 81/72.

9. Swisdak, M.M., "Explosion Effects and Properties, Part I-Explosions in Air," NWSC-WOL, TR 75-116, October 1975.

10. Skjeltorp, A.T., Jenssen, A., and Rinnan, A., "Blast Propagation Outside a Typical Ammunition Storage Site," Proceedings of the Fifth International Symposium on Military Applications of Blast Simulation, Stockholm, Sweden, May 22-26, 1977.

11. "Explosive Series, Properties of Explosives of Military Interest," U.S. Army Materiel Command (AMC) Pamphlet 706-177, January 1971.

12. Bhargava, Rai Bishesheer Nath, "Experimental Investigation of the Effect of Surface Roughness on Shock Attenuation," Faculty of Pure Science, Columbia University, New York, Ph.D Dissertation, 1956.

13. Kawanmura, Ryuma, and Kawada, Harris, "A Study on the Attenuation of Shock Waves Due to Obstacles in the Passage," Journal of the Physical Society of Japan, 12, 1290-1298, 1957.

REFERENCES (Cont)

14. Porzel, Francis B., "Synopsis of a Theory for Shock Impedance Effects in a Rough Walled Tunnel," IDA/HQ 67-5809 Research Paper, p306, Institute for Defense Analyses, Research and Engineering Support Division, Arlington, VA, May 1967.

15. Coulter, George A., "Attenuation of Shock Waves in Roughened Tunnels," BRL Memorandum Report BRL-MR-1903, January 1968.

16. Skjeltorp, A.T., and Jenssen, A., "One-Dimensional Blast Wave Propagation," 4th International Symposium on Military Applications of Blast Simulations, Southend-on-Sea, England, September 9-12, 1974.

APPENDIX A

PRESSURE-TIME RECORDS

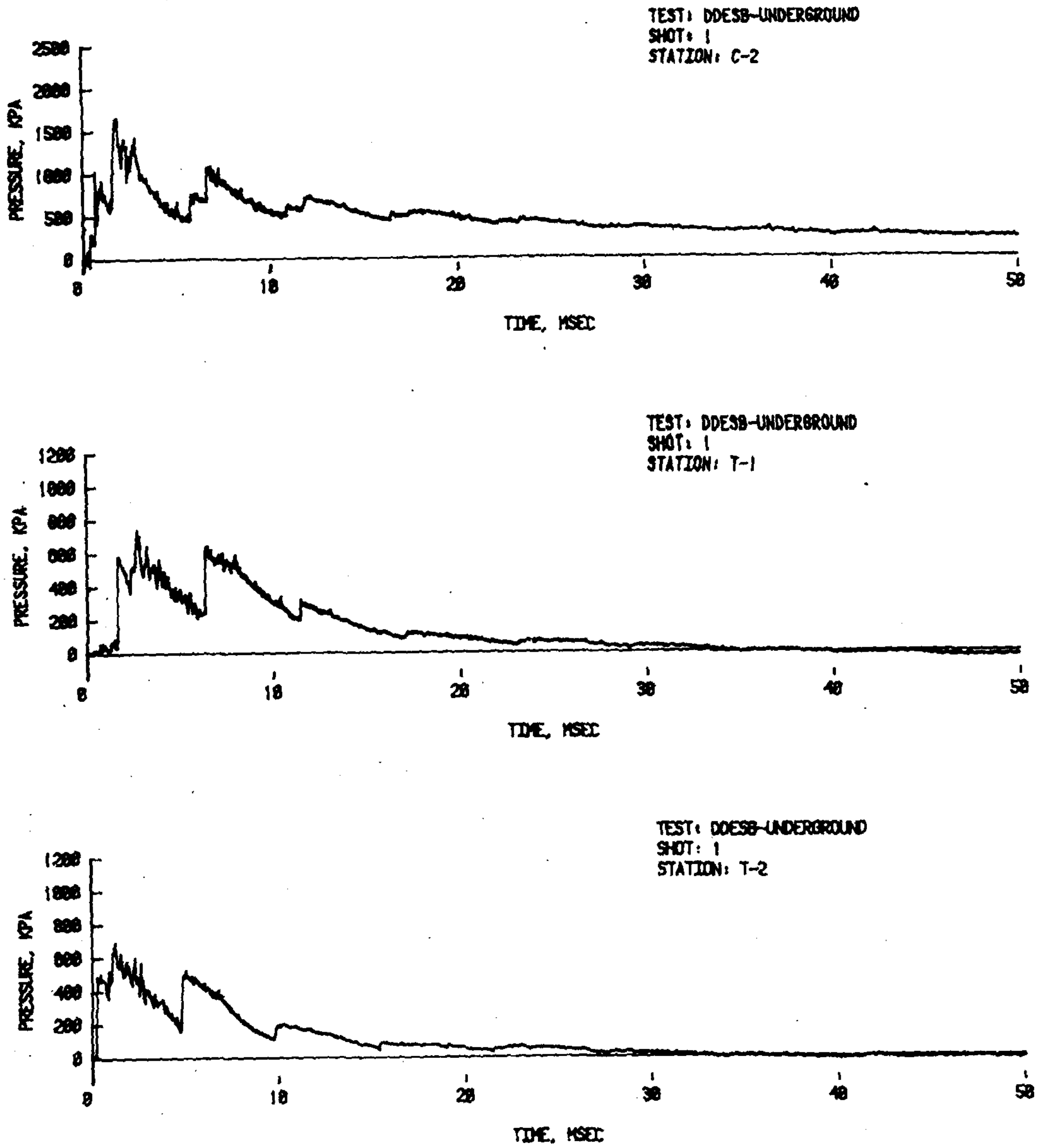

FIGURE A1. Shot 1, Chamber Loading Density - 0.356 kg/m^3 of PRIMACORD

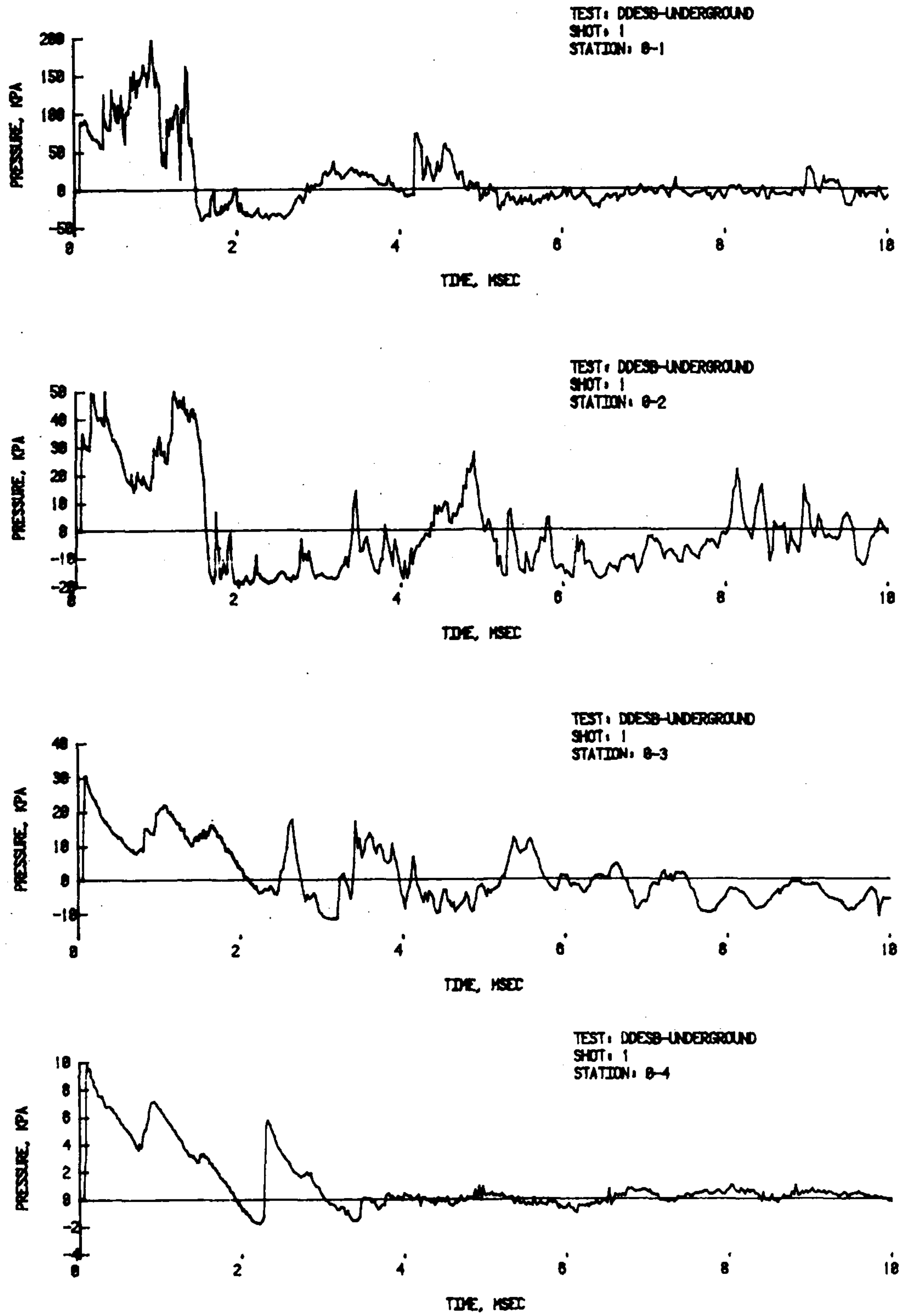

FIGURE A1. Shot 1, Chamber Loading Density - 0.356 kg/m^3 of PRIMACORD (Cont)

STATION: 45-1

NO RECORD

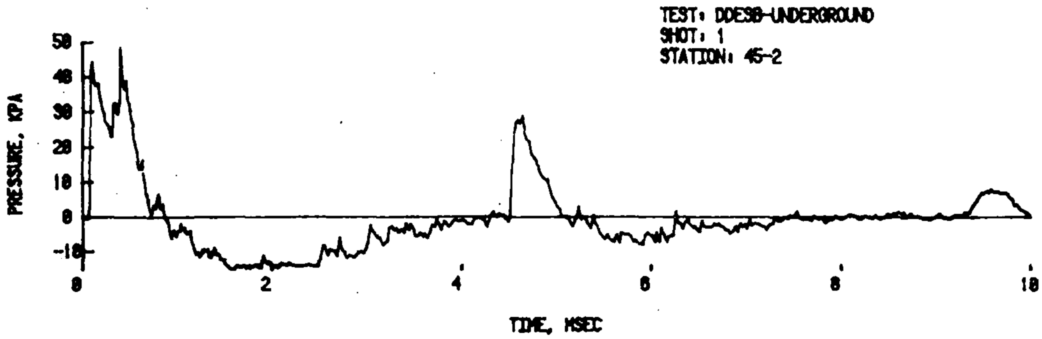

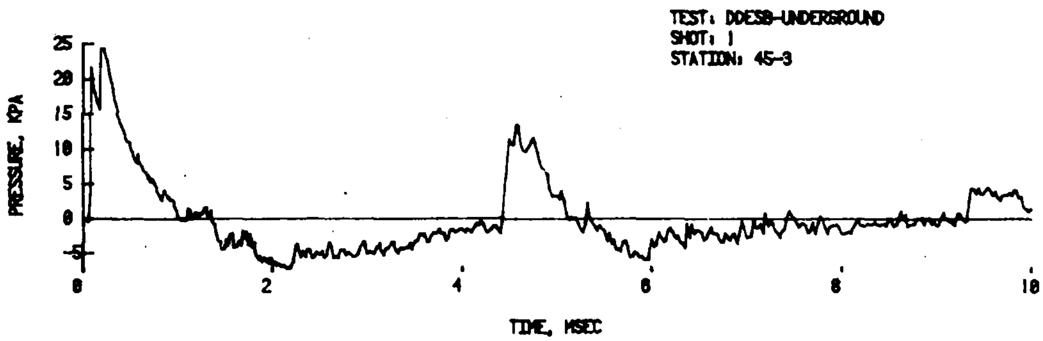

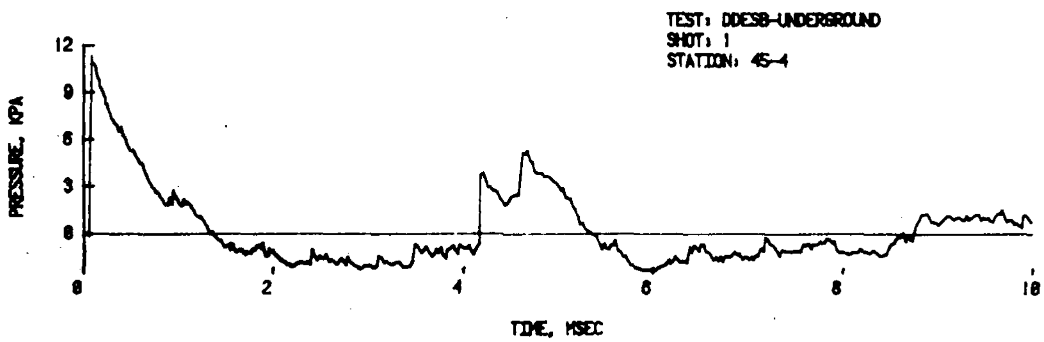

FIGURE A1. Shot 1, Chamber Loading Density - 0.356 kg/m^3 of PRIMACORD (Cont)

STATION: 45-1

NO RECORD

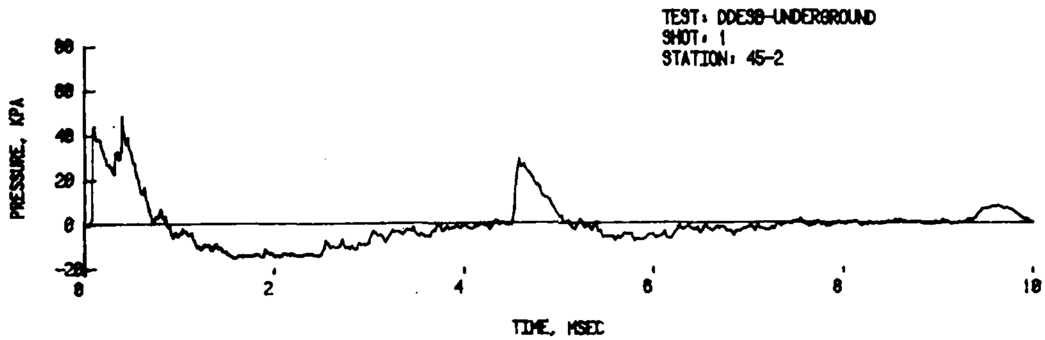

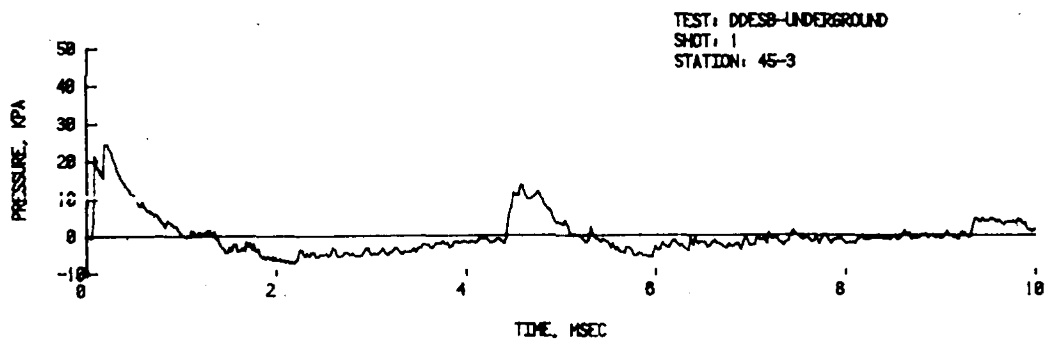

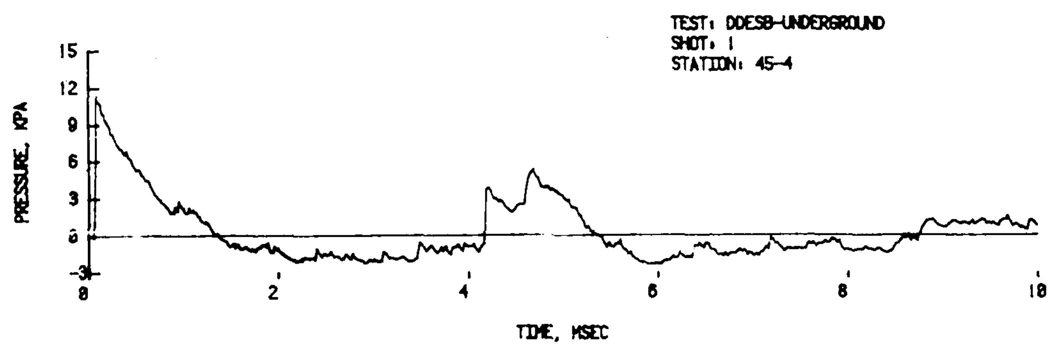

FIGURE A1. Shot 1, Chamber Loading Density - 0.356 kg/m^3 of PRIMACORD (Cont)

STATION: 90-1

NO RECORD

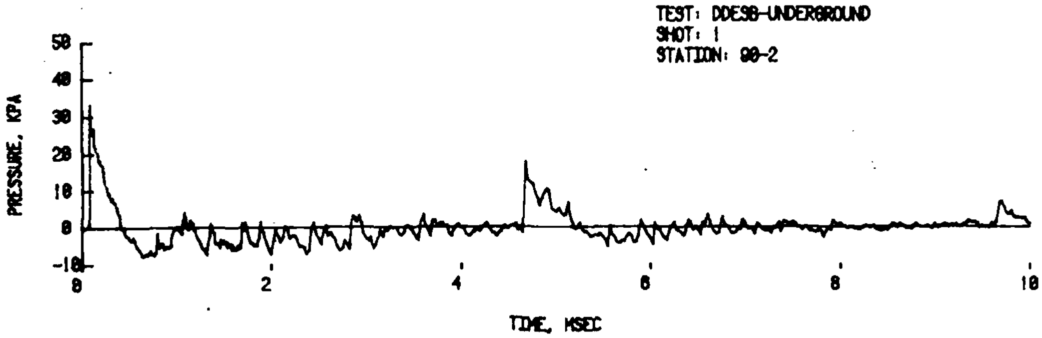

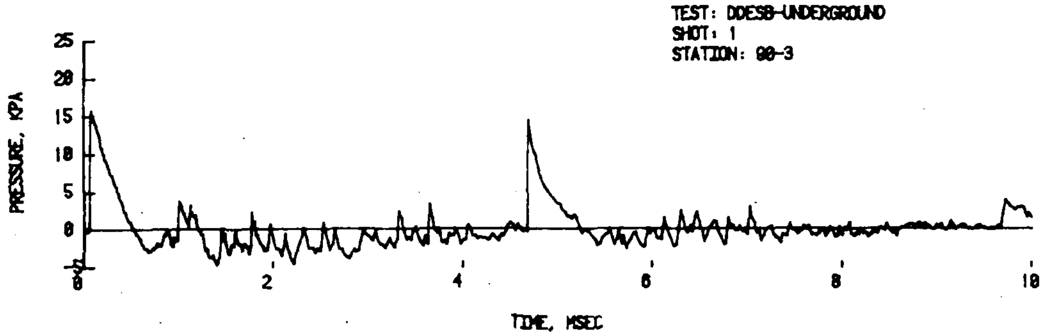

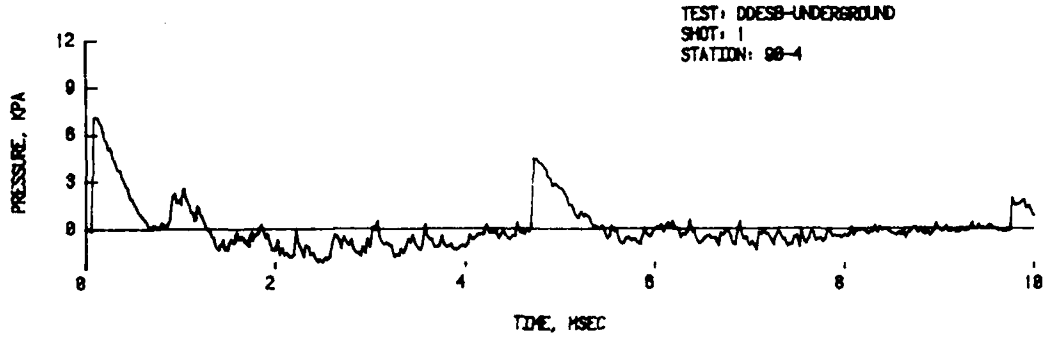

FIGURE A1. Shot 1, Chamber Loading Density - 0.356 kg/m^3 of PRIMACORD (Cont)

STATIONS: 135-1, 135-2, AND 135-3

NO RECORDS

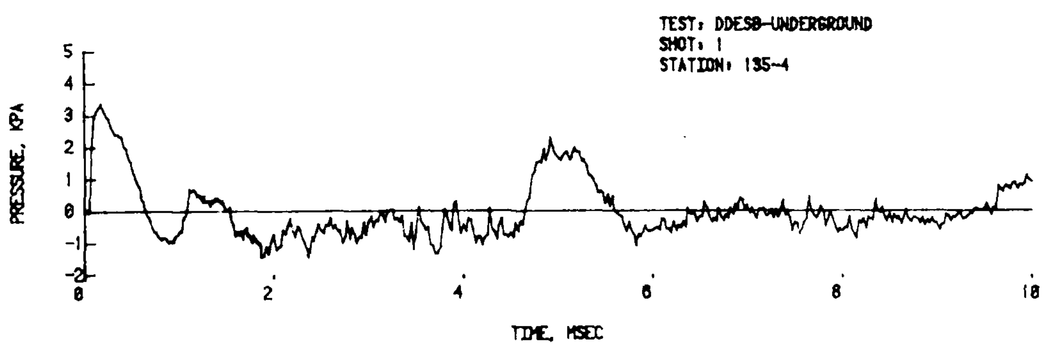

FIGURE A1. Shot 1, Chamber Loading Density - 0.356 kg/m^3 of PRIMACORD (Cont)

STATIONS: C-1 AND C-2

NO RECORDS

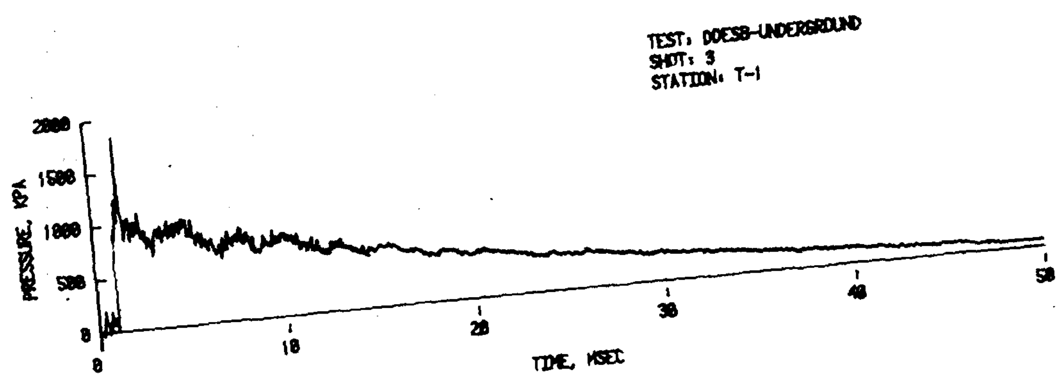

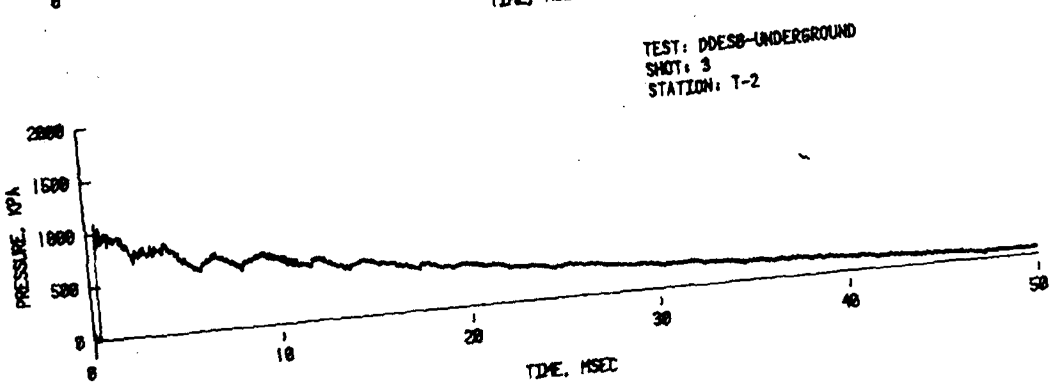

FIGURE A2. Shot 3, Chamber Loading Density - 1.459 kg/m^3 of PRIMACORD

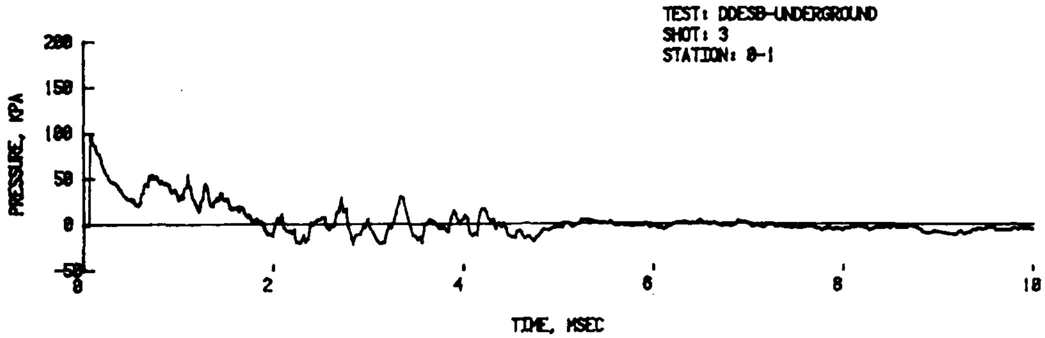

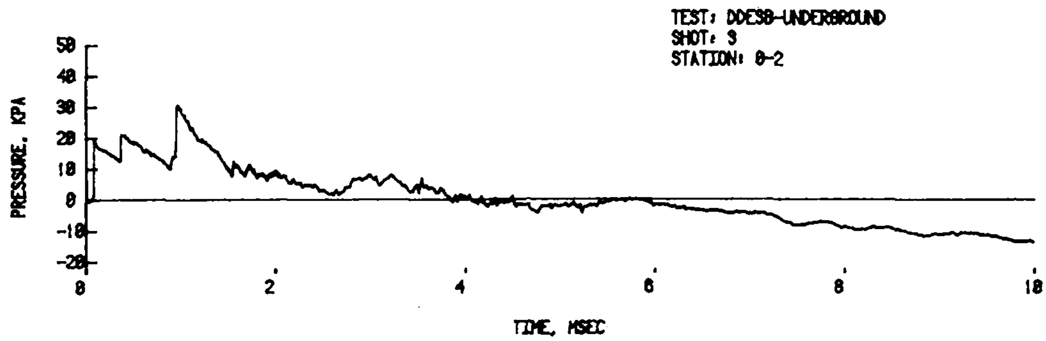

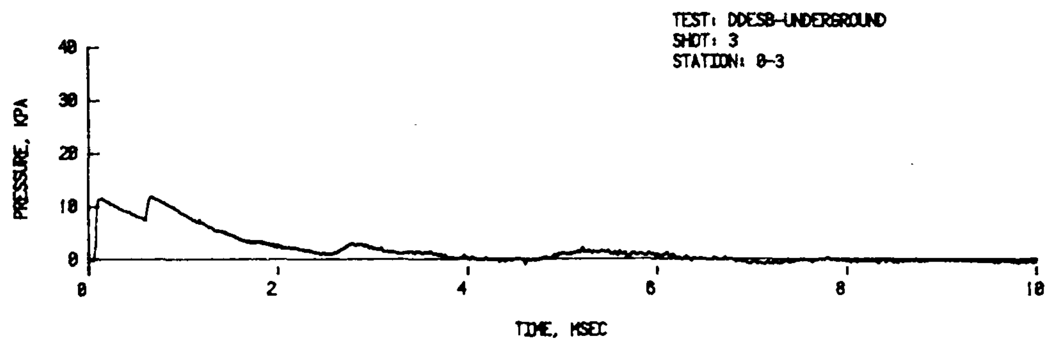

STATION: 8-4

NO RECORD

FIGURE A2. Shot 3, Chamber Loading Density - 1.459 kg/m^3 of PRIMACORD (Cont)

STATION: 45-1

NO RECORD

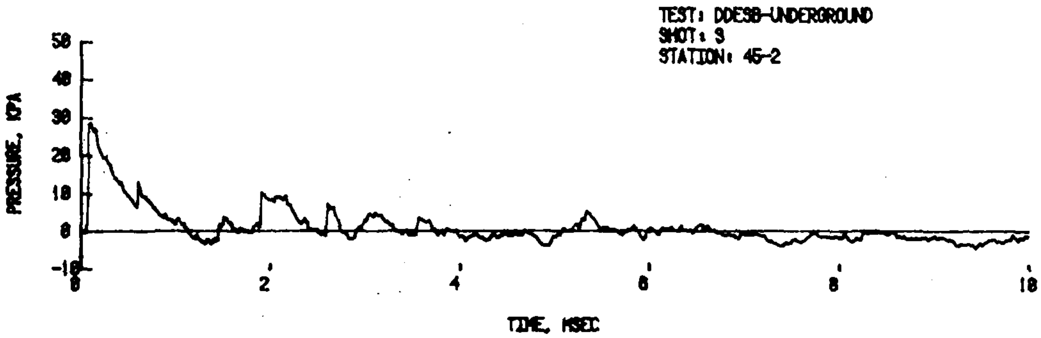

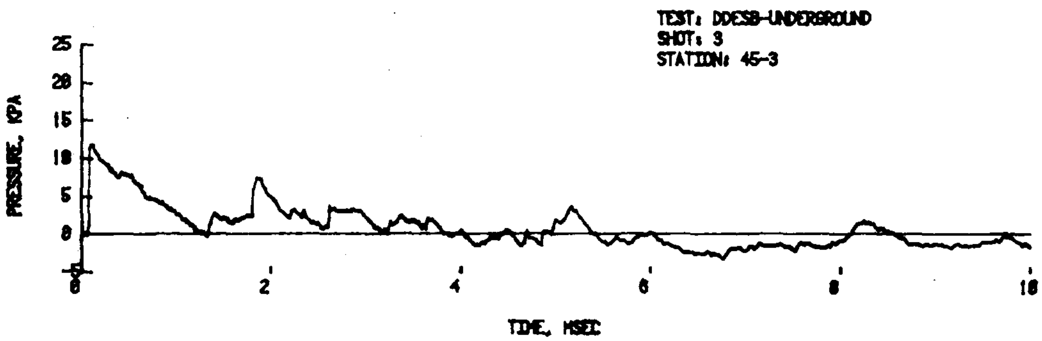

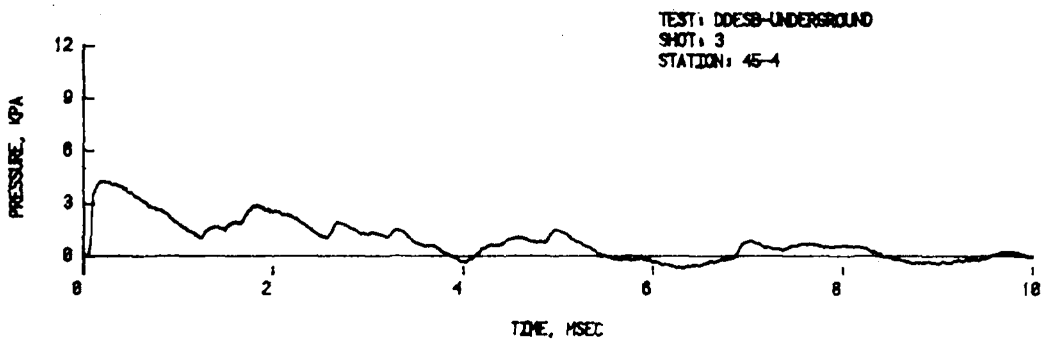

FIGURE A2. Shot 3, Chamber Loading Density - 1.459 kg/m^3 of PRIMACORD (Cont)

STATION: 90-1

NO RECORD

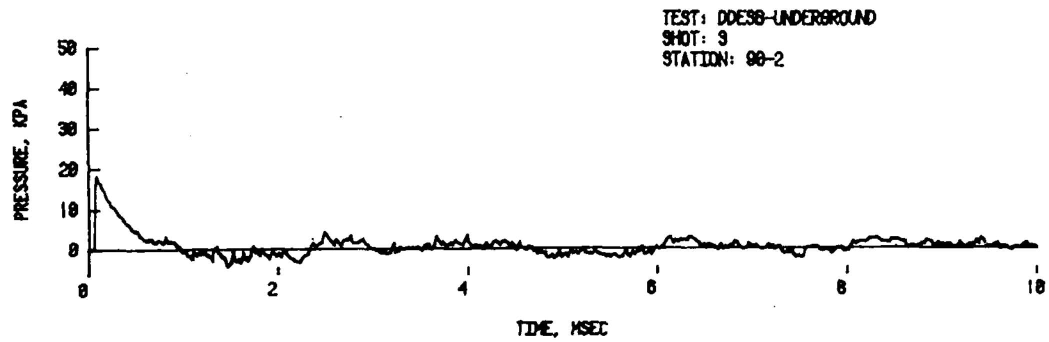

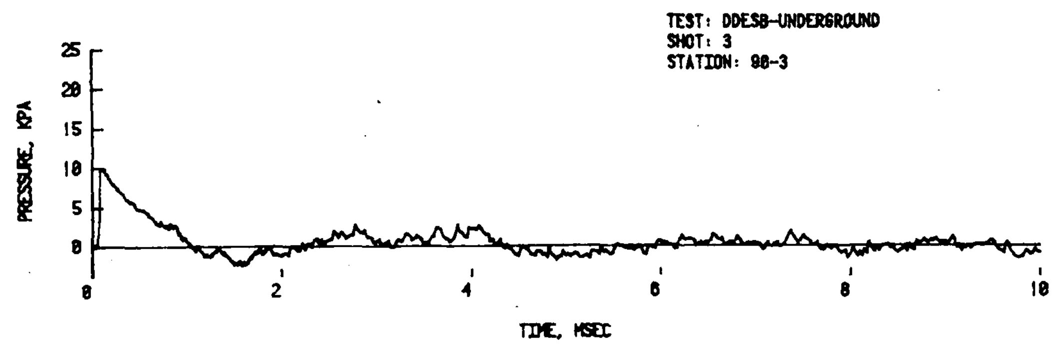

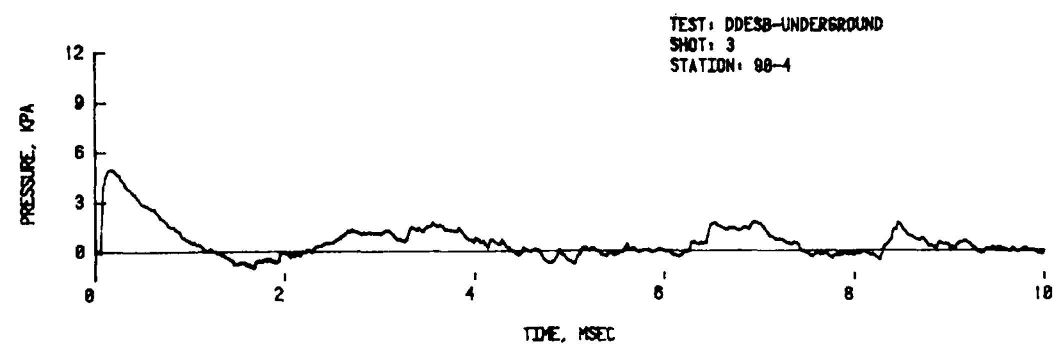

FIGURE A2. Shot 3, Chamber Loading Density - 1.459 kg/m^3 of PRIMACORD (Cont)

STATIONS: 135-1, AND 135-2

NO RECORDS

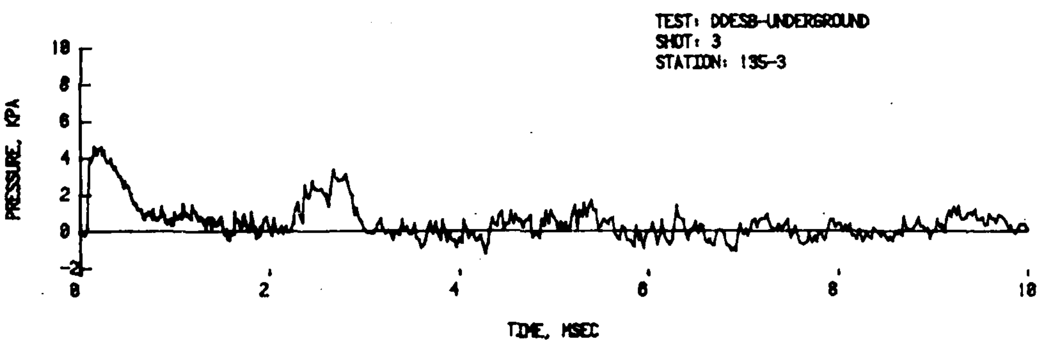

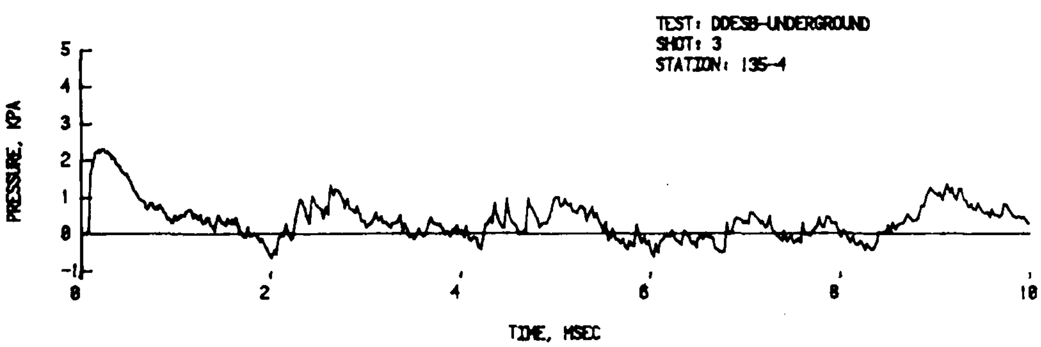

FIGURE A2. Shot 3, Chamber Loading Density - 1.459 kg/m^3 of PRIMACORD (Cont)

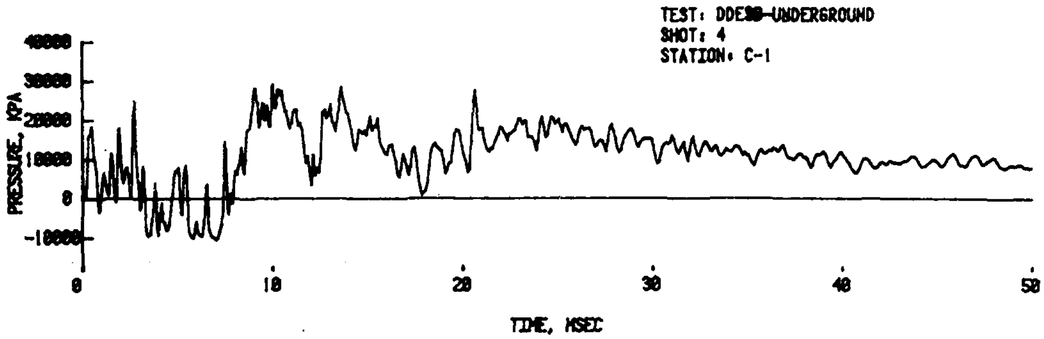

STATION: C-2

NO RECORD

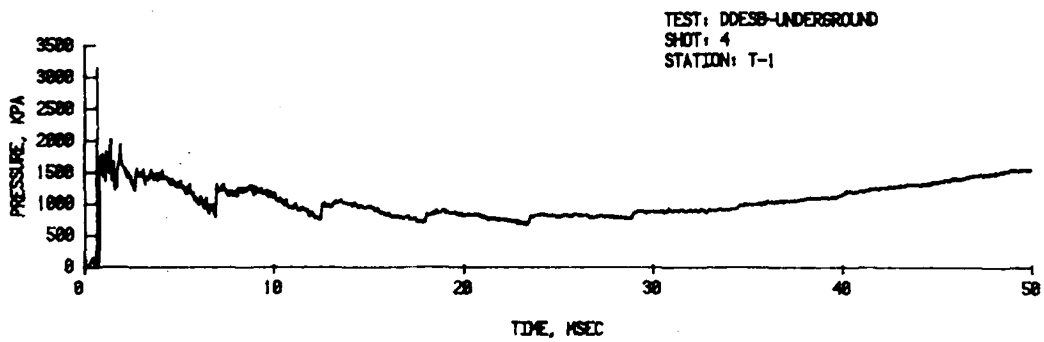

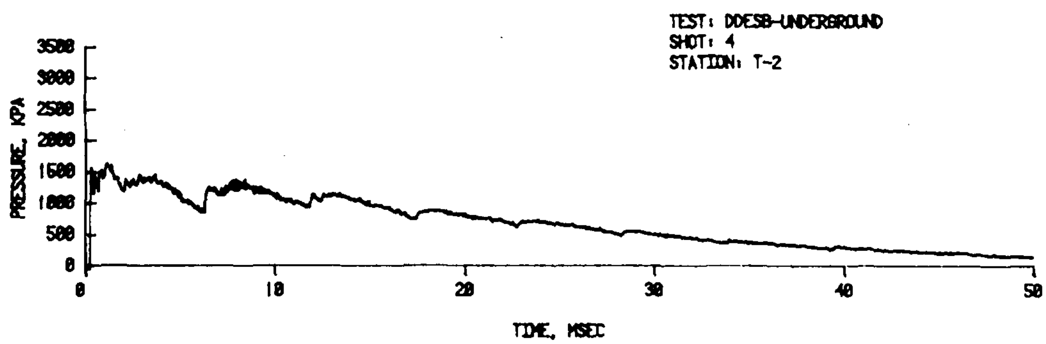

FIGURE A3. Shot 4, Chamber Loading Density - 3.405 kg/m^3 of PRIMACORD

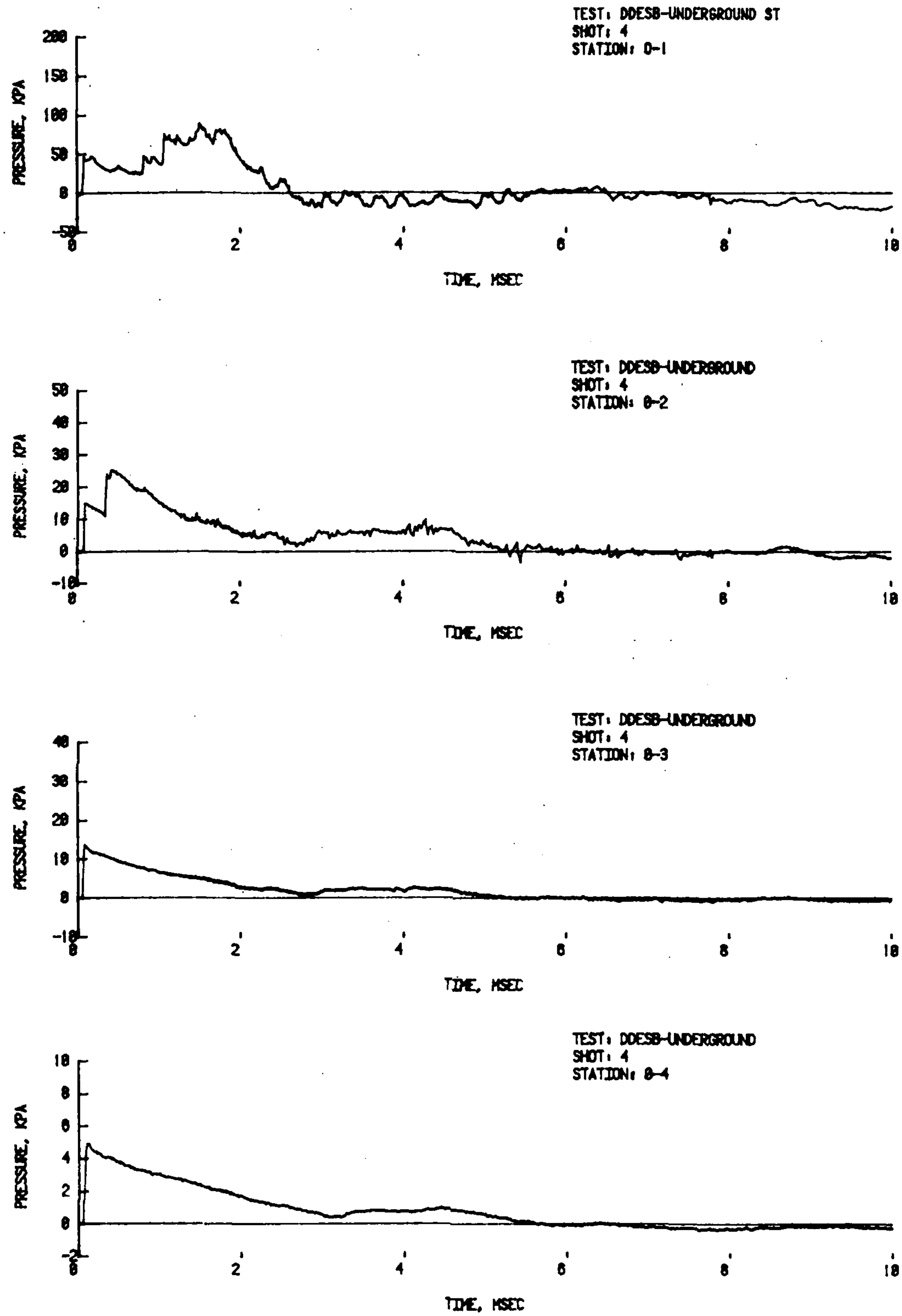

FIGURE A3. Shot 4, Chamber Loading Density - 3.405 kg/m^3 of PRIMACORD (Cont)

STATION: 45-1

NO RECORD

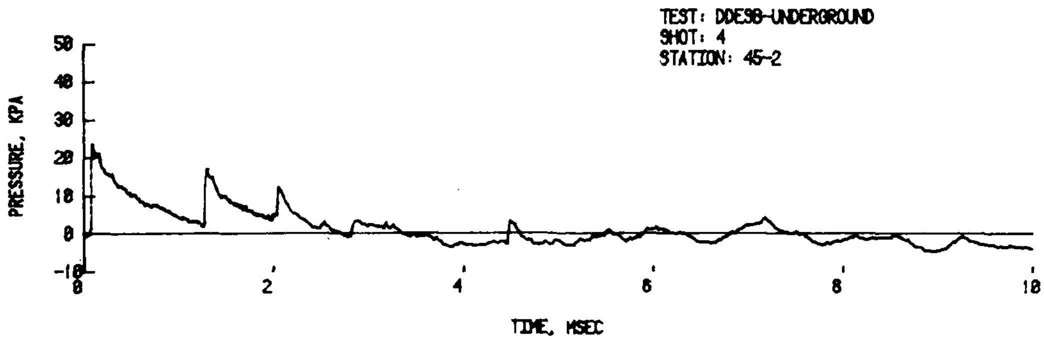

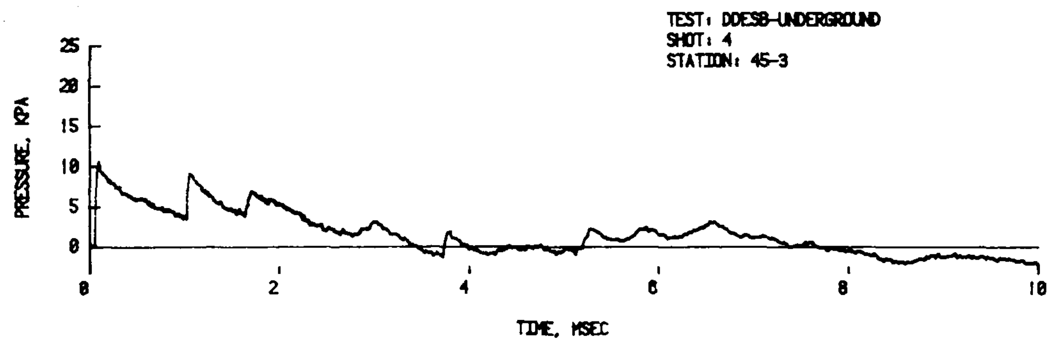

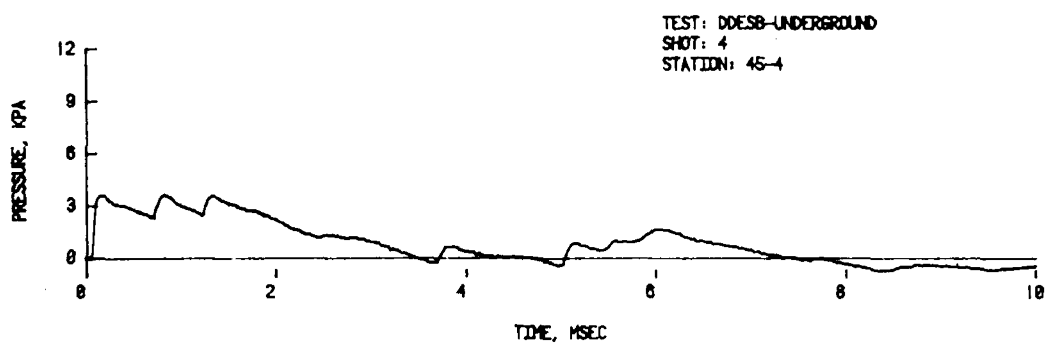

FIGURE A3. Shot 4, Chamber Loading Density - 3.405 kg/m^3 of PRIMACORD (Cont)

STATION: 90-1

NO RECORD

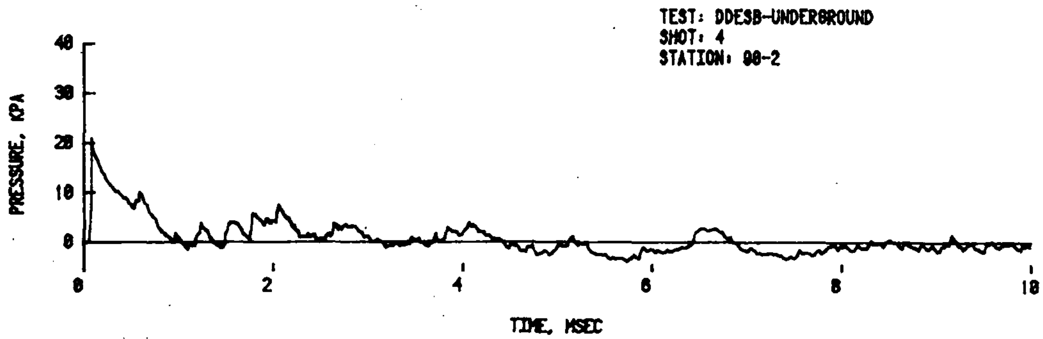

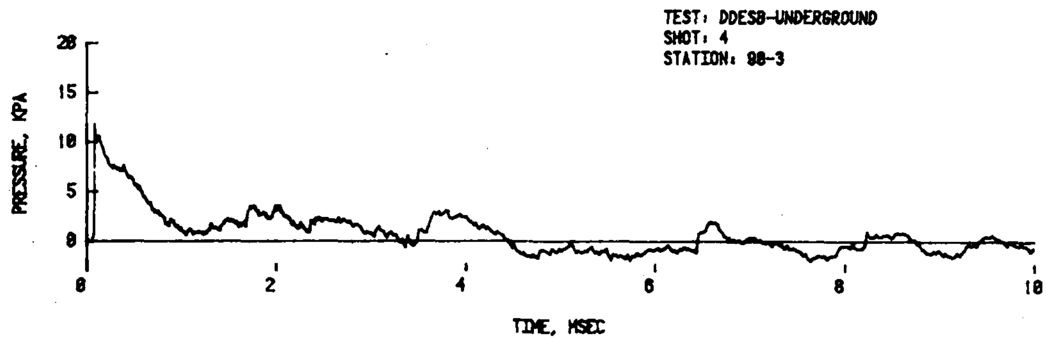

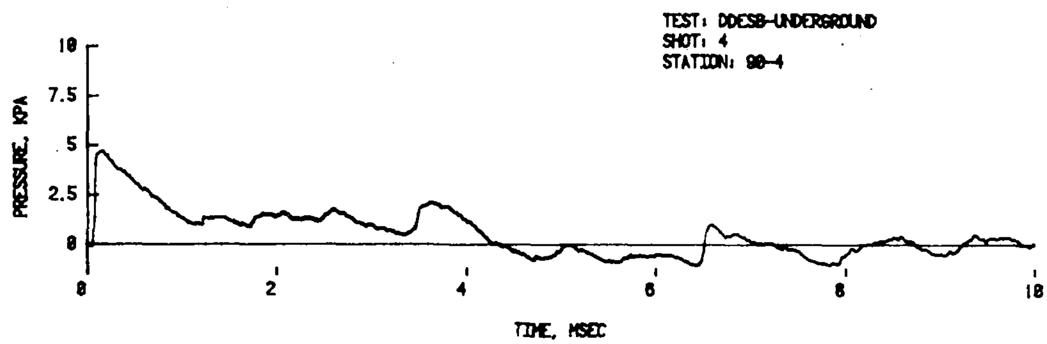

FIGURE A3. Shot 4, Chamber Loading Density - 3.405 kg/m^3 of PRIMACORD (Cont)

STATION: 135-1

NO RECORD

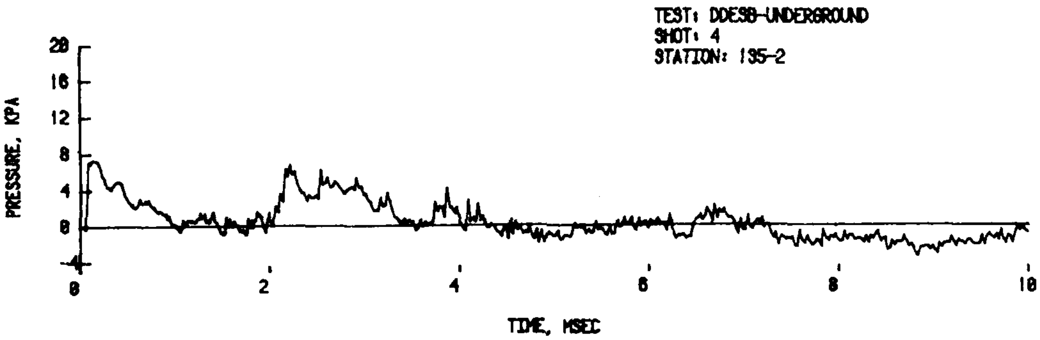

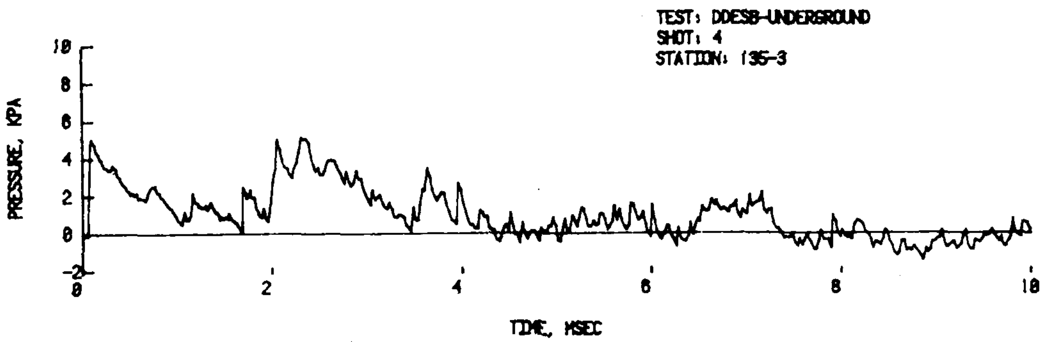

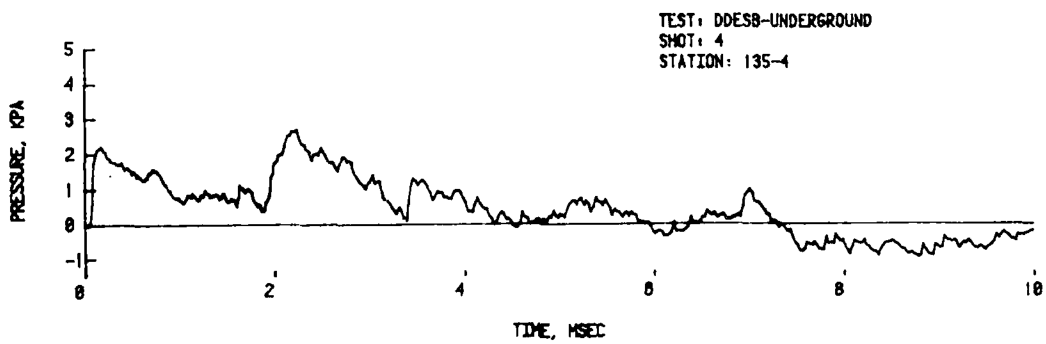

FIGURE A3. Shot 4, Chamber Loading Density - 3.405 kg/m^3 of PRIMACORD (Cont)

STATIONS: C-1 AND C-2

NO RECORDS

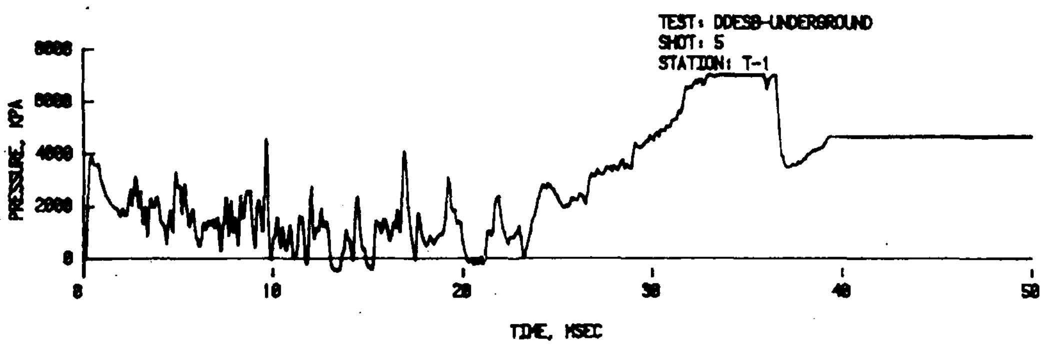

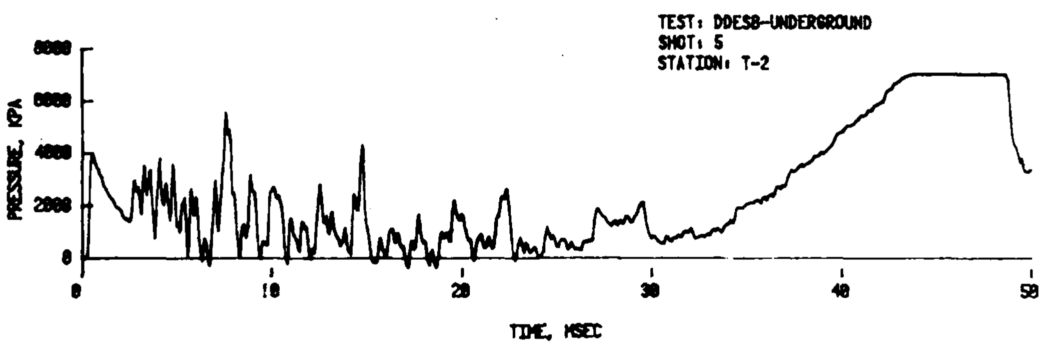

FIGURE A4. Shot 5, Chamber Loading Density - 3.942 kg/m^3 of C-4

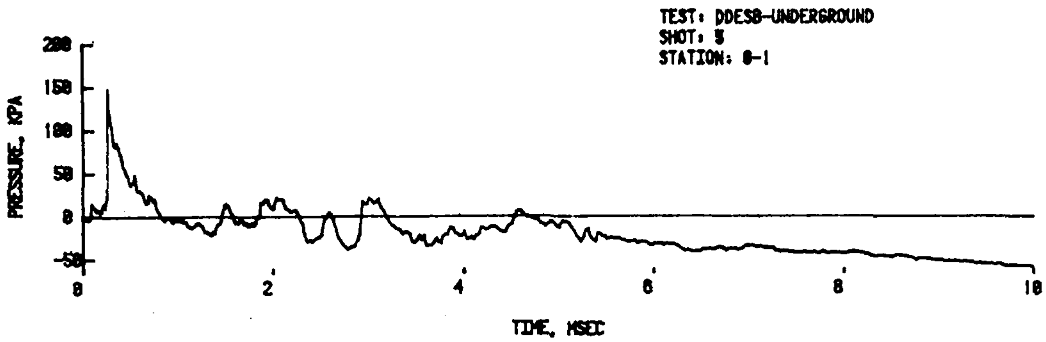

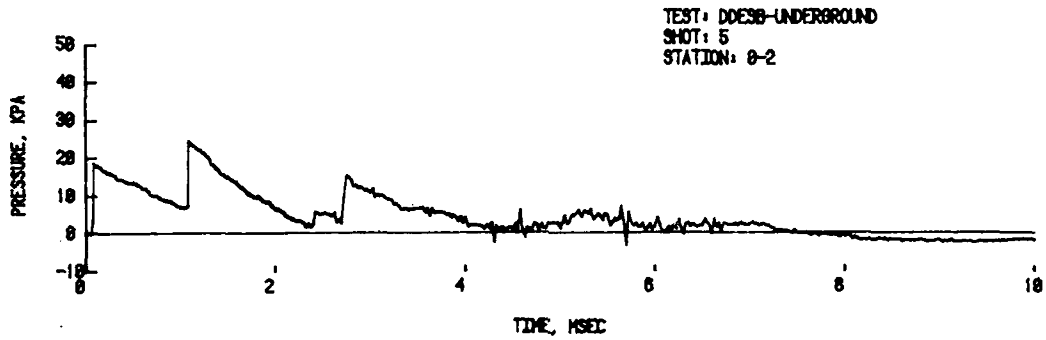

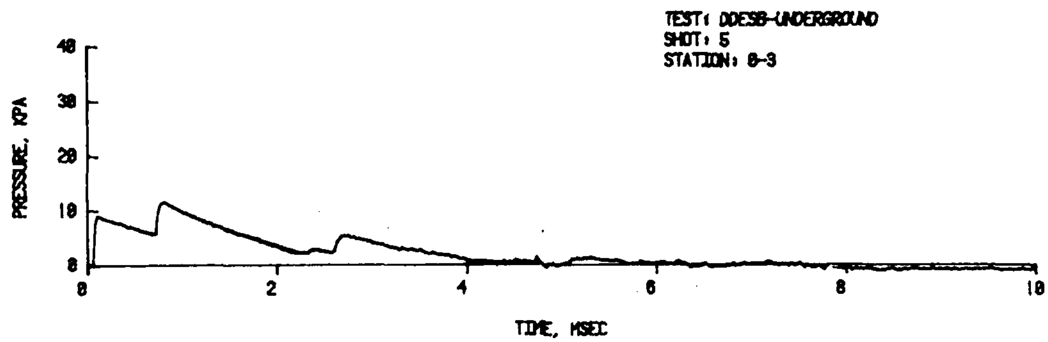

STATION: 8-4

NO RECORD

FIGURE A4. Shot 5, Chamber Loading Density - 3.942 kg/m^3 of C-4 (Cont)

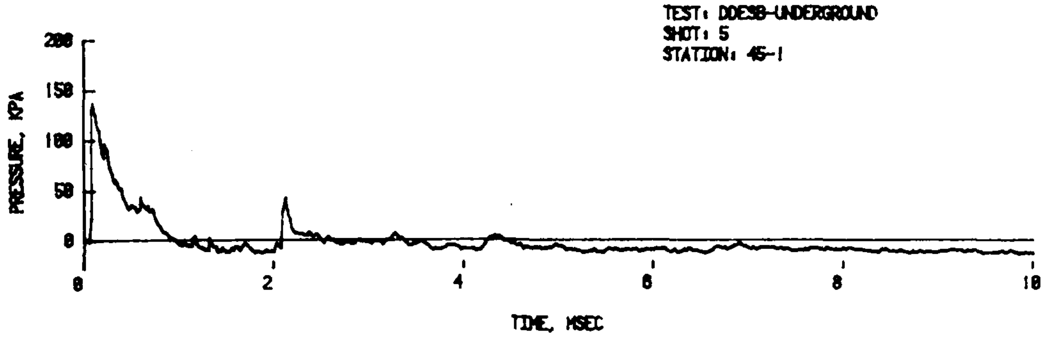

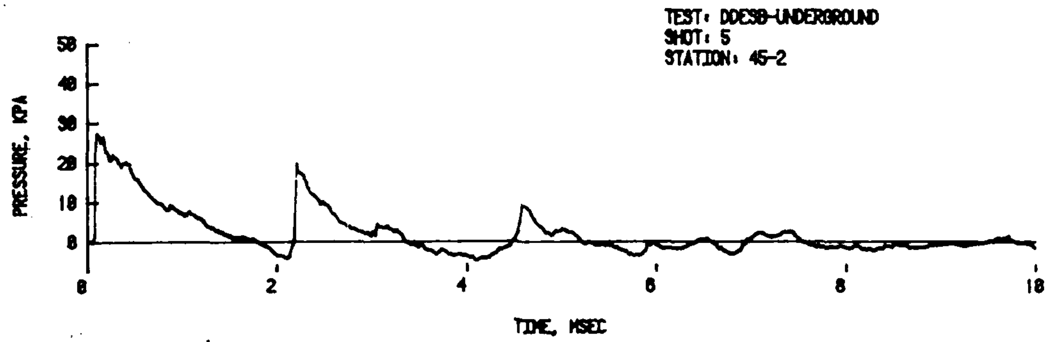

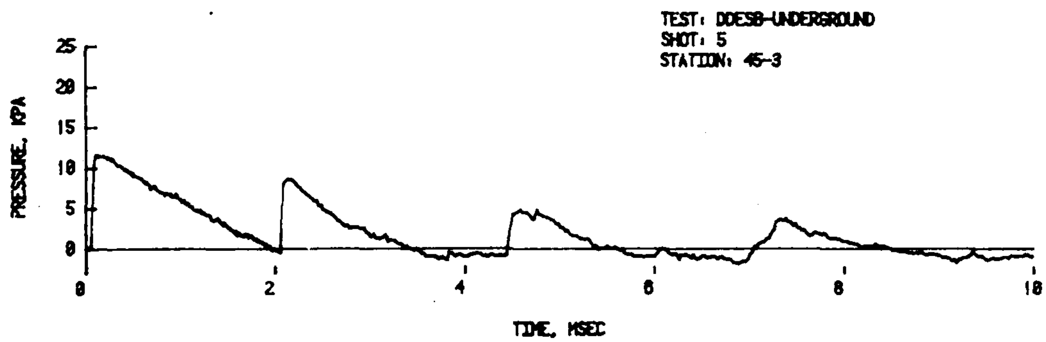

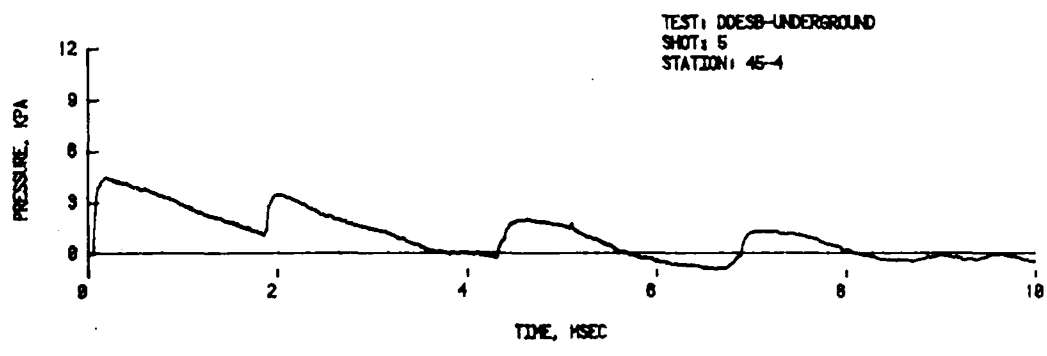

FIGURE A4. Shot 5, Chamber Loading Density - 3.942 kg/m^3 of C-4 (Cont)

STATION: 90-1

NO RECORD

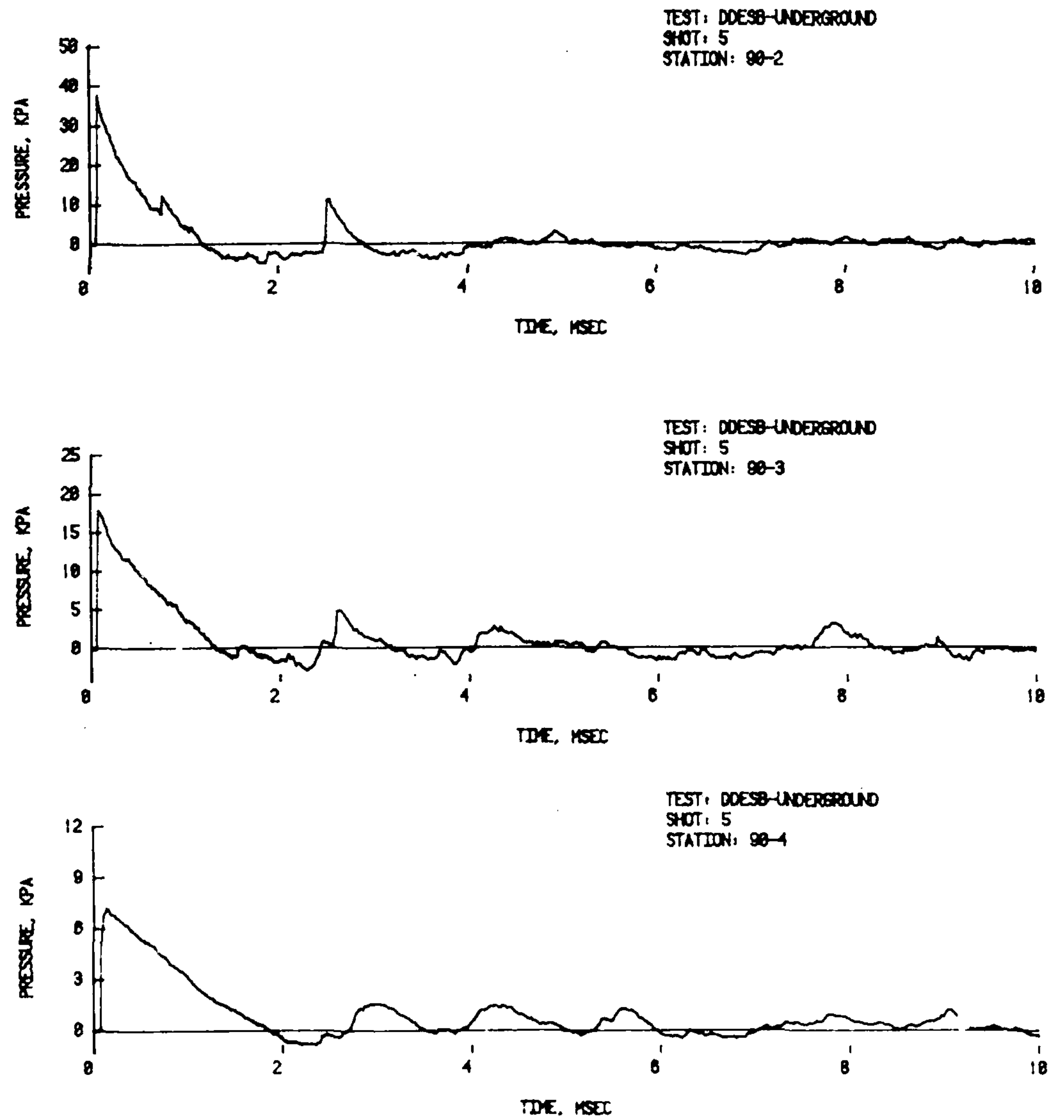

FIGURE A4. Shot 5, Chamber Loading Density - 3.942 kg/m^3 of C-4 (Cont)

STATION: 135-1

NO RECORD

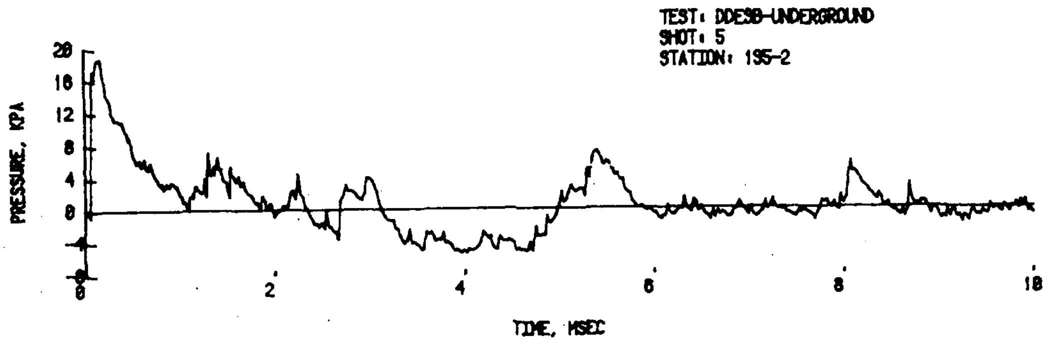

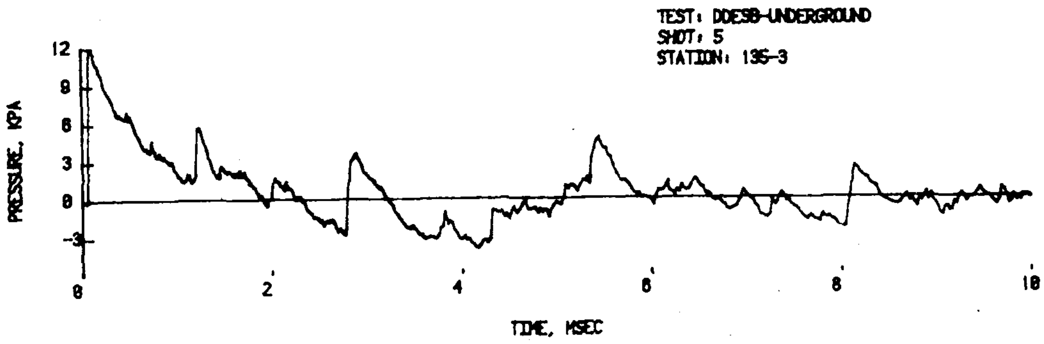

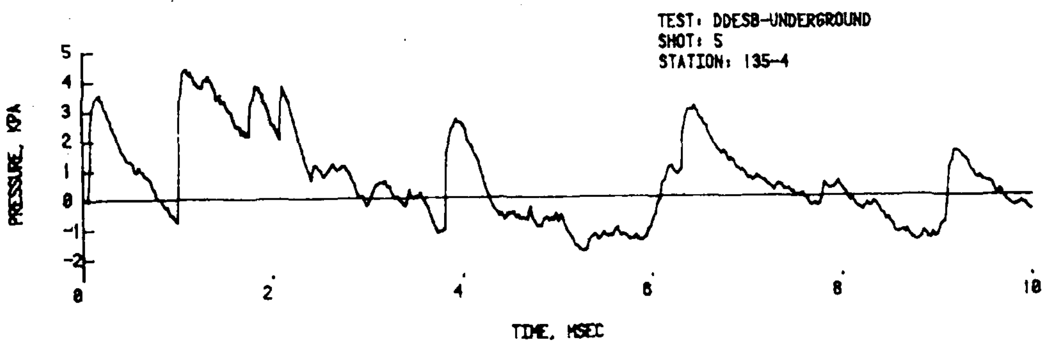

FIGURE A4. Shot 5, Chamber Loading Density - 3.942 kg/m^3 of C-4 (Cont)

APPENDIX B

EXAMPLES OF IMPULSE-TIME CALCULATIONS

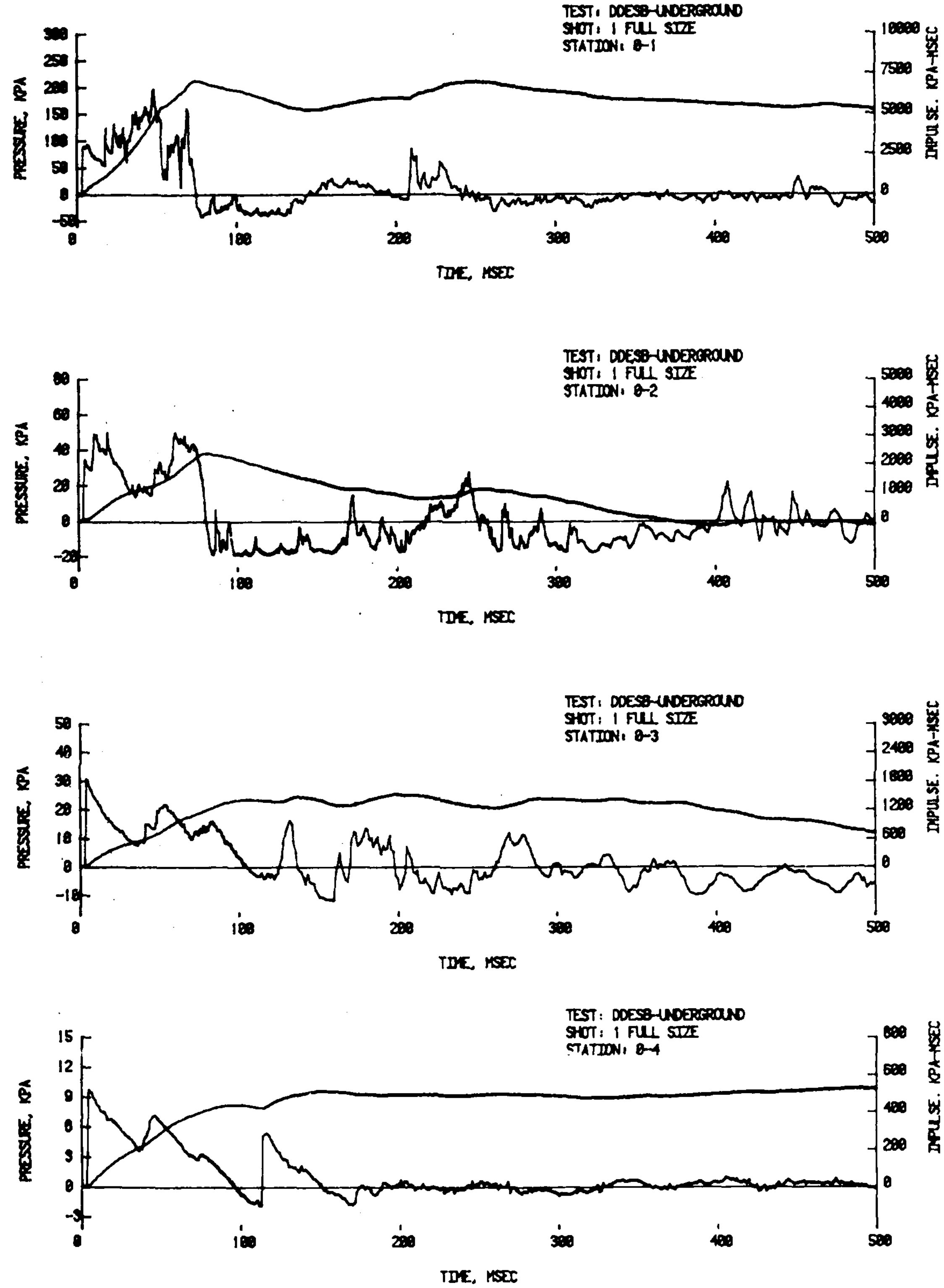

FIGURE B1. Predicted Full Scale Impulse for 0° Line, 0.356 kg/m^3, W/V$_c$

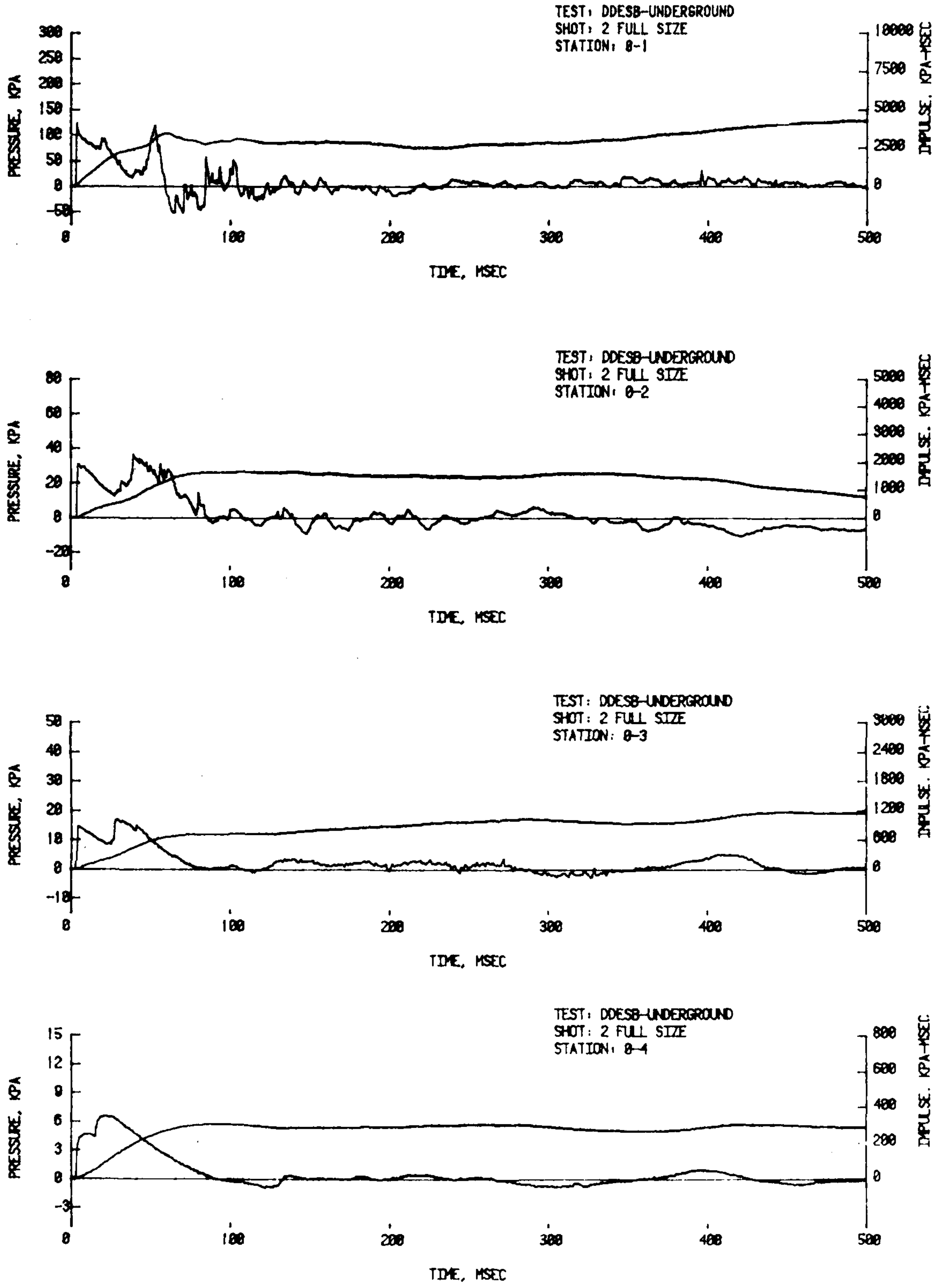

FIGURE 82. Predicted Full Scale Impulse for 0° Line, [illegible] kg/m^3, Q/V

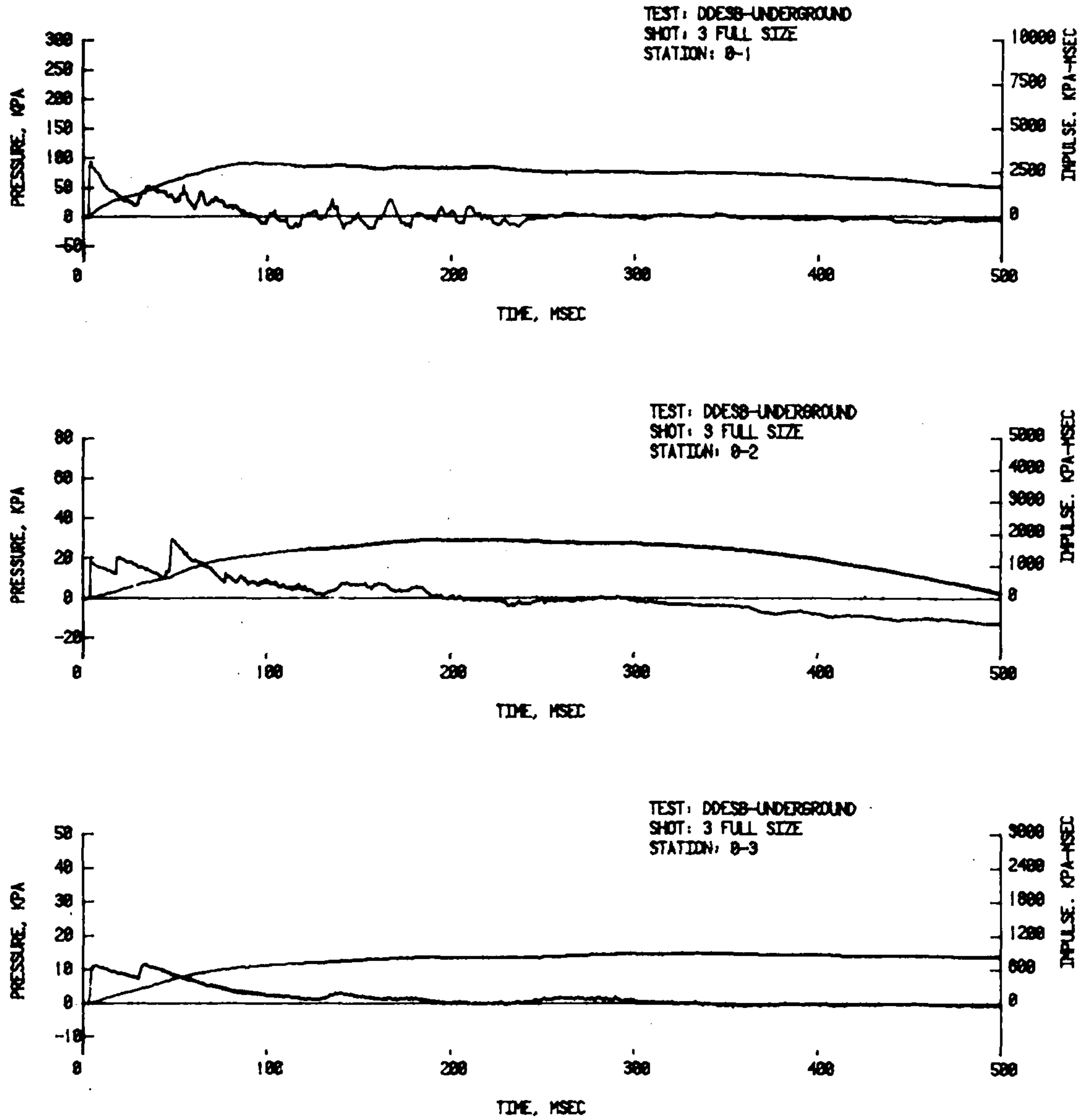

FIGURE 83. Predicted Full Scale Impulse for 0° Line, 1.459 kg/m^3, Q/V_c

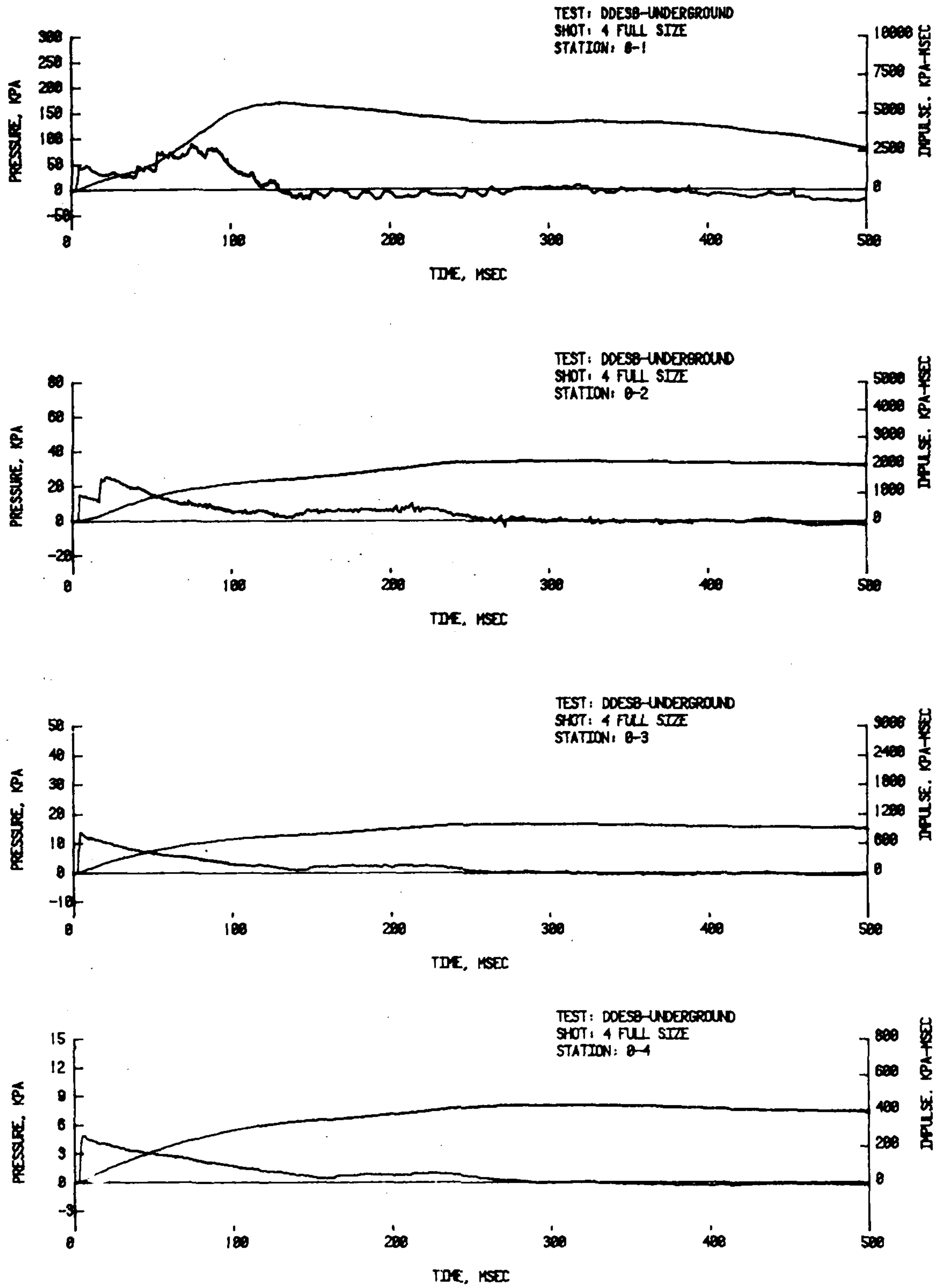

FIGURE B4. Predicted Full Scale Impulse for 0° Line, 3.405 kg/m^3, Q/V_c

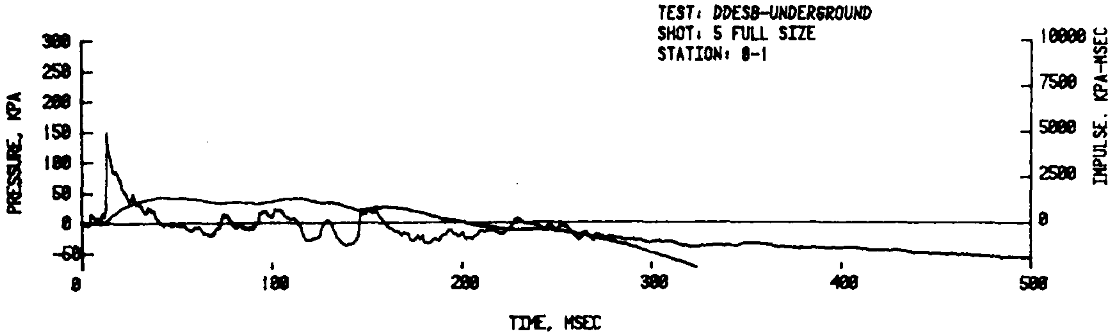

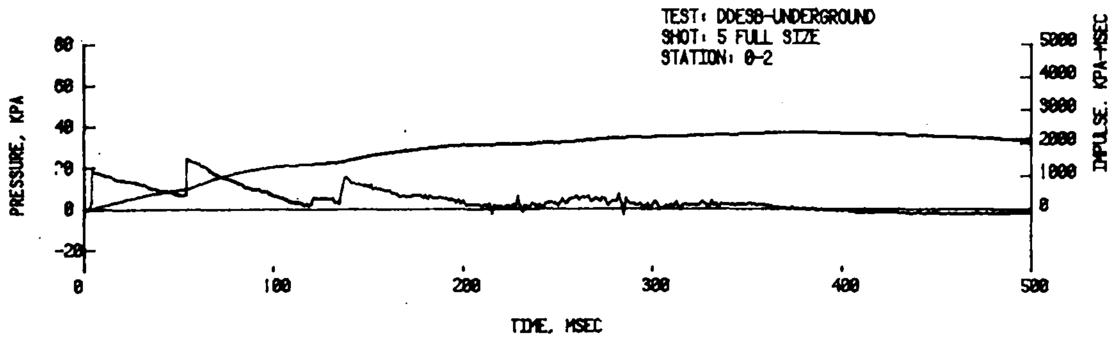

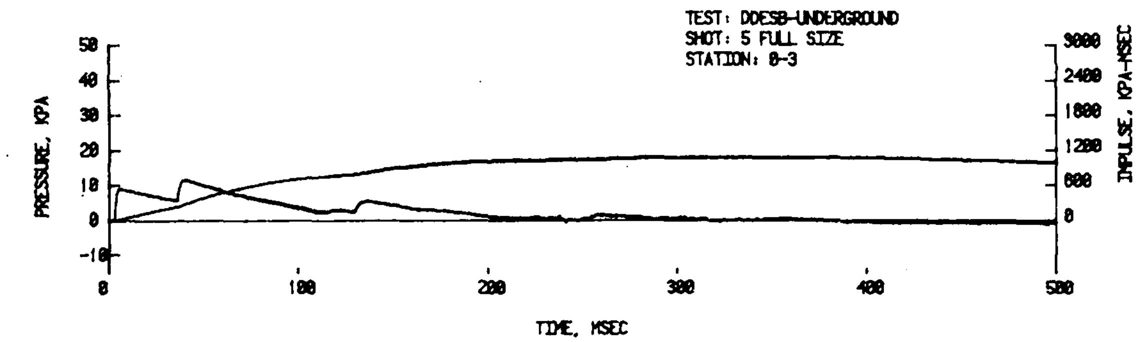

FIGURE B5. Predicted Full Scale Impulse for 0° Line, 3.942 kg/m^3, Q/V$_c$

SYMBOLS

g	Convergent tube parameter.
A_1	Ambient air sound speed, m/s.
A_4	Shock tube chamber sound speed, m/s.
A_{41}	Ratio chamber sound speed to ambient sound speed.
A_c	Chamber cross-section area at exit end, m^2.
A_j	Tunnel cross-section area, m^2.
D_t	Diameter of tunnel, m.
M_e	Mach number at convergent section.
M_3	Mach number behind the contact surface.
M_5	Mach number in chamber gas near area convergence.
P_1	Ambient pressure, kPa.
P_2	Shock wave pressure, kPa.
P_{21}	Ratio of shock wave pressure to ambient pressure.
P_4	Shock tube chamber pressure, kPa.
P_{41}	Ratio of shock tube chamber pressure to ambient pressure.
P_{VT}	Quasi-static overpressure in total volume, kPa.
P_W	Side-on overpressure at tunnel exit, kPa.
Q	Explosive charge mass, kg.
R	Distance outside of tunnel, m.
S_1	Tube cross-section area, m^2 (A_j).
S_4	Chamber cross-section area, m^2 (A_c)
T_1	Ambient temperature, ^oC.
U_2	Particle velocity behind shock front, m/s.
U_{21}	Ratio of particle velocity to ambient sound speed.

SYMBOLS
(Cont)

V_c	Storage chamber volume, m^3.
V_j	Tunnel volume, m^3.
V_t	Total volume, $V_c + V_j$, m^3.
ΔP	Side-on overpressure outride of tunnel, kPa.
γ_1	Ratio of specific heats in ambient air.
γ_4	Ratio of specific heats in chamber.
θ	Degrees off the tunnel aris.

DISTRIBUTION LIST

No. of Cys	Organization
12	Administrator Defense Technical Info Center ATTN: DTIC-FDAC Cameron Station, Bldg 5 Alexandria, VA 22304-6145
30	Chairman DOD Explosives Safety Board ATTN: JDDESB Hoffman Bldg 1, Room 856-C 2461 Eisenhower Avenue Alexandria, VA 22331-0600
1	OSD, ADUSDRE (R/AT,ET) ATTN: Mr. J. Persh Washington, DC 20301-3110
1	Under Secretary of Defense for Research & Engineering Department of Defense Washington, DC 20301
1	Director of Defense Research & Engineering Washington, DC 20301
1	Assistant Secretary of Defense (Atomic Energy) ATTN: Document Control Washington, DC 20301
1	Assistant Secretary of Defense (MRA&L) ATTN: EO&SP Washington, DC 20301
1	Director Defense Advanced Research Projects Agency 1400 Wilson Boulevard Arlington, VA 22209-2308

No. of Cys	Organization
1	Director Defense Intelligence Agency ATTN: DT-1B (Dr. Vorona) Washington, DC 20301
2	Chairman Joint Chiefs of Staff ATTN: J-3 (Operations) J-5 (P&P/R&D Div) Washington, DC 20301
3	Director Institute for Defense Analyses ATTN: Dr. H. Menkes Dr. J. Bengston Tech Info Ofc 1801 Beauregard Street Alexandria, VA 22311
4	Director Defense Nuclear Agency ATTN: SPTD (Mr. Kennedy) DDST(E) (Dr. Sevin) OALG (Mr. Jeffers) LEEE (Mr. Eddy) Washington, DC 20305
1	Information & Analysis Ctr-DNA Kaman Tempo ATTN: DASIAC PO Drawer QQ Santa Barbara, CA 93102
1	Commander Field Command, DNA ATTN: FCWS-SC (Tech Library) Kirtland AFB, NM 87115

DISTRIBUTION LIST

No. of Cys	Organization
10	HQDA (DAMA-ART-M) (DAEN-ECE-T/Mr. Wright) (DAEN-MCC-D/Mr. Foley) (DAEN-RDL/Mr. Simonini) (DAEN-RDZ-A/Dr. Choromokos) (DALO-SMA/COL Paris) (DAMA-CSM-CA) (DAMA-AR/NCL Div) (DAMA-NCC/COL Orton) (DAPE-HRS) WASH DC 20310
2	Commander US Army Materiel Command ATTN: AMCDRA-ST AMCSF 5001 Eisenhower Avenue Alexandria, VA 22333-0001
1	Director AMC Field Safety Activity ATTN: AMXOS-OES Charlestown, IN 47111-9669
1	Director AMC ITC ATTN: Dr. Chiang Red River Depot Texarkana, TX 75501
1	Commander USA Laboratory Command ATTN: AMSLC-AS-SE (R. Oden) 2800 Powder Mill Road Adelphi, MD 20783-1145
1	Director Materials Technology Laboratory ATTN: AMXMR-ATL Watertown, MA 02172-0001

No. of Cys	Organization
1	Commander USA Harry Diamond Laboratory ATTN: SLCHD-TI 2800 Powder Mill Road Adelphi, MD 20783-1197
1	Director Benet Weapons Laboratory ATTN: SMCAR-CCB-TL Watervliet, NY 12189-4050
1	Commander USA Natick R&D Laboratories ATTN: AMDNA-D (Dr. Seiling) Natick, MA 01760
2	Commander USA Armament Materiel Readiness Command ATTN: Joint Army/Navy/AF Conven Ammo Prof Coord GP/E1 (Jordan) Rock Island, IL 61299
1	Commander USA Armament Command ATTN: AMSAR-SA Rock Island Arsenal Rock Island, IL 61201
1	Commander US Army Armament, Munitions and Chemical Command ATTN: AMSMC-IMP-L Rock Island, IL 61299-7300
3	Commander USA Armament Research, Development & Engineering Center ATTN: SMCAR-LCM-SPC SMCAR-MSI SMCAR-TDC Picatinny Arsenal NJ 07806-5000

DISTRIBUTION LIST

No. of Cys	Organization
1	Commander USA Rock Island Arsenal Rock Island, IL 61299
1	Commander Indiana Army Ammunition Plant Charlestown, IN 47111
1	Commander Joliet Army Ammunition Plant Joliet, IL 60436
1	Commander Kansas Army Ammunition Plant Parsons, KS 67357
1	Commander Lone Star Army Ammunition Plant Texarkana, TX 75502
1	Commander Longhorn Army Ammunition Plant Marshall, TX 75671
1	Commander Milan Army Ammunition Plant Milan, TN 38358
1	Commander Radford Army Ammunition Plant Radford, VA 24141
1	Commander Ravenna Army Ammunition Plant Ravenna, OH 44266
1	Commander Pine Bluff Arsenal Pine Bluff, AR 71601

No. of Cys	Organization
1	Commander USA Aviation Systems Command ATTN: AMSAV-ES 4300 Goodfellow Boulevard St. Louis, MO 63120-1798
1	Director USA Aviation Research & Technology Activity Ames Research Center Moffett Field, CA 94035-1099
1	Commander USA Research Office PO Box 12211 Research Triangle Park, NC 27709-2211
1	Director Lewis Research Center ATTN: Mail Stop 77-5 21000 Brookpark Road Cleveland, OH 44135
1	Commander USA Dugway Proving Ground ATTN: STEDP-TO-H (Mr. Miller) Dugway, UT 84022
2	Commander USA Communications Electronics Command ATTN: AMSEL-ED AMSEL-IM-L (RptSec,B2700) Fort Monmouth, NJ 07703-5000
4	Commander US Army Missile Command ATTN: AMSMI-R (Mr. Cobb) AMSMI-RD AMSMI-RR (Mr. Lively) AMSMI-RX (M. Thauer) Redstone Arsenal, AL 35898-5249

DISTRIBUTION LIST

No. of Cys	Organization
1	Commander USA Ballistic Missile Defense Systems Command ATTN: M. Whitfield, ATC ATTN: J. Veeneman P.O. Box 1500 Huntsville, AL 35807-3801
1	Director Missile & Space Intelligence Center ATTN: AIAMS-YDL Redstone Arsenal, AL 35898-5500
1	Commander USA Tank Automotive Command ATTN: AMSTA-TSL Warren, MI 48397-5000
1	Commander USA Development & Employment Agency ATTN: MODE-ORO Fort Lewis, WA 98433-5000
1	Director USA TRADOC Analysis Center ATTN: ATOR-TSL White Sands Missile Range, NM 88002-5502
1	Commandant USA Infantry School ATTN: ATSH-CD-CS-OR Fort Benning, GA 31905-5400
1	Commandant USA Engineer School ATTN: ATSE-CD Fort Belvoir, VA 22060

No. of Cys	Organization
1	Commander USA Belvoir R&D Center ATTN: STRBE-NN Fort Belvoir, VA 22060-5606
1	Commander USA Engineer Division-Europe ATTN: EUDED (Dr. Crowson) APO New York, NY 09757
1	Division Engineer USA Engineer Division Fort Belvoir, VA 22060
1	Corps of Engineers-HSV Division ATTN: HNDDE (Mr. Char) PO Box 1600 Huntsville, AL 35807
1	Director USA Engineer Waterways Experimental Station ATTN: WESNB (K. Davis) PO Box 631 Vicksburg, MS 39180-0631
1	Commander USA Construction Engineering Research Laboratory PO Box 4005 Champaign, IL 61820
1	Commander USA Foreign Science & Technology Center ATTN: Rsch & Data Br Federal Office Building 220 7th Street, NE Charlottesville, VA 22901

DISTRIBUTION LIST

No. of Cys	Organization
1	Assistant Secretary of the Navy (R&D) Department of the Navy Washington, DC 20350
3	Chief of Naval Operations ATTN: OP-411 (C. Ferraro) OP-41B CPT Wernsman Washington, DC 20350
2	Commander Naval Sea Systems Command ATTN: SEA-06H (Van Slyke) SEA-0333 Washington, DC 20362
1	Commander Naval Surface Weapons Center ATTN: E-23 (Mr. Walsh) Dahlgren, VA 22448-5000
5	Commander Naval Surface Weapons Center ATTN: Dr. Schindel Dr. Victor Dawson Dr. P. Huange R15 (Swisdak/Smith) Silver Spring, MD 20902-5000
1	Commander Naval Weapons Center ATTN: Code 0632 (Osterman) China Lake, CA 93555
1	Commander Naval Research Lab ATTN: Code 2027 Washington, DC 20375

No. of Cys	Organization
1	Commander Naval Weapons Evaluation Facility ATTN: Document Control Kirland AFB Albuquerque, NM 87117
1	Officer-In-Charge Naval EOD Facility ATTN: Code D (Dickenson) Indian Head, MD 20640
1	Commander Naval Weapons Support Center ATTN: Code 502 Crane, IN 47522
1	Commander Naval Facilities Engineering Cmd ATTN: Code 04T5 Washington, DC 22360
1	Commander Naval Air Systems Command ATTN: AIR 532 Washington, DC 20360
2	Commander David W. Taylor Naval Ship R&D Center ATTN: Code 17 (Mr. Murray) Code 1747 (Mr. Wilner) Bethesda, MD 20084-5000
1	Commander Naval Ship R&D Center ATTN: Underwater Explosions Rsch Div (Mr. L.T. Butt) Portsmouth, VA 23709

DISTRIBUTION LIST

No. of Cys	Organization
2	Civil Engineering Laboratory Naval Construction Battalion Ctr ATTN: Code L31 Code L51 (Mr. Keenan) Port Hueneme, CA 93041
4	HQ USAF (AFNIE-CA) (AFRIDO/AFRODXM/AFRDPM) WASH DC 20330
1	USAF Systems Command ATTN: IGFG Andrews Air Force Base Washington, DC 20334
1	Commander Air Force Rocket Propulsion Laboratory ATTN: Code AFRPL MKPA (Geisler) Edwards AFB, CA 93523
3	Air Force Armament Laboratory ATTN: AFATL/DOIL (TIC) DLYV (Mr. McGuire) AFTAWC (OA) Eglin AFB, FL 32542-5438
1	Ogden ALC/MMWRE ATTN: Mr. Comins Hill Air Force Base, UT 84056
7	US Air Force ATTN: AFML (LNN/Nicholas; MAS; MBC/Schmidt) AFWAL AFLC (MMWM/Rideout; IGYE/Shopker) FTD (ETD) Wright-Patterson AFB, OH 45433
1	AFWL/SUL Kirtland AFB, NM 87117

No. of Cys	Organization
3	Director of Aerospace Safety ATTN: JDG/AFISC(SEVV) (COL McQueen) IDG/AFISC (SEW)(Gavitt) (SEV)(Gopher) Norton AFB, CA 92409
2	Director Joint Strategic Target Planning Staff ATTN: JLTW TPTP Offutt AFB, Omaha, NE 68113
1	HQ AFESC/RDC ATTN: Walter Buckholtz Tyndall AFB, FL 32403
1	Director Office of Operational & Environmental Safety US Department of Energy Washington, DC 20545
1	Director Office of Military Application US Department of Energy Washington, DC 20545
1	US Department of Energy Albuquerque Operations Office ATTN: Operational Safety PO Box 5400 Albuquerque, NM 87115
1	Director Pittsburgh Mining & Safety Research Center Bureau of Mines, Department of Interior 4800 Forbes Avenue Pittsburgh, PA 15213

DISTRIBUTION LIST

No. of Cys	Organization
1	Director Lawrence Livermore National Laboratory University of California P.O. Box 808 Livermore, CA 94550
1	Director Los Alamos National Laboratory ATTN: Dr. J. Taylor P.O. Box 1663 Los Alamos, NM 87545
1	Director Sandia National Laboratories ATTN: Div 6442 (von Riesemann) P.O. Box 5800 Albuquerque, NM 87115
1	Director NASA-George C. Marshall Space Center Huntsville, AL 35812
2	Director NASA-Aerospace Safety Research & Data Institute Lewis Research Center 21000 Brook Park Road Cleveland, OH 44135
1	Director NASA-Scientific & Technical Information Facility PO Box 8757 Baltimore/Wash International Airport, MD 21240
1	National Academy of Science ATTN: Mr. Groves 2101 Constitution Avenue, NW Washington, DC 20418

No. of Cys	Organization
1	Central Intelligence Agency OIR/DB/Standard GE47 HQ Washington, DC 20505
1	Institute of Makers of Explosives ATTN: Exec Dir, Suite 550 1575 Eve Street, NW Washington, DC 20005
1	Aberdeen Research Center ATTN: Mr. John Keefer PO Box 548 Aberdeen, MD 21001
1	Agbabian Associates ATTN: Dr. D.P. Reddy 250 N. Nash Street El Segundo, CA 90245
1	Ammann & Whitney ATTN: Mr. Dobbs, Suite 1700 Two World Trade Center New York, NY 10048
1	Black & Veatch Consulting Engineers ATTN: Mr. Callahan 1500 Meadow Lake Parkway Kansas City, MO 64114
1	Dr. Wilfred E. Baker Wilfred Baker Engineering PO Box 6477 San Antonio, TX 78209
1	Aeronautical Research Associates of Princeton, Inc. ATTN: Dr. Donaldson PO Box 2229 Princeton, NJ 08540

DISTRIBUTION LIST

No. of Cys	Organization
1	Applied Research Associates, Inc. ATTN: Mr. Drake 1204 Openwood Street Vicksburg, MS 39180
1	J.G. Engineering Research Associates 3831 Menlo Drive Baltimore, MD 21215
2	Kaman-AviDyne ATTN: Dr. N.P. Hobbs Mr. S. Criscione Northwest Industrial Park 83 Second Avenue Burlington, MA 01803
3	Kaman-Nuclear ATTN: Dr. F.H. Shelton Dr. D. Sachs Dr. R. Keffe 1500 Garden of the Gods Road Colorado Springs, CO
1	Knolls Atomic Power Laboratory ATTN: Dr. R.A. Powell Schenectady, NY 12309
1	McDonnell Douglas Astronautics Western Division ATTN: Dr. Lea Cohen 5301 Bosla Avenue Huntington Beach, CA 92647
1	Physics International 2700 Merced Street San Leandro, CA 94577
1	R&D Associates ATTN: Mr. John Lewis PO Box 9695 Marina del Rey, CA 90291
1	R&D Associates ATTN: G.P. Ganong PO Box 9335 Albuquerque, NM 87119
2	The Boeing Company-Aerospace Div ATTN: Dr. Peter Grafton Dr. D. Strome (Mail Stop 8C-68) PO Box 3707 Seattle, WA 98124
2	AVCO Corporation Structures & Mechanics Dept ATTN: Dr. William Broding Dr. J. Gilmore 201 Lowell Street Wilmington, MA 01887
1	Aerospace Corporation PO Box 92957 Los Angeles, CA 90009
1	General American Trans Corp General American Research Div ATTN: Dr. J.C. Shang 7449 N. Natchez Avenue Niles, IL 60648
1	Hercules, Inc. ATTN: Billings Brown Box 93 Magna, UT 84044
1	Mason & Hanger-Silas Mason Co, Inc. Plantex Plant PO Box 647 Amarillo, TX 79117

DISTRIBUTION LIST

No. of Cys	Organization
1	Lovelace Research Institute ATTN: Dr. E.R. Fletcher PO Box 5890 Albuquerque, NM 87115
1	Massachusetts Institute of Technology Aeroelastic & Structures Research Laboratory ATTN: Dr. E.A. Witmar Cambridge, MA 02139
1	Monsanto Research Corporation Mound Laboratory ATTN: Frank Neff Miamisburg, OH 45342
1	Science Applications, Inc. Suite 310 1216 Jefferson Davis Highway Arlington, VA 22202
2	Battelle Memorial Institute ATTN: Dr. L.E. Hulbert Mr. J.E. Backofen, Jr. 505 King Avenue Columbus, OH 43201
1	Georgia Institute of Tech ATTN: Dr. S. Atluri 225 North Avenue, NW Atlanta, GA 30332
1	IIT Research Institute ATTN: Mrs. H. Napadensky 10 West 35th Street Chicago, IL 60616
2	Southwest Research Institute ATTN: Dr. H.N. Abramson Dr. U.S. Lindholm 8500 Culebra Road San Antonio, TX 78228

No. of Cys	Organization
1	Brown University Division of Engineering ATTN: Prof. R. Clifton Providence, RI 02912
1	Florida Atlantic University Dept of Ocean Engineering ATTN: Prof. K.K. Stevens Boca Raton, FL 33432
1	Texas A&M University Dept of Aerospace Engineering ATTN: Dr. J.A. Stricklin College Station, TX 77843
1	University of Alabama ATTN: Dr. T.L. Cost PO Box 2908 University, AL 35486
1	University of Delaware Dept of Mechanical & Aerospace Engineering ATTN: Prof. J.R. Vinson Newark, DE 19711

Aberdeen Proving Ground

No. of Cys	Organization
1	Cdr, TECOM, ATTN: AMSTE-SI-F
3	Cdr, CRDEC, ATTN: SMCCR-RSP-A SMCCR-MU SMCCR-SPS-IL
1	Cdr, USATHMA, ATTN: AMXTH-TE
5	Dir, AMSAA, ATTN: AMXSY-D AMXSY-MP (H. Cohen)

USER EVALUATION SHEET/CHANGE OF ADDRESS

This Laboratory undertakes a continuing effort to improve the quality of the reports it publishes. Your comments/answers to the items/questions below will aid us in our efforts.

1. BRL Report Number__________ ____________________Date of Report_____________

2. Date Report Received____

3. Does this report satisfy a need? (Comment on purpose, related project, or other area of interest for which the report will be used.)_____________________

____

____

4. How specifically, is the report being used? (Information source, design data, procedure, source of ideas, etc.)____

____

____

5. Has the information in this report led to any quantitative savings as far as man-hours or dollars saved, operating costs avoided or efficiencies achieved, etc? If so, please elaborate.____

____

____

6. General Comments. What do you think should be changed to improve future reports? (Indicate changes to organization, technical content, format, etc.)

____

____

____

CURRENT ADDRESS

____
Name

____
Organization

____
Address

____
City, State, Zip

7. If indicating a Change of Address or Address Correction, please provide the New or Correct Address in Block 6 above and the Old or Incorrect address below.

OLD ADDRESS

____
Name

____
Organization

____
Address

____
City, State, Zip

(Remove this sheet, fold as indicated, staple or tape closed, and mail.)